UNIVERSITY OF MODENA AND REGGIO EMILIA

Doctor of Philosophy (Ph.D.) Program in Clinical and experimental medicine (CEM) - Medicina clinica e sperimentale

XXXVIII° cycle

Study of host-microorganism interactions by *in vitro* models of mono- and polymicrobial vaginal infections, and evaluation of the protective effect of new bioactive molecules

Candidate: Francesco Ricchi

Supervisor: Prof. Eva Pericolini

Ph.D. program coordinator: Prof. Marco Vinceti

INDEX

ABSTRACT

The homeostasis of the vaginal microenvironment is finely regulated. The bacteria belonging to the genus *Lactobacillus* play a key role in retaining the homeostasis; in addition, their immunomodulatory and anti-inflammatory activity have been described in literature. When this balance breaks down, dysbiosis occurs and causes the onset of infections by microorganisms and viruses that normally behave as commensals. *Candida albicans* (*C. albicans*), can overgrow and trigger vulvovaginal candidiasis (VVC). The shifting from commensalism to pathogenicity is due to the capacity to undergo a dimorphic transition from yeast to hyphal morphology. In such form the fungus expresses several virulence factors, such as candidalysin (CL) and the hydrolytic enzymes secreted aspartyl proteases (SAP), and it promotes inflammation and damage to the vaginal mucosa; the latter are responsible of the clinical symptoms: itching, burning sensation, vaginal discharge and strangury.

To date, the mechanisms driving host-microrganism and host-virus interactions in the context of the vaginal environment is incomplete. The increase of drug resistance, and the lack of knowledge on the pathogenetic mechanisms that lead to vulvovaginal infections, requires to establish novel therapeutic approaches and advanced *in vitro* models for the study of such diseases.

For this reason, the experimental approach used for the present Ph.D. project includes the setting up of vaginal epithelial cells arranged in monolayers or multilayers (RVE) systems to be infected by microbes and viruses responsible of vaginal infections (specifically, the fungus *C. albicans*, the bacteria *Gardnerella vaginalis* and *Escherichia coli* and the Herpes simplex 2 virus). These models have been used to assess the beneficial effects of bioactive molecules and to analyse the molecular mechanisms used by the cells to respond to the infectious agents. In addition, an "untargeted" metabolomic approach has been employed to reveal the production of bioactive metabolites released by different species of *Lactobacillus*.

The results indicate that: a) specific bacterial lysates can improve the host cells response against the pathogens; b) an *in vitro* RVE model employed in combination with artificial vaginal fluid has provided a tool that better resembles the human vaginal mucosa, and it is useful to study the interaction of the infected epithelial cells with microorganisms and viruses; c) *C. albicans* triggers a rapid activation of epithelial cells mitochondria, which is protective against several virulence traits of the fungus (release of candidalysin and hyphal formation); d) by using an "untargeted" metabolomic approach, significant differences in metabolites production by *Lacticaseibacillus* (*L.*) *rhamnosus*, *Lactobacillus* (*L.*) *acidophilus*, *Lactiplantibacillus* (*L.*) *plantarum* and *Limosilactobacillus* (*L.) reuteri* could be detected; specifically, inosine (a nucleoside with antioxidant, anti-inflammatory, antiinfective and neuroprotective properties) was found to be

overproduced by *L. rhamnosus*.

In conclusion, by using *in vitro* models of vaginal infections, this study has contributed to acquire data concerning the possible interactions between vaginal epithelial cells and microorganisms and viruses. Such results have been obtained by analysing the mechanisms underlying the cell responses to the different pathogens. In addition, the possible beneficial effects of novel bioactive molecules in the treatment of vaginal infections have been proposed. Finally, by this study it has been possible to highlight how different bacterial species are able to produce several metabolites with possible beneficial effects for the vaginal mucosa.

RIASSUNTO

Il microambiente vaginale è finemente regolato per mantenere l'omeostasi. I batteri lattici del genere *Lactobacillus* svolgono un ruolo chiave nel preservare questa omeostasi ed è noto il loro effetto immunomodulante ed antinfiammatorio. L'alterazione di questo equilibrio porta a disbiosi, con conseguente insorgenza di infezioni sostenute da microrganismi e virus che possono anche far parte del microbiota vaginale. Per esempio, *Candida albicans* (*C. albicans*), un lievito commensale della mucosa vaginale, può proliferare eccessivamente e causare candidosi vulvovaginale (VVC). Il passaggio da commensale a patogeno di *C. albicans* nella VVC è legato alla sua transizione morfologica da lievito a ifa che, insieme alla produzione di fattori di virulenza come la candidalisina (CL) ed enzimi idrolitici come le proteasi aspartiche (SAP), promuove l'infiammazione e il danno della mucosa vaginale con sintomi caratteristici quali: prurito, bruciore, perdite vaginali e dolori alla minzione.

Ad oggi, i meccanismi che regolano le interazioni ospite-microrganismo e virus nell'ambiente vaginale rimangono poco chiari. Alla luce dell'aumento della resistenza ai farmaci e della scarsa comprensione dei meccanismi patogenetici delle infezioni vulvovaginali, vi è un urgente bisogno di nuovi approcci terapeutici e di modelli *in vitro* avanzati per studiare queste patologie. Per questo, l'approccio sperimentale utilizzato per questo lavoro di dottorato ha incluso la messa a punto di sistemi di monostrato o multistrato (RVE) di cellule epiteliali vaginali, successivamente infettati con microrganismi e virus responsabili di infezioni vulvovaginali (in particolare *C. albicans* ma anche *Gardnerella vaginalis*, *Escherichia coli* e virus Herpes simplex di tipo 2). Questi modelli di infezione sono stati utilizzati per saggiare l'effetto benefico di molecole bioattive, nonché per analizzare i meccanismi molecolari di risposta ai microrganismi e virus dell'epitelio vaginale. Inoltre, è stato utilizzato un approccio di metabolomica "untargeted" per analizzare la produzione di possibili metaboliti bioattivi rilasciati da differenti specie di lattobacilli.

I risultati ottenuti indicano che: a) specifici lisati batterici possono migliorare la risposta cellulare contro i patogeni; b) l'utilizzo di un modello RVE *in vitro,* in presenza di fluido vaginale artificiale, è un modello più rappresentativo della mucosa vaginale umana e si è rivelato utile per studiare l'interazione delle cellule epiteliali infettate con microrganismi e virus; c) *C. albicans* induce una rapida attivazione mitocondriale nelle cellule epiteliali vaginali, che lo utilizzano come meccanismo protettivo nei confronti di diversi fattori di virulenza del fungo (rilascio di candidalisina e formazione di ife); d) utilizzando un approccio di metabolomica "untargeted", abbiamo rilevato differenze consistenti nei metaboliti prodotti da *Lacticaseibacillus* (*L.*) *rhamnosus*, *Lactobacillus* (*L.*) *acidophilus*, *Lactiplantibacillus* (*L.*) *plantarum* e *Limosilactobacillus* (*L.) reuteri* con una over-produzione di inosina, nucleoside con proprietà antiossidanti, antinfiammatorie, anti-infettive e

neuroprotettive, da parte di *L. rhamnosus*.

In conclusione, questo studio ha esplorato tramite modelli *in vitro* di infezione vaginale, le possibili interazioni tra cellule epiteliali vaginali, microrganismi e virus analizzando i meccanismi che mediano le risposte cellulari ai diversi patogeni microbici e virali; questo studio ha inoltre evidenziato il potenziale effetto benefico di nuove molecole bioattive nel trattamento delle infezioni vaginali e ha messo in luce come specie diverse di batteri lattici possano produrre diversi metaboliti con possibili effetti benefici per la salute della mucosa vaginale.

PREFACE

This Ph.D. Thesis is the synthesis of three years of dedicated work in the field of clinical microbiology, and it shows the results of the research projects in which I have been involved. The common thread of these projects is the study of host-pathogens interactions, by means of *in vitro* models of mono- and polymicrobial vaginal infections, with emphasis on the protective role and the therapeutic potential of selected bioactive molecules.

The studies included in this Thesis reflect a forward-looking scientific approach, aimed at handling real-world situations through a rigorous scientific method. My efforts have been driven by a strong intellectual curiosity, accompanied by a deep devotion to scientific integrity, both of which have significantly contributed to my personal and professional growth.

I would like to acknowledge also the individuals and institutions whose support has been essential in completing this work.

I am deeply grateful to my supervisor, Professor Eva Pericolini, for her invaluable guidance and continuous support throughout these years. I would also wish to acknowledge Professors Claudio Cermelli, Andrea Ardizzoni, and Elisabetta Blasi for their scientific advice and for promoting a stimulating research setting.

I would also like to extend my sincere thanks to Professor Attila Gacser and his research group at the University of Szeged (Hungary) for their warm welcome and scientific support during my six-month research stay. Their professionalism and cooperation provided a highly supportive and dynamic research environment that greatly enriched my experience, both personally and in terms of scientific academic research development.

I extend my special thanks to Dott. Paola Della Zorza, Dott. Chiara Pistorello and the entire Depofarma company group for funding and supporting part of this research project.

Lastly, I also wish to express my sincere gratitude to my colleagues in the Microbiology laboratory and all the coworkers of other research groups who made these studies possible. Their support and scientific competence have been invaluable throughout these years.

CHAPTER 1

Cutibacterium acnes lysate improves cellular response against *Candida albicans*, *Escherichia coli* and *Gardnerella vaginalis* in an *in vitro* model of vaginal infection

Francesco Ricchi[1], Samyr Kenno[2], Natalia Pedretti[3], Giulia Brenna[2], Francesco De Seta[3,4], Andrea Ardizzoni[2] and Eva Pericolini[2]

[1] Clinical and Experimental Medicine PhD Program, University of Modena and Reggio Emilia, Modena, Italy;

[2] Department of Surgical, Medical, Dental and Morphological Sciences with Interest in Transplant, Oncological and Regenerative Medicine, University of Modena and Reggio Emilia, Modena, Italy;

[3] Department of Medical Sciences, University of Trieste, Trieste, Italy;

[4] Department of Obstetrics and Gynecology, Istituto di Ricovero e Cura a Carattere Scientifico (IRCCS) San Raffaele Scientific Institute, University Vita and Salute, Milano, Italy.

***Frontiers in cellular and infection microbiology*. 2025, doi:10.3389/fcimb.2025.1578831**

1. INTRODUCTION

The vagina of healthy women during the reproductive age is colonized by many microbial species, mainly *Lactobacillus* spp. (up to 95%) (Ravel et al., 2011). The healthy vaginal microbiota helps the host to keep pathogens at bay through mechanisms of competitive inhibition, production of bacteriocins and lactic acid and by stimulating the host cells to release antimicrobial peptides and anti-inflammatory cytokines (Niu et al., 2017; Ilhan et al., 2019). The microecological balance of the vagina is a finely tuned dynamic process, capable of self-regulation. The breaking up of such balance leads to dysbiosis, with the resident microbiota overcome by pathogens, triggering the onset of gynecological infectious diseases (Chao et al., 2019; Zhang et al., 2021). Vulvovaginal candidiasis (VVC), bacterial vaginosis (BV) (and to a lesser extent aerobic vaginitis, AV) are the most common infections of the lower genital tract.

VVC is a symptomatic inflammation of the vagina, that affects 70-75% of healthy women at least once during their reproductive age (Blostein et al., 2017; Denning et al., 2018). It is caused by several species of the genus *Candida*, mainly by *C. albicans*. VVC is mainly endogenous because *C. albicans* is a member of the human microbiota and it dwells in the mucosae of the oropharynx, genital and gastrointestinal tracts (Odds, 1987; Kauffman, 2006; Pappas, 2006; Pfaller and Diekema, 2007). In the context of VVC the infection and disease frequently occur in healthy women and to date a higher incidence of the disease has not been described under conditions of immunodepression. However, some studies indicated increased susceptibility in specific categories (i.e., diabetics and immunocompromised women) (Talaei et al., 2017; O'Laughlin and McCoy, 2023). Even though *Candida* causes damage *per se*, the host response plays an important role in VVC onset, by exacerbating the fungal-mediated damage and causing the symptoms, which include itching, burning, pain, redness of the vulva and vaginal mucosa and a typically thick and white (cottagecheese-like) vaginal discharge (Ardizzoni et al., 2021).

Bacterial vaginosis (BV) is a condition characterized by a modification of the bacterial milieu, where beneficial healthy vaginal microbiota is dramatically reduced and overwhelmed by facultative and strictly anaerobic pathogens, such as *Gardnerella* spp., *Prevotella* spp., *Peptostreptococcus* spp., *Mobiluncus* spp., *Atopobium vaginae* and *Mycoplasma hominis* (Srinivasan and Fredricks, 2008; Turovskiy et al., 2011; Chen et al., 2021). It affects women during their fertile age, it is characterized by specific clinical symptoms (thin, homogeneous and grayish-white vaginal discharge, rotten fish vaginal odor, and less commonly itching and burning sensation) and it is accompanied by serious obstetrics and gynecologic complications: spontaneous abortion, preterm birth, endometritis, pelvic inflammatory disease, postoperative infections (Jacobsson et al., 2002; Leitich et al., 2003; Rothman

et al., 2003; Guerra et al., 2006; Kavoussi et al., 2006) and increased susceptibility to sexually transmitted diseases (Brotman, 2011).

Aerobic vaginitis (AV) is a less common vaginal infection, where the normal vaginal microbiota is overcome by aerobic bacteria often deriving from the Gastro-Intestinal (GI) tract, such as *Escherichia coli*, *Streptococcus agalactiae*, *Staphylococcus aureus* and *Enterococcus faecalis* (Donders et al., 2002, 2011, 2017; Kaambo et al., 2018). These bacteria can become dangerous, especially during pregnancy, because not only do they affect fetal health, but the pregnancy status aggravates the symptoms and the consequences of the infection (Donders et al., 2017; Fan et al., 2021; Plisko et al., 2021). The etiology and pathogenesis of AV are not completely clear (Fan et al., 2021; Mohankumar et al., 2022). The pathogenic bacteria are retained to produce different toxins or, similarly to VVC, to affect the local immunity of patients, thus leading to the disease onset (Ma et al., 2022). AV symptoms are viscous and yellow vaginal discharge, sticky fishy odor, stinging and burning sensations and dyspareunia (Donders et al., 2017).

To date, antibiotics (metronidazole, clindamycin and tinidazole) and antifungal drugs (fluconazole, amphotericin B, nystatine, flucytosine) are the gold standard treatments for BV/ AV and VVC, respectively (Gaziano et al., 2020). However, given the ever-growing problem of drug resistance, it is necessary to develop novel therapeutic strategies as an aid or an alternative to the current pharmacological approach.

The alteration of vaginal mucosa integrity is a key step in the pathological process of lower genital tract infections. For example, *G. vaginalis* can disrupt the epithelial barrier integrity and alter the immune microenvironment in the vaginal tract (Rahman et al., 2024). Preservation of the integrity and functionality of the epithelial barrier is crucial to counteract infections, hence the potentiation of epithelial cells play a pivotal role against pathogens.

In recent years, the emerging concept of "trained immunity" modified the idea of memory responses that traditionally were a prerogative only of the adaptive branch of the immune system (Netea et al., 2016). Indeed, increasing data show that also the cells of the innate immunity, as well as the epithelial cells, are able to acquire a memory phenotype through the modulation of epigenetic, metabolic and functional changes in response to several stimuli of infectious (Liu et al., 2016; Kaufmann et al., 2018; Bigot et al., 2019; Covián et al., 2019, 2021), and non-infectious nature (Bekkering et al., 2014). It has been demonstrated that following these changes, such cells can increase cytokines production and antigen presentation, ultimately improving the antimicrobial responses. The basis of this phenomenon has been reconducted to the presence of several Pathogen Associated Molecular Pattern

(PAMP) molecules that trigger the trimethylation of the lysine residue in position 4 on the histone H3 (H3K4me3). This chemical modification facilitates the transcription of several genes, especially those coding for proinflammatory cytokines (Acevedo et al., 2021). Epigenetic and metabolic reprogramming act on epithelial cells by improving their mechanical barrier, enabling them to modulate cytokines production and stimulating them to produce alarmins and other antimicrobial peptides. They act also on innate immune cells, such as macrophages and NK cells, by increasing their mitochondrial activity, triggering the inflammasome, and modulating cytokines production and their phagocytic activity (Chalifour et al., 2004; Zhang and Mosser, 2008). By taking advantage of the new knowledge of the mechanisms of trained immunity, new approaches have been introduced to potentiate the response of the host, such as the use of bacterial lysates. Bacterial lysates are obtained by mechanical or chemical crushing of the bacterial cell walls (Bizzini et al., 1984; Pfefferle et al., 2013), and the fragments obtained contain several antigens and PAMP molecules. Literature reports the successful employment of bacterial lysates to prevent recurrent respiratory diseases, to avoid the flare-up of respiratory chronic infections and as a defense against urinary infections (Braido et al., 2007; Ahumada-Cota et al., 2020).

Cutibacterium acnes (*C. acnes*) (formerly knownas *Propionibacterium acnes*) lysate proved effective for the treatment of type 1 hypersensitivity caused by soaps, solvents, chemicals and cosmetics (Mangano et al., 2017). Because this species normally dwells on the skin, it is prone to several kinds of stressful stimuli and therefore it is endowed with as many defense systems. In particular, *C. acnes* is equipped with the enzyme radical oxygenase that allows the bacteria to reduce the reactive oxygen species (ROS), thus counteracting the oxidative stress (Allhorn et al., 2016). One particular fraction of the *C. acnes* lysate, the P40, has been previously demonstrated to be effective for the treatment of chronic obstructive bronchitis as well as recurrent infections of the genitourinary tract from *C. albicans*, *E. coli* and Herpes Simplex Virus (Jurkiewicz and Zielnik-Jurkiewicz, 2018; Triantafillou et al., 2019; Yang et al., 2019). The present study aims at evaluating the activity of the *C. acnes* bacterial lysate (BL) in *in vitro* models of microbial infections from the fungus *C. albicans*, the Gram-variable bacterium *G. vaginalis* and the Gram-negative bacterium *E. coli*.

2. MATERIALS AND METHODS

2.1 Cells, microorganisms and bacterial lysate

2.1.1 Cells

The human vaginal epithelial cell line A-431(ATCC-CRL-1555) and the murine macrophages J774A.1 cell line (ATCC-TIB-67) employed in this study were purchased from American Type Culture Collection. Cells were cultured, as previously described, with slight modifications (Spaggiari et al., 2023). Briefly, both cell lines were cultured in Dulbecco's Minimum Essential Medium (DMEM) (Sial S.r.l., Rome, Italy), supplemented with heatinactivated fetal bovine serum (Hi FBS Sial) at 10% (vol/vol) in the growth medium and 5% (vol/vol) in the maintenance medium, 100 U/ml Penicillin-Streptomycin (Lonza Walkersville Inc., Walkersville, MD, U.S.A.), 2.5 mg/ml Ciprofloxacin (Gibco, Thermo Fisher Scientific Italia) and 2 mM L-glutamine (Gibco).

2.1.2 Microbial strains and growth conditions

All the microorganisms employed in the present study had been stocked frozen at -80°C in Microbank® cryovials (ProLab Diagnostics, Richmond Hill, ON, Canada). After thawing, the reference strains *C. albicans* SC5314 (ATCC MYA-2876) and *C. parapsilosis* CLIB214 (ATCC 22019) were grown in Yeast Extract Peptone Dextrose (YEPD) broth (Condalab, Madrid, Spain) and subcultured in Sabouroud Dextrose Agar (SDA – Oxoid, Thermo Scientific Italia) through weekly passages. *E. coli* (ATCC 13762) was grown in Tryptic Soy Broth (TSB – Biolife S.r.l., Milano, Italy) and subcultured in MacConkey agar (BioChemika, Sigma-Aldrich, Germany) through weekly passages. *G. vaginalis* (ATCC 14018) was grown in New York City III (NYC III) broth (ATCC Medium 1685) and *L. crispatus* (ATCC 33280) was grown in De Man, Rogosa Sharpe (MRS) broth (Oxoid). All the microorganisms were used in their exponential growth phase for the infection assays (see below). *C. albicans* and *C. parapsilosis* were subcultured in SDA and *E. coli* was subcultured in TSB; the incubations were carried out for 24 h at 37°C under agitation (120 rpm) and in aerobic conditions. For both *L. crispatus* and *G. vaginalis*, an aliquot from the frozen stock was placed in broth and cultured at 37°C under agitation (120 rpm) and in anaerobic conditions for 24 h and 48 h respectively.

2.1.3 Bacterial lysate

Bacterial lysate (BL) was prepared from *C. acnes* (ATCC 6919) as described elsewhere (Ohashi et al., 1983; Basal et al., 2004). Whole cells, suspended in an appropriate volume of distilled water, were disrupted through ultrasonication. The mixture was then centrifuged at 2,200 × g for 20 min to remove any intact cells. The resulting supernatant underwent further centrifugation at 20,000 × g for 30 min. The obtained pellet was treated with pronase at 80°C for 2 h. Following another centrifugation at 20,000 × g for 30 min, the final pellet was lyophilized and designated as the cell wall fraction. After the preparation of the lyophilized cell wall fraction, a mother solution at 10 mg/ml in dimethyl-sulfoxide (DMSO) was prepared. Then, BL was used at 100, 10 or 1 mg/ml, diluted in the respective media. In all the experiments, the respective dilution of DMSO was included, as internal control, and it did not show any effect.

2.2 Effect of BL on fungi and bacteria by MIC determination

The broth microdilution method was employed to evaluate the possible direct effect of BL on pathogens viability. Specifically, BL starting from the concentration of 0.160 mg/ml was serially diluted 1:2 in 96-well, flat-bottomed plates in Roswell Park Memorial Institute (RPMI) 1640 (Sigma Aldrich) added with glucose 18 g/l (Carlo Erba, Milano, Italy) and 4-Morpholinapro-pansulphonic acid (MOPS, 35 g/l) (Sigma Aldrich) for *Candida* and *E. coli*. The broth microdilution method was carried out for *G. vaginalis* by using NYC III broth and for *L. crispatus* by using MRS broth. Subsequently, 100 ml of the microorganism ($5x10^5$ CFU/ml for all microorganisms except for *G. vaginalis* and *L. crispatus*, $5x10^6$ CFU/ml) were added to each well. The growth of the microorganisms was assessed by measuring the optical density (OD) with a spectrophotometric plate reader (Sunrise, Tecan, Männedorf, Switzerland), 24 h and 48 h after inoculation. Readings were performed at 540 nm (for fungi) and 595 nm (for bacteria) wavelengths. Each species, seeded in its specific medium without bacterial lysate and diluent, served as a positive control.

2.3 Effect of BL on A-431 and J774A.1 cells by flow cytometry analysis

A-431 and J774A.1 cell cultures ($1x10^5$ cells/well) were grown for 24 h or 2 h, respectively, in 96-well plates. Then, cells were washed with 200 µl of warm PBS to remove dead cells and antibiotic residues. Next, 100 ml of 10-fold serially diluted BL in maintenance medium (with or without antibiotics) were added in triplicate to the cell cultures and incubated for a further 24 h. A-431 cells were then detached by Trypsin-EDTA solution (0,25%) in HBSS (1×) (GIBCO) whereas J774A.1 cells were then detached with a cellscraper. Cells were then centrifuged for 10 min at 4°C at 350 × g

and the supernatants were harvested. Next, the cells were stained with eBioscience™ Fixable Viability Dye eFluor™ 780 (Thermo Fisher Scientific, U.S.A.), diluted in BSA/PBS 0.5% w/vol, to discriminate live cells from dead cells. Each sample was incubated for 15 min in ice, in the dark. Next, the cells were centrifuged for 10 min at 4°C at 350 × g, the supernatant was discarded, and the pellet was resuspended in Fixation Buffer (BioLegend, U.S.A.) and incubated for 20 min in the dark at room temperature. Each sample was centrifuged one last time for 10 min at room temperature at 350 × g, the supernatant was discared, and the pellet was resuspended in 350 µl of PBS for analysis. The FACSymphony™ (Becton Dickinson, U.S.A.) was employed and the software FlowJo™ was used for the data analysis. Heat-killed (HK) A-431 and J774A.1 cells were included as internal controls.

2.4 A-431 and J774A.1 cell assays

The assays performed on the A-431 cells are depicted in Figure 1A. Briefly, 24 h after seeding (at day 1), the A-431 cells were primed by removing the growth medium and adding BL into the fresh medium (day 2). At day 3 the BL-primed A-431 cells were infected with *C. albicans* or the bacteria and the production of mtROS in response to the infection was kinetically evaluated. Finally, at day 4 after seeding, the growth of microorganisms, the A-431 cell-damage and cytokines and chemokines production in response to the infection were assessed. All the assays performed on the J774A.1 cells are depicted in Figure 2A. Briefly, the J774A.1 cells were seeded and primed with BL (day 1). At day 2 the BL-primed J774A.1 cells were infected with *C. albicans* or the bacteria and the production of mtROS in response to the infection was kinetically evaluated. Finally, at day 2 after seeding, the phagocytosis and killing activity of the BL-primed J774A.1 were assessed.

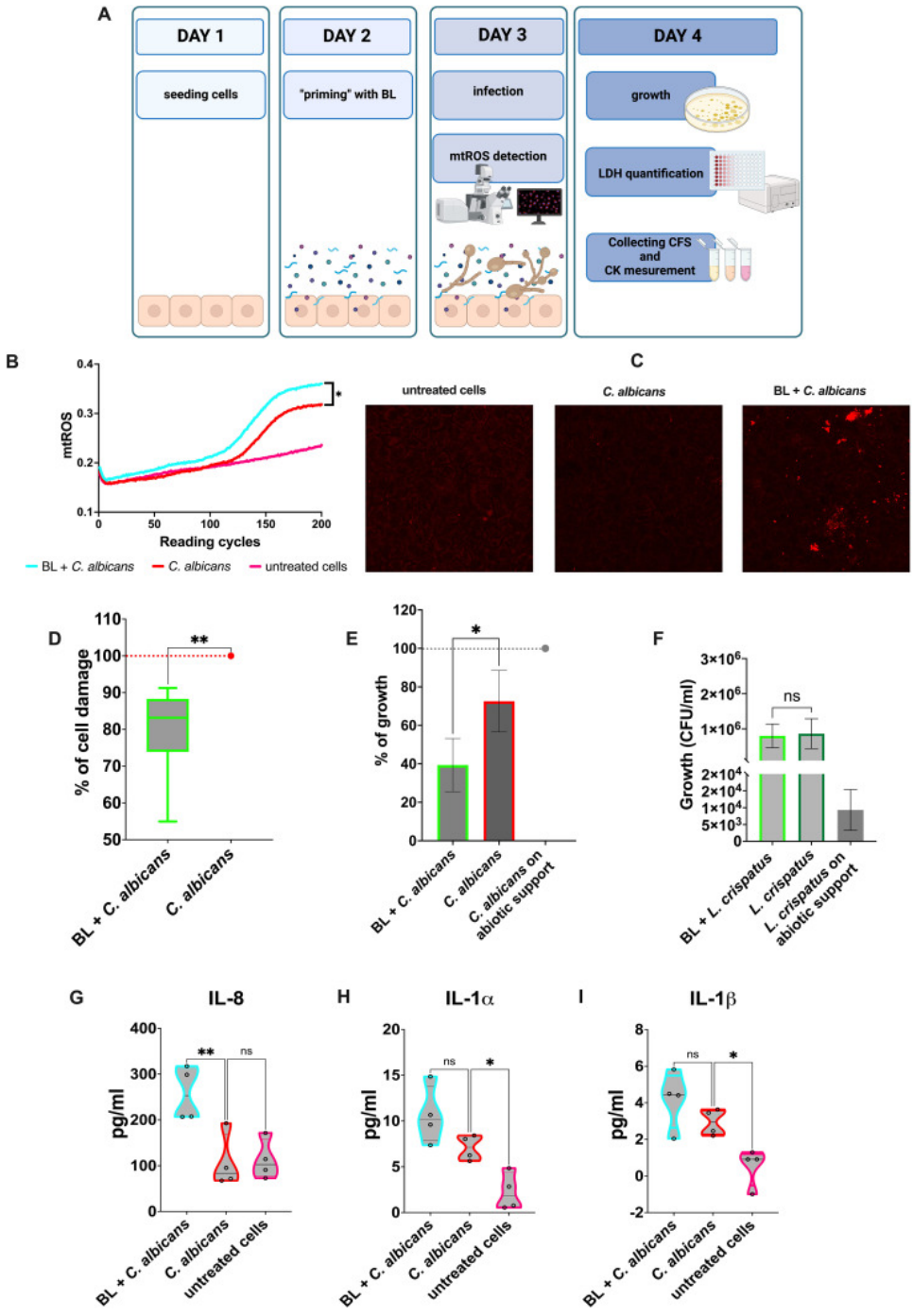

Figure 1

Effects of BL priming on A-431 cells infected with *C albicans*. (**A**) Schematics representing the treatment and the experiments carried out (created with BioRender.com). (**B**) Kinetic quantification of mtROS production by infected A-431 cells primed or not with BL (10 mg/ml). Data are from 3 experiments performed in triplicate (**C**) Visualization of mtROS production in A-431 cells primed or not with BL (10 mg/ml) by confocal microscopy, 30 min after infection with *C. albicans*. (**D**) Percentage of damage in BL-primed (1 mg/ml) and infected A-431 cells. The boxplot results from six experiments conducted in triplicate. (**E**, **F**) Effect of BL-primed (1 mg/ml) A-431 cells on the growth of *C. albicans* (**E**) and *L. crispatus* (**F**) determined through Colony Forming Units (CFU) counts; the data are expressed as the mean ± SD of at least 3 experiments. (**G**–**I**) IL-8 (**G**), IL-1α (**H**) and IL-1β (**I**) production by BL-primed (10 mg/ml) infected A-431 cells. Each truncated violin results from 4 experiments. The values of $*p < 0.05$ and $**p < 0.01$ were considered statistically significant. ns, not significant.

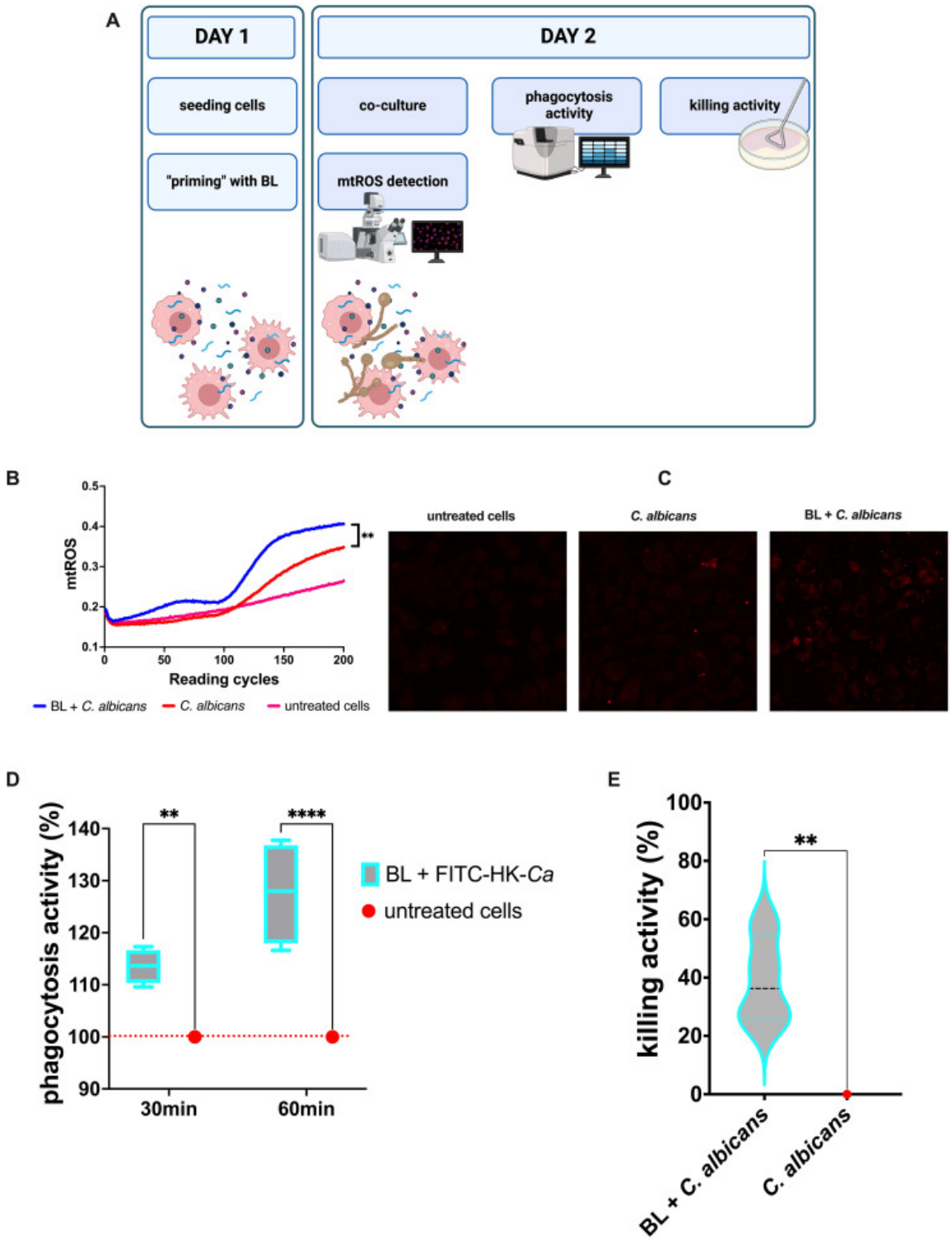

Figure 2

Effects of LB priming on J774A.1 cells infected with *C. albicans*. (**A**) Schematics representing the treatment and the experiments carried out (created with BioRender.com). (**B**) Kinetic quantification of mtROS production by BL-primed (100 mg/ml) infected J774A.1 cells. Data are from 3 experiments performed at least in duplicate. (**C**) Visualization of mtROS production in J774A.1 cells primed or not with BL (100 mg/ml) by confocal microscopy, 30 min after infection with *C. albicans*. (**D**) Percentage of phagocytic activity of BL-primed (10 mg/ml) J774A.1 cells after 30 and 60 min of coculture with FITC-labelled heat-killed *C. albicans* (FITC-HK-*Ca*). Each boxplot results from 4 experiments conducted in triplicate. (**E**) Percentage of killing activity by BL-primed (10 mg/ml) J774A.1 cells against *C. albicans*. Data results from four experiments conducted in duplicate. The values of $^{**}p < 0.01$ and $^{****}p < 0.0001$ were considered statistically significant.

2.4.1 Evaluation of microorganisms-induced cell damage by lactate-dehydrogenase quantification

Serially diluted BL was added to cell cultures grown for 24 h, as described in paragraph 2.3. Finally, the infection was performed at different MOI (Multiplicity of infection, defined as the ratio between the number of cells and the number of microorganisms). One hundred µl of each microorganism suspension, in maintenance medium, was added. Specifically, MOI 1:5 was used for *C. albicans*, MOI 1:1000 was employed for *E. coli*, whereas for *G. vaginalis* a MOI 1:1 was applied. The plate was then placed again for 24 h at 37°C with 5% CO_2. Cytotoxicity was quantified by analyzing the LDH release in the culture medium, by employing a commercially available kit (Roche, via Sigma-Aldrich) following the Manufacturer's instructions. The percentage of damage was calculated as follows:

$$\%\ \text{of cells damage} = \frac{\text{sample} - \text{low control}}{\text{high control} - \text{low control}} \times 100$$

where: low control is the average value of uninfected cells and high control is the average value of uninfected cells lysed with 1% (vol/vol) Triton-X-100 (Fluka). Then, the data were expressed as percentages, assuming as 100% the damage of infected cells not primed with BL.

2.4.2 Evaluation of microorganisms' growth after coculture with BL-primed epithelial cells

BL was added to cell cultures grown for 24 h, as described in the previous paragraph. *C. albicans* (MOI 1:5) or *L. crispatus* (MOI 1:50) were then added to the cells. After 24 h of culture, the cells were detached with 0.2% (vol/vol) Tryton-X-100. The samples were collected in 1.5 ml tubes. All the wells were then washed with 100 ml of Soybean–Casein Digest Broth prepared with Lecithin and Polysorbate 80 (SCLDP 80) medium (Biotec) to completely detach the fungi and the bacteria, and the detached microorganisms were added to the respective tubes. Next, the tubes were centrifuged at 3,500 rpm for 5 min, the supernatants were discarded, and the pellets were resuspended with 1 ml of PBS. Finally, serial dilutions were performed and seeded onto SDA plates (*C. albicans*) or MRS plates (*L. crispatus*). The data were expressed as percentages, assuming as 100% the maximum growth of *C. albicans* in wells not containing cells. Normalization was not performed on *L. crispatus*, and its growth was expressed as CFU/ml.

2.4.3 Kinetic quantification of mtROS in BL-primed and *C. albicans* infected cells

For the determination of mtROS production, A-431 cells were seeded on black-transparent 96 well plates, infected by *C. albicans* at MOI 1:5 and then 2.5 mM/well MitoSOX™ Red (Invitrogen™, Thermo-Fisher Scientific) were added immediately to each well. Then, the fluorescence intensity was measured in kinetics (1 reading cycle every 5 min) by means of a Fluoroskan FL microplate fluorometer (Thermo Scientific, Waltham, MA, U.S.A.) under stable temperature of 37°C. The fluorescence emission was analyzed at excitation/emission wavelengths of 544 nm/590 nm, according to an established protocol (Spaggiari et al., 2024). The assay was carried out under the same experimental conditions also for J774A.1 cells but using a different MOI (1:10). Confocal microscopy was employed for the visualization of mtROS in A-431 and J774A.1 cells. The cells were seeded at a density of $5x10^5$ cells per compartment in a 4-compartments cell culture dish (Greiner Bio-One, Italy). Imaging was then performed using a confocal microscope (Leica SP8 confocal microscope equipped with 405nm and white light lasers) and the resulting images were analyzed using Fijii software (ImageJ).

2.4.4 Quantification of cytokines production in BL-primed infected cells

The secretion of IL-1α, IL-1β, TNF-α and IL-8 by BL-primed A-431 cells 24 h after infection with *C. albicans*, *E. coli* and *G. vaginalis* was assessed, using the same MOI described above (see paragraph 2.4.1). The detection of cytokines and chemokines was achieved by using commercial ELISA kits (PeproTech™, ThermoFischer Scientific, Cranbury, NJ, USA for IL-1α and TNF-α; Invitrogen™, Thermo-Fisher Scientific for IL-1β and IL-8), which were used according to the Manufacturers' instructions. The analyses were carried out on the supernatants that had been collected after LDH quantification or from *ad-hoc* experiments carried out with the same protocol used for LDH detection and stored at -20°C.

2.4.5 Phagocytosis and killing activity of BL primed J774A.1 cells

C. albicans, subcultured for 24 h on SDA, was resuspended in PBS at the working concentration of $1x10^9$ CFU/ml. The fungal cells were then inactivated by heating them at 90°C for 30 min. Next, the killed yeasts were labelled with 0.1 mg/ml fluorescein 5(6)isothiocyanate (FITC) (Sigma Aldrich) for 15 min at room temperature, in the dark and occasionally flipping. The labelled heat-killed (HK)

Candida cells were then aliquoted and kept as frozen stocks at -20°C. The FITC stock solution was prepared at 1 mg/ml in 0.05 M carbonate-bicarbonate buffer. Cell cultures ($1x10^5$ cells/well) were grown for 2 h in a black-transparent 96-well plates. Then, the growth medium was removed and 100 µl of 10-fold serially diluted BL in maintenance medium were added to the cell cultures and incubated for a further 24 h. Next, 100 µl of $1x10^6$ FITC-labeled HK *Candida* suspension in maintenance medium were added to each well, and the multiwell plate was incubated for further 30 min and 60 min. After these incubation times, the medium was removed and 100 µl of 0.4% (w/vol) Trypan Blue solution (Corning, U.S.A.) were added; then, the plate was further incubated for 1 min. Finally, the Trypan Blue was removed, and the fluorescence emission was analyzed by Fluoroskan FL microplate fluorometer at excitation/emission wavelengths of 490 nm/521 nm. The percentage of phagocytosis was calculated as follows:

$$\%\ \text{of phagocytosis} = \frac{\text{sample} - \text{blank control}}{\text{untreated cells} - \text{blank control}} \times 100$$

where blank control is represented by average fluorescence value of medium with FITC labelled HK *Candida* and the untreated cells represents the average level of cell phagocytosis. To evaluate the killing activity of BL-primed J774A.1 cells, the growth medium was removed, and serially diluted BL was added to cell cultures that had been grown for 2 h in growth medium with or without antibiotics, according to the microorganism assessed. Then, the cells were infected with *C. albicans*, *E. coli* and *G. vaginalis*, all employed with MOI 1:1. After 4 h of infection with *C. albicans* or 2 h of infection with the bacteria, the cells were detached with 0.2% (vol/vol) Tryton-X-100 and the samples were collected in 1.5 ml tubes. Control samples consisting of microorganisms growth in the wells without cells were detached with SCDLP80. Next, serial dilutions were performed and seeded onto SDA plates for *C. albicans*, Tryptic Soy Agar (TSA, Condalab, Spain) for *E. coli*, and *Gardnerella vaginalis* agar (Microbiol, Uta, CA, Italy) for *G. vaginalis*. All the plates were incubated at 37°C with 5% CO_2. The percentage of killing activity was calculated as follows:

$$\%\ \text{of killing activity} = 100 - \frac{\text{CFU sample} \times 100}{\text{CFU m. o. on abiotic support}}$$

where "CFU m.o. on abiotic support" is represented by the average number of CFU of the microorganism grown under the same conditions, without cells. The percentage of killing increase was then calculated as follows:

$$\%\ \text{of killing increase} = 100 - \frac{\%\ \text{of killing sample} \times 100}{\%\ \text{of killing of untreated cells}} - 100$$

where “% of killing of untreated cells” represents the basal killing activity of the untreated cells, infected with the pathogen.

2.5 Statistical analysis

The Shapiro-Wilk test was used to analyze data distribution within each experimental group. Subsequently, statistical analysis was performed by one-way ANOVA or the Kruskal Wallis test, depending on the distribution of data; Dunnett’smultiple comparisons or Dunn’s test respectively were chosen as post-hoc tests. For the kinetic curve obtained in the mtROS assessment procedures, the Area Under the Curve (AUC) was calculated to summarize the curve into a single value. Subsequently, statistical analysis was performed on the AUC values of each experimental group using one-way ANOVA. Don’t corrected test for multiple comparison was chosen as a post-hoc test. To analyze the data of the phagocytosis activity in terms of dose and infection time, a two-way ANOVA test, followed by Dunnett’s multiple comparisons, were used. All statistical analyses were carried out using GraphPad Prism 10 software. Values of * $p < 0.05$, ** $p < 0.01$ and **** $p < 0.0001$ were considered statistically significant.

3. RESULTS

3.1 Effect of BL on microorganisms

By employing the broth microdilution method, the direct effect of BL on fungi (*C. albicans* and *C. parapsilosis*) as well as on bacteria (*E. coli*, *L. crispatus* and *G. vaginalis*) was evaluated after 24 h and 48 h of incubation. The results show that BL did not impair the growth of any of the microorganisms, regardless of BL concentrations (0.16 mg/ml to 0.63 μg/ml), as shown in the charts of Supplementary Figure S1.

3.2 Effect of BL on A-431 and J774A.1 cells viability

In order to establish the lack of toxic effects of BL on the vaginal epithelial cell line A-431 and on the murine phagocytic cell line J774A.1, a cytofluorimetric analysis was carried out to quantify the percentage of live cells after the treatment with BL. As shown in Supplementary Figure S2, BL did not affect the viability of epithelial (Supplementary Figure S2A) and phagocytic (Supplementary Figure S2B) cell lines, regardless of its concentrations.

3.3 A-431 vaginal epithelial cells primed with BL increased mtROS production, reduced cell damage, impaired microbial growth and modulated cytokines and chemokines secretion in response to *C. albicans* infection

A-431 vaginal epithelial cells responded to *C. albicans* infection by increasing the mitochondrial activity as a defense mechanism against the fungus. Such an increase was achieved through the production of mitochondrial ROS (mtROS), whose level was much higher than that of the untreated cells. Interestingly, when the vaginal cells had been primed with BL prior to being infected by *C. albicans*, the mtROS production was significantly higher compared to vaginal cells that were not subjected to such pretreatment (Figure 1B). Representative microscopy images showed an increased production of mtROS in BL-primed cells after 30 min of *C. albicans* infection, as compared to *C. albicans* infected cells (Figure 1C). The production of higher levels of mtROS suggests that epithelial cells primed with BL could respond more efficiently to the fungal pathogen. Not only did BL treatment make A-431 cells more responsive against the pathogen, but it caused them to become also more resistant to the fungal-induced cell damage. Indeed, A-431 cells primed with BL prior to fungal infection, significantly reduced the levels of LDH release, a marker of cell damage, with respect to the control cells (Figure 1D). In addition, the effect of BL on A-431 cells caused indirect damage to

the fungus. Indeed, *C. albicans* recovered after the infection of BL-primed A-431 cells grew significantly less than *C. albicans* recovered from A-431 unprimed cells (Figure 1E). It is worth noting that such an effect could not be observed when A-431 cells were colonized with *L. crispatus*, a species considered beneficial for the vaginal tract. This *Lactobacillus* could grow efficiently after recovering from both BLprimed and un-primed A-431 cells (Figure 1F). Moreover, when primed with BL, infected A-431 cells significantly increased IL-8 secretion with respect to un-primed infected cells (Figure 1G). The secretion of IL-1α (Figure 1H) and IL-1β (Figure 1I) in primed infected cells resulted slightly increased, but the levels of both these cytokines remained comparable to those of *C. albicans* un-primed infected cells. Finally, the assessment of TNF-α levels returns cytokine levels below the detection limit in response to *C. albicans* infection, irrespective of the pretreatment with BL (data not shown).

3.4 J774A.1 murine macrophages primed with BL increased mtROS production, phagocytosis activity and killing capacity in response to *C. albicans* infection

As for the vaginal epithelial cell line, the J774A.1 murine macrophages responded to *C. albicans* infection by increasing the oxidative burst, which for this kind of cell is one of the main defense mechanisms against microbial pathogens. Similarly to the results observed for the vaginal epithelial cells, in the BL-primed and infected macrophages the levels of mtROS were significantly higher than in the un-primed *C. albicans* infected cells (Figures 2B). Representative microscopy images showed an increased production of mtROS in BL-primed cells after 30 min of *C. albicans* infection, as compared to *C. albicans* infected cells (Figure 2C). This result strongly suggests that BL has all the potential to improve macrophages' antimicrobial activity. Indeed, the priming with BL significantly increased the phagocytosis activity of J774A.1 of FITC labelled heat-inactivated (HK) *C. albicans* after 30 min (and even more after 60 min) of coculture (Figure 2D). In addition, the percentage of killing activity of J774A.1 cells against *C. albicans* was significantly higher when the macrophages were primed with BL, with respect to the un-primed cells (Figure 2E).

3.5 A-431 vaginal epithelial cells primed with BL reduced cell damage and modulated cytokines and chemokines secretion in response to bacterial infections

Similarly to what was observed in *C. albicans* infection, our results show a significant reduction of cell damage in the vaginal epithelial cells primed with BL and infected with *E. coli* (Figure 3A) or *G.*

vaginalis (Figure 3B). Following *E. coli* infection, a significant increase of IL-8 (Figure 4A) was observed in BL-primed cells. Differently, the levels of the inflammatory cytokine TNF-α were significantly reduced in BL-primed cells in response to *E. coli* infection, reaching levels similar to those secreted by the untreated cells (Figure 4B). Finally, the levels of IL-1α (Figure 4C) and IL-1β (Figure 4D) did not increase when the infected cells had been primed with BL, and the levels of both these cytokines remained comparable to those of *E. coli* infected unprimed cells. Upon A-431 cells infection with *G. vaginalis*, the levels of IL-8 (Figure 4E), IL-1α (Figure 4F), and IL-1β (Figure 4G) did not change, irrespective of the pretreatment or not with BL, even though a trend of increased IL-8 could be observed in BL-primed as compared to un-primed infected cells (Figure 4E). Differently from *E. coli*, TNF-α levels returns cytokine levels below the detection limit in response to *G. vaginalis* infection, irrespective of the pretreatment with BL (data not shown).

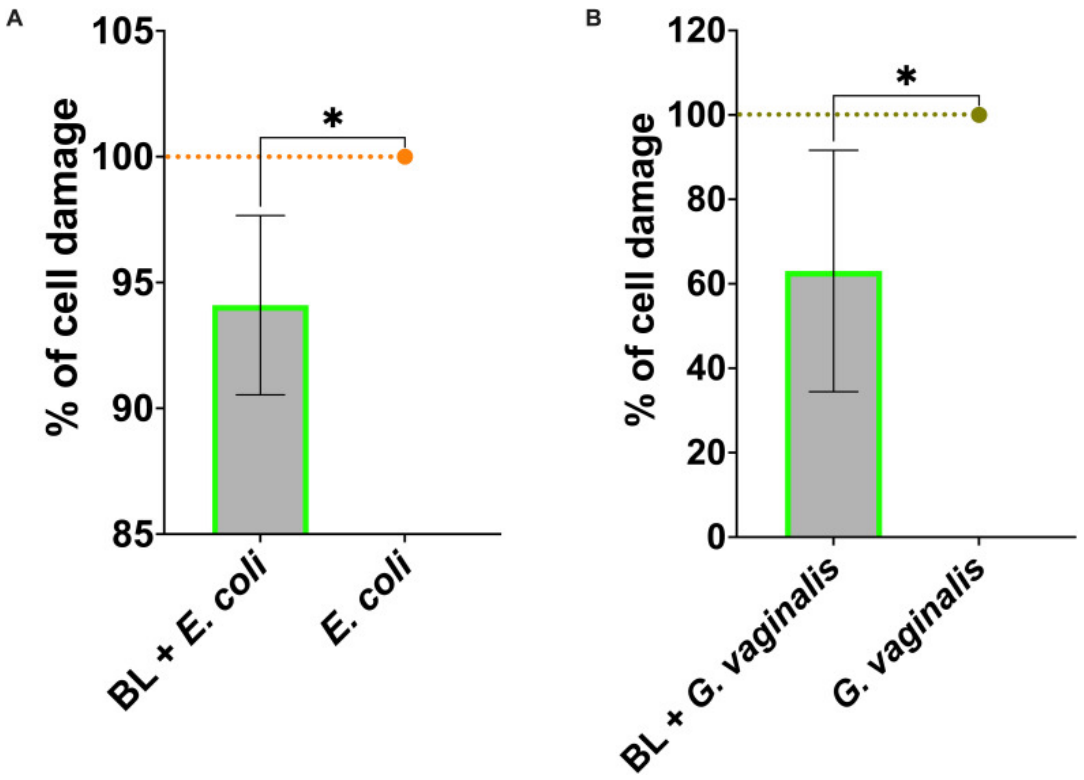

Figure 3
Effect of BL priming on A-431 cell damage induced by *E. coli* (**A**) and *G. vaginalis* (**B**). Percentage of cell damage of BL-primed (1 mg/ml) and infected A-431 cells. The data are expressed as the mean ± SD of at least 3 experiments. The values of $*p < 0.05$ were considered statistically significant.

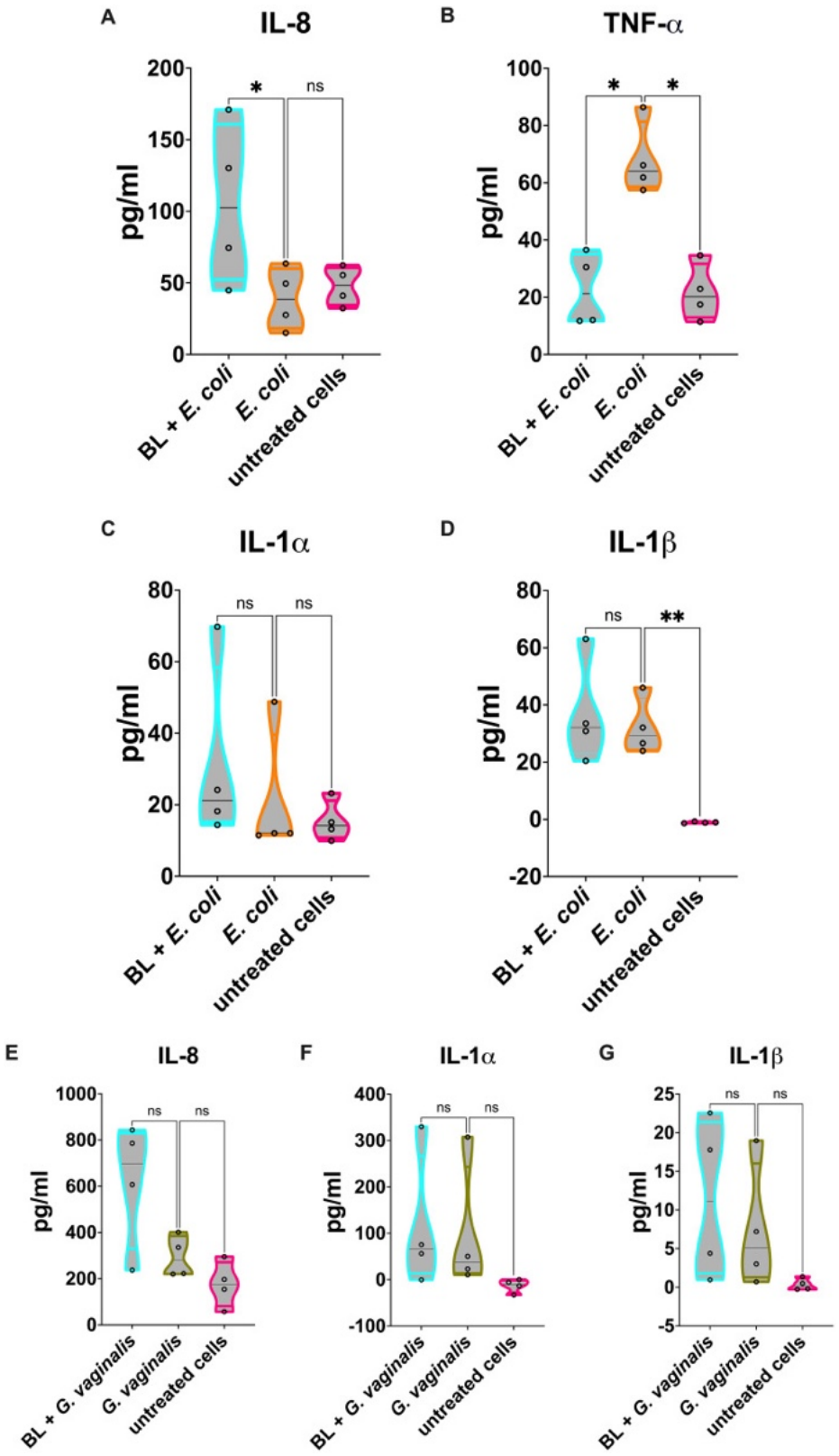

Figure 4

Cytokines and chemokines released by BL-primed A-431 cells infected with *E coli* or *G vaginalis*. (**A**-**D**) IL-8 (**A**), TNF-α (**B**), IL-1α (**C**) and IL-1β (**D**) production by *E. coli* infected A-431 cells primed or not with BL (10 mg/ml). (**E**-**G**) IL-8 (**E**), IL-1α (**F**) and IL-1β (**G**) production by *G. vaginalis* infected A-431 cells primed or not with BL (10 mg/ml). Each truncated violin results from 4 experiments. The values of $*p < 0.05$ and $**p < 0.01$ were considered statistically significant, ns, not significant.

3.6 J774A.1 cells primed with BL increased killing activity against *E. coli* and *G. vaginalis*

Similarly to what was observed for *C. albicans* infection, the killing activity of J774A.1 macrophages primed with BL was significantly increased against both *E. coli* (Figure 5A) and *G. vaginalis* (Figure 5B) as compared to un-primed infected cells.

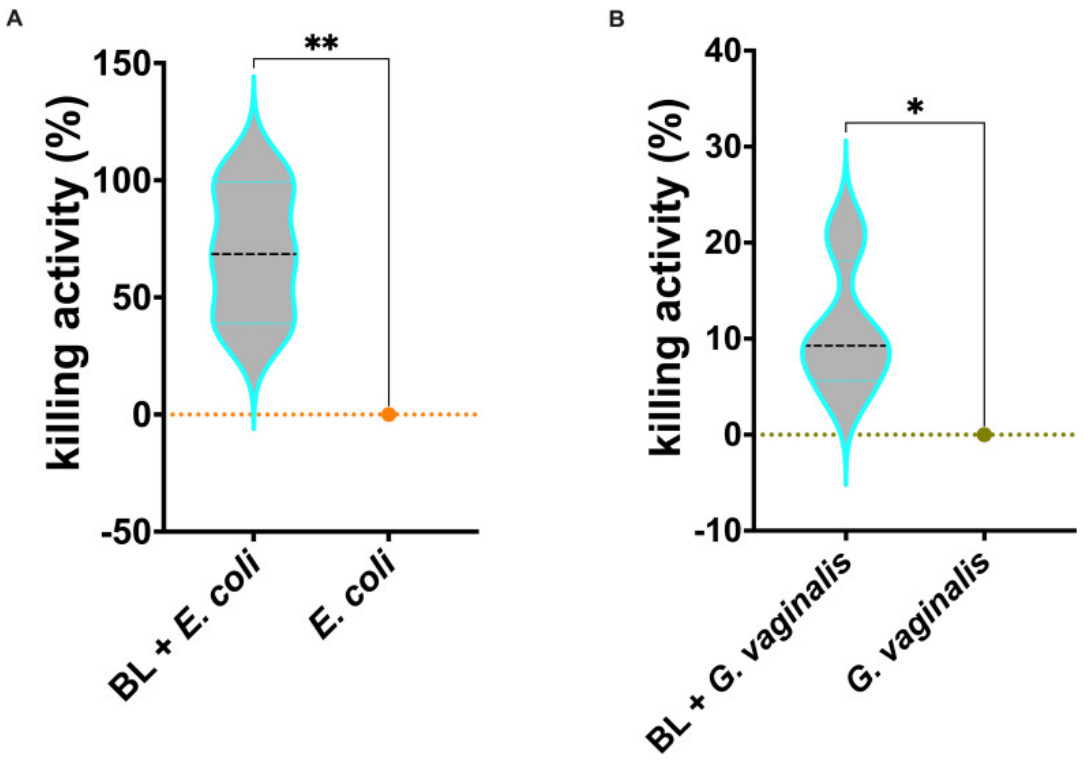

Figure 5
Effects of BL priming on J774A.1 cells infected with *E. coli* (**A**) or *G. vaginalis* (**B**). Percentage of BL-primed (10 µg/ml) J774A.1 killing activity against *E. coli* and *G. vaginalis*. Data result from at least 3 experiments conducted in duplicate. The values of $*p < 0.05$ and $**p < 0.01$ were considered statistically significant.

4. DISCUSSION

Candida albicans is a normal commensal of the human body. It dwells on the skin and on the mucosal surfaces of oro-pharynx, gastro-intestinal and female genital tract. When the immune system is compromised, *Candida* shifts from commensalism to opportunism, becoming a pathogen and causing disease. Interestingly, in the context of VVC the infection and disease are not necessarily associated with the immune system impairment; indeed, VVC frequently affects healthy women. However, some studies indicated increased susceptibility in specific categories, such as diabetics and immunocompromised women (Talaei et al., 2017; O'Laughlin and McCoy, 2023). Furthermore, it has been demonstrated that even though *Candida* causes damage *per se*, the host response plays an important role in VVC onset, by exacerbating the fungal-mediated damage and causing the symptoms, which include itching, burning, pain, redness of the vulva and vaginal mucosa and vaginal discharge (Ardizzoni et al., 2020, 2021).

Bacterial vaginosis (BV) is characterized by alterations in the vaginal environment and a shift in the vaginal microbiota from *Lactobacillus* species to a high bacterial diversity, including facultative anaerobes. *Gardnerella* spp. dwells in the vagina of patients with BV and it and it represents the key bacteria in the pathogenesis of BV (Salinas et al., 2020). Aerobic vaginitis (AV), has an incidence ranging from 2.0 to 25.8% (Donders et al., 2009), and the associated pathogenic microorganisms are mainly *Escherichia coli*, *Enterococcus* spp., *Streptococcus angina*, and *Streptococcus agalactiae*.

The treatment with antifungal drugs (the gold standard, to date) is accompanied by the risk of developing drug resistance. Similarly, in both BV and AV, the antimicrobial agents are widely used. However, resistance to these agents is the major cause of recurrent vaginitis. Therefore, the definition of novel therapeutic strategies is warranted as an alternative to the current pharmacological approach.

By using *in vitro* models of microbial infection, here we have evaluated the protective activity of the *C. acnes* bacterial lysate (BL) against the most common lower genital tract pathogens.

In order to establish whether BL acts by improving epithelial and innate immune cells response to the infections, without exerting a direct effect on vaginal microorganisms, we have performed experiments where bacteria and fungi have been incubated with a range of BL dilutions for 24 or 48 h. The lack of any effect demonstrates that BL at least in our *in vitro* system, does not exert any direct antimicrobial activity, thus suggesting that in an eventual therapeutic treatment it should not affect the resident microbiota. However, we assessed the effect of BL only on 5 microorganisms. A broader analysis covering more strains and species is warranted to support our results. Then, to exclude a possible toxic effect of BL, epithelial and phagocytic cell lines have been treated or not with BL at

different concentrations, and the percentage of alive cells has been assessed. The results demonstrate the absence of any toxicity of BL at least under our experimental conditions, thus suggesting that it might be well tolerated by human cells. Therefore, the response to the infections by BL-primed cells is very likely to occur mainly through mechanisms involving the improved reactivity of vaginal epithelial cells and macrophages against microbial pathogens. Among such responses, the increase of mtROS plays a crucial role in innate immunity (West et al., 2011). In line with this phenomenon, both our *in vitro* models (A-431 vaginal epithelial cells and J774A.1 macrophages) show an increase in mtROS production upon infection with *C. albicans* in BL-primed cells. In line with our recent results, demonstrating that mtROS is a key element of vaginal epithelial cells response to *C. albicans* (Spaggiari et al., 2024), the data reported here show that not only does the BL make the cells capable of responding better to an infectious insult, but it makes them also less prone to being damaged by fungal and bacterial pathogens. This is evident by the significantly lower levels of cell damage in BL-primed vaginal epithelial cells infected with *C. albicans*, *E. coli* and *G. vaginalis*. By strengthening the vaginal epithelial cells, BL also counteracts microbial growth, albeit indirectly. Indeed, *C. albicans* retrieved from BL-primed vaginal epithelial cells have grown significantly less than *C. albicans* retrieved from the un-primed cells. Interestingly, such effect has not been observed upon colonization with the beneficial microbe *L. crispatus*, thus strengthening the idea that BL "instructs" the vaginal epithelial cells to respond specifically only to harmful microorganisms.

The improvement of vaginal epithelial cells performance passes also through the modulation of cytokines and chemokines release in response to the infection. In particular, the BL-primed A-431 cells produce significantly higher levels of IL-8, upon infection with *C. albicans* and *E. coli* and increased (albeit not significant) levels of IL-8 upon infection with *G. vaginalis*. In addition, significantly lower levels of TNF-α following *E. coli* infection have been observed. IL-8 is a chemokine also known as "neutrophils chemotactic factor" because it induces chemotaxis in neutrophils and in other granulocytes, causing them to migrate to the site of infection. Notably, previous clinal studies demonstrate that the absence of leukocytes in most women with BV is likely due to the lack of IL-8 induction (Cauci et al., 2002, 2003; Cauci, 2004). Should this BLinduced enhancement of IL-8 secretion be demonstrated also *in vivo*, it would imply that this lysate could play an active role in the establishment of the innate immune response. TNF-α is a cytokine that plays a central role in the inflammatory responses, by inducing either survival or death in target cells. The levels of this cytokine are reported to increase in AV, but not in VVC (Hedges et al., 2006; Kalia et al., 2019). Consequently, upon *E. coli* infection of BL primed A-431 vaginal epithelial cells, the reduction of TNF-α suggests BL may have an immunomodulatory role, but more evidence is needed to directly link this to AV treatment.

The effect of BL cell priming has been assessed also on macrophages, which are typical cells involved in innate immune responses. As shown by the results presented here, the effects of BL on the phagocytic cells are not limited to the increase of mtROS. Indeed, BL-primed J774A.1 cells significantly improve their phagocytic activity against HK *C. albicans*. In addition, BL priming makes the macrophages more effective in their killing activity with respect to un-primed J774A.1, and such killing capacity has been shown to increase significantly against *C. albicans*, *E. coli* and *G. vaginalis*. These results strengthen our idea that BL-primed immune cells are more responsive to microbial pathogens. Overall, the results shown here point to the possible role of BL in priming epithelial and phagocytic cells to improve their response against bacterial and fungal pathogens. Such effects should be assessed also on other microorganisms or even viruses relevant for lower genital tract infections. These data indicate that the use of this (and, in future, other bacterial lysates) may provide a promising novel approach to handle lower genital tract infections through the reinforcement of local immunity. It should be pointed out that while *C. acnes* lysate (and possibly other microbial lysates) may be a promising novel approach for the management of lower genital tract infections, further *in vivo* and clinical studies are warranted to confirm its efficacy.

SUPPLEMENTARY MATERIAL

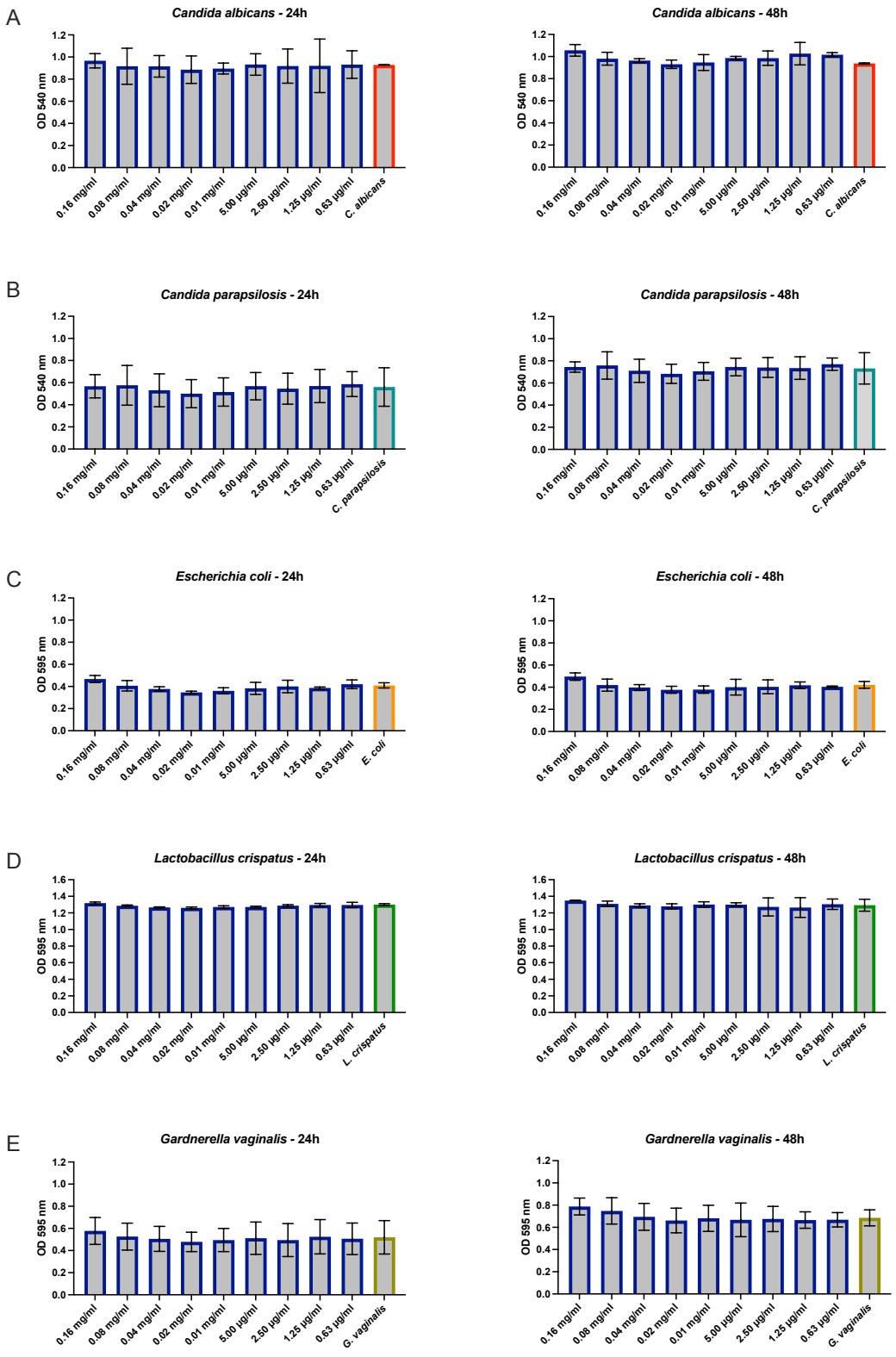

Figure S1. Effects of scalar doses of BL on microorganisms' viability. The effect of serially diluted BL (0.16 µg/ml to 0.63 µg/ml) on microorganisms' viability was assessed after 24 h (left panels) and 48 h (right panels) contact with *C. albicans* (**A**), *C. parapsilosis* (**B**), *E. coli* (**C**), *L. crispatus* (**D**) and *G. vaginalis* (**E**). Data are expressed as mean ± SD of 3 different experiments.

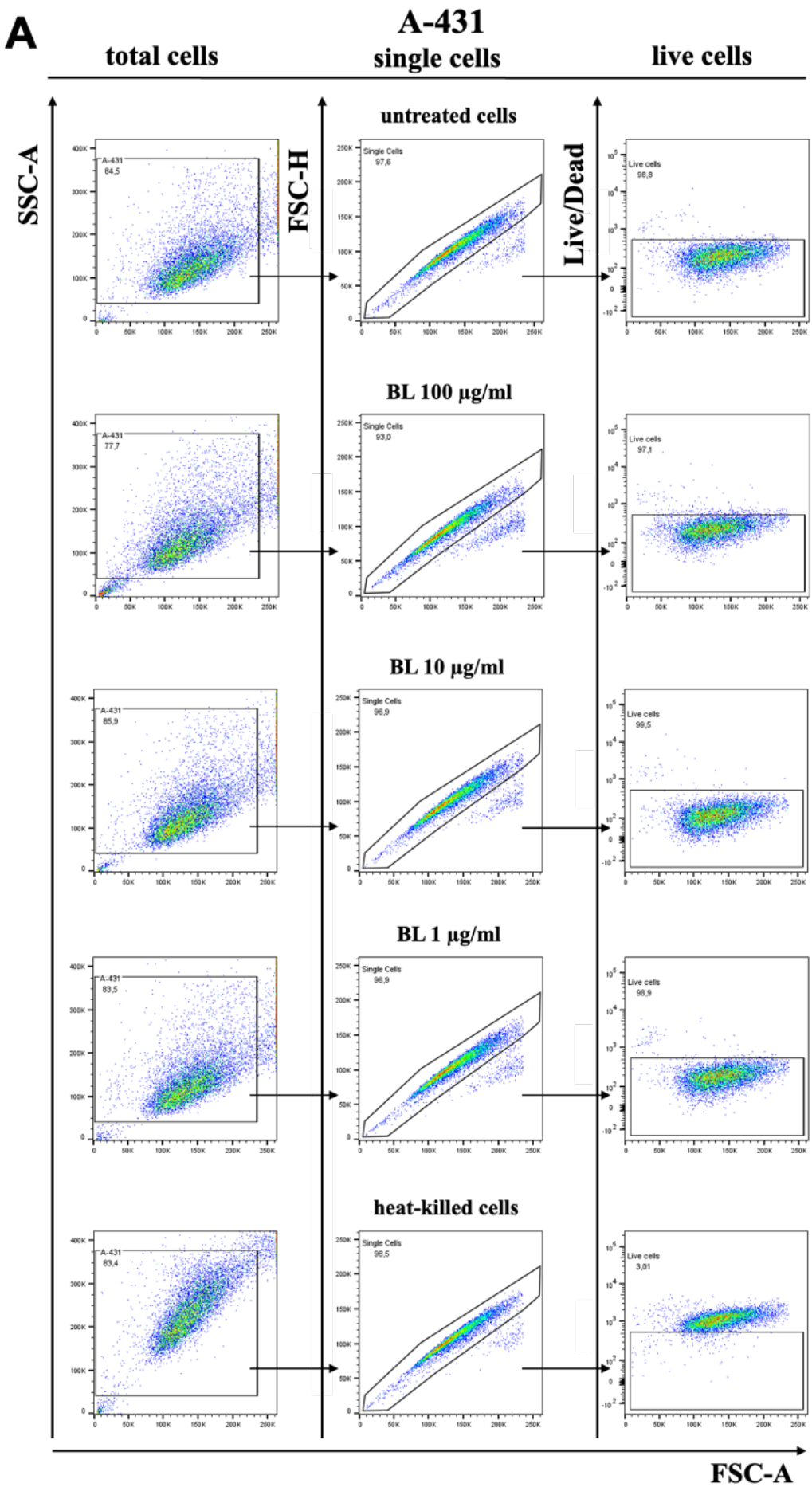
A
A-431
total cells
single cells
live cells
SSC-A
FSC-H
Live/Dead
FSC-A
untreated cells
A-431
84,5
Single Cells
97,6
Live cells
98,8
BL 100 µg/ml
A-431
77,7
Single Cells
93,0
Live cells
97,1
BL 10 µg/ml
A-431
85,9
Single Cells
96,9
Live cells
99,5
BL 1 µg/ml
A-431
83,5
Single Cells
96,9
Live cells
98,9
heat-killed cells
A-431
83,4
Single Cells
98,5
Live cells
3,01

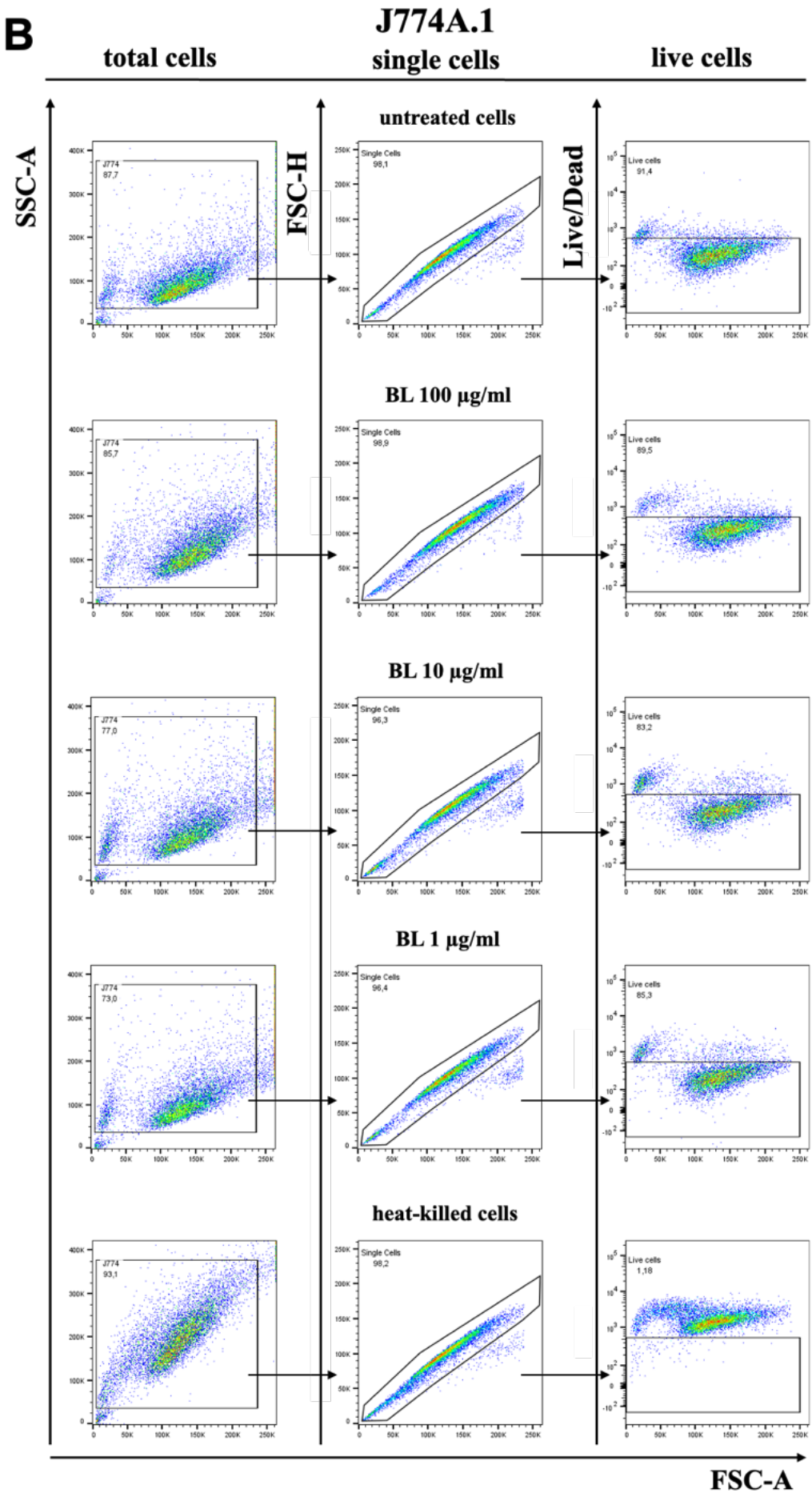
B
J774A.1
total cells
single cells
live cells
SSC-A
FSC-H
Live/Dead
FSC-A
untreated cells
J774
87,7
Single Cells
98,1
Live cells
91,4
BL 100 µg/ml
J774
85,7
Single Cells
98,9
Live cells
89,5
BL 10 µg/ml
J774
77,0
Single Cells
96,3
Live cells
83,2
BL 1 µg/ml
J774
73,0
Single Cells
96,4
Live cells
85,3
heat-killed cells
J774
93,1
Single Cells
98,2
Live cells
1,18

Figure S2. Effect of BL on cells viability.
Effect of serially diluted BL (100, 10 and 1 μg/ml) on the viability of A-431 cells (**A**) and J774A.1 macrophages (**B**) was assessed by cytofluorimetric analysis. Heat-killed cells were used as positive controls, whereas untreated cells were included as negative controls. Cytofluorimetric plots with the gating strategy are shown.

REFERENCES

Acevedo, O. A., Berrios, R. V., Rodrí guez-Guilarte, L., Lillo-Dapremont, B., and Kalergis, A. M. (2021). Molecular and cellular mechanisms modulating trained immunity by various cell types in response to pathogen encounter. Front. Immunol. 12. doi: 10.3389/fimmu.2021.745332

Ahumada-Cota, R. E., Hernandez-Chiñas, U., Milián-Suazo, F., Chávez-Berrocal, M. E., Navarro-Ocaña, A., Martí nez-Gómez, D., et al. (2020). Effect and analysis of bacterial lysates for the treatment of recurrent urinary tract infections in adults. Pathogens 9, 102. doi: 10.3390/pathogens9020102

Allhorn, M., Arve, S., Brüggemann, H., and Lood, R. (2016). A novel enzyme with antioxidant capacity produced by the ubiquitous skin colonizer Propionibacterium acnes. Sci. Rep. 6, 36412. doi: 10.1038/srep36412

Ardizzoni, A., Sala, A., Colombari, B., Giva, L. B., Cermelli, C., Peppoloni, S., et al. (2020). Perinuclear anti-neutrophil cytoplasmic antibodies (pANCA) impair neutrophil candidacidal activity and are increased in the cellular fraction of vaginal samples from women with vulvovaginal candidiasis. JoF 6, 225. doi: 10.3390/ jof6040225

Ardizzoni, A., Wheeler, R. T., and Pericolini, E. (2021). It takes two to tango: how a dysregulation of the innate immunity, coupled with candida virulence, triggers VVC onset. Front. Microbiol. 12. doi: 10.3389/fmicb.2021.692491

Basal, E., Jain, A., and Kaushal, G. P. (2004). Antibody response to crude cell lysate of propionibacterium acnes and induction of pro-inflammatory cytokines in patients with acne and normal healthy subjects. J. Microbiol. 42, 117–125

Bekkering, S., Quintin, J., Joosten, L. A. B., van der Meer, J. W. M., Netea, M. G., and Riksen, N.P. (2014). Oxidizedlow-density lipoprotein induces long-term proinflammatory cytokine production and foam cell formation via epigenetic reprogramming of monocytes. ATVB 34, 1731–1738. doi: 10.1161/ATVBAHA. 114.303887

Bigot, J., Guillot, L., Guitard, J., Ruffin, M., Corvol, H., Chignard, M., et al. (2020). Respiratory epithelial cells can remember infection: A proof of concept study. J. Infect. Dis. 221 (6), 1000–1005. doi: 10.1093/infdis/jiz569

Bizzini, B., Henocq, E., Reynier, J., and Relyveld, E. H. (1984). Experimental and clinical results with the Corynebacterium granulosum-derived immunomodulator P40. Asian Pac. J. Allergy Immunol. 2, 144–153.

Blostein, F., Levin-Sparenberg, E., Wagner, J., and Foxman, B. (2017). Recurrent vulvovaginal candidiasis. Ann. Epidemiol. 27, 575–582.e3. doi: 10.1016/j.annepidem. 2017.08.010 Braido, F., Tarantini, F., Ghiglione, V., Melioli, G., and Canonica, G. W. (2007). Bacterial lysate in the prevention of acute exacerbation of COPD and in respiratory recurrent infections. Int. J. Chron. Obstruct. Pulmon. Dis. 2, 335–345.

Brotman, R. M. (2011). Vaginal microbiome and sexually transmitted infections: an epidemiologic perspective. J. Clin. Invest. 121, 4610–4617. doi: 10.1172/JCI57172 Cauci, S. (2004). Vaginal immunity in bacterial vaginosis. Curr. Infect. Dis. Rep. 6, 450–456. doi: 10.1007/s11908-004-0064-8

Cauci, S., Guaschino, S., De Aloysio, D., Driussi, S., De Santo, D., Penacchioni, P., et al. (2003). Interrelationships of interleukin-8 with interleukin-1beta and neutrophils in vaginal fluid of healthy and bacterial vaginosis positive women. Mol. Hum. Reprod. 9, 53–58. doi: 10.1093/molehr/gag003

Cauci, S., Guaschino, S., Driussi, S., De Santo, D., Lanzafame, P., and Quadrifoglio, F. (2002). Correlation of local interleukin-8 with immunoglobulin A against Gardnerella vaginalis hemolysin and with prolidase and sialidase levels in women with bacterial vaginosis. J. Infect. Dis. 185, 1614–1620. doi: 10.1086/340417

Chalifour, A., Jeannin, P., Gauchat, J.-F., Blaecke, A., Malissard, M., N'Guyen, T., et al. (2004). Direct bacterial protein PAMP recognition by human NK cells involves TLRs and triggers a-defensin production. Blood 104, 1778–1783. doi: 10.1182/blood2003-08-2820

Chao, X.-P., Sun, T.-T., Wang, S., Fan, Q.-B., Shi, H.H., Zhu, L., et al. (2019). Correlation between the diversity of vaginal microbiota and the risk of high-risk human papillomavirus infection. Int. J. Gynecol. Cancer 29, 28–34. doi: 10.1136/ijgc-2018-000032

Chen, X., Lu, Y., Chen, T., and Li, R. (2021). The female vaginal microbiome in health and bacterial vaginosis. Front. Cell. Infect. Microbiol. 11. doi: 10.3389/ fcimb.2021.631972 Covián, C., Fernández-Fierro, A., Retamal-Dí az, A., Dí az, F. E., Vasquez, A. E., Lay, M. K., et al. (2019). BCG-induced cross-protection and development of trained immunity: implication for vaccine design. Front. Immunol. 10. doi: 10.3389/ fimmu.2019.02806

Covián, C., Rí os, M., Berrí os-Rojas, R. V., Bueno, S. M., and Kalergis, A. M. (2021). Induction of trained immunity by recombinant vaccines. Front. Immunol. 11. doi: 10.3389/fimmu.2020.611946

Denning, D. W., Kneale, M., Sobel, J. D., and Rautemaa-Richardson, R. (2018). Global burden of recurrent vulvovaginal candidiasis: a systematic review. Lancet Infect. Dis. 18, e339–e347. doi: 10.1016/S1473-3099(18)30103-8

Donders, G. G. G., Bellen, G., Grinceviciene, S., Ruban, K., and Vieira-Baptista, P. (2017). Aerobic vaginitis: no longer a stranger. Res. Microbiol. 168, 845–858. doi: 10.1016/j.resmic.2017.04.004

Donders, G., Bellen, G., and Rezeberga, D. (2011). Aerobic vaginitis in pregnancy: Aerobic vaginitis in pregnancy. BJOG: Int. J. Obstet. Gynecol.118, 1163–1170. doi: 10.1111/j.1471-0528.2011.03020.x

Donders, G., Van Calsteren, K., Bellen, G., Reybrouck, R., Van Den Bosch, T., Riphagen, I., et al. (2009). Predictive value for preterm birth of abnormal vaginal flora, bacterial vaginosis and aerobic vaginitis during the first trimester of pregnancy. BJOG 116, 1315–1324. doi: 10.1111/j.1471-0528.2009.02237.x

Donders, G. G. G., Vereecken, A., Bosmans, E., Dekeersmaecker, A., Salembier, G., and Spitz, B. (2002). Definition of a type of abnormal vaginal flora that is distinct from bacterial vaginosis: aerobic vaginitis. BJOG 109, 34–43. doi: 10.1111/j.14710528.2002.00432.x Fan, C., Dai, Y., Zhang, L., Rui, C., Wang, X., Luan, T., et al. (2021). Aerobic vaginitis induced by escherichia coli infection during pregnancy can result in adverse pregnancy outcomes through the IL-4/JAK-1/STAT-6 pathway. Front. Microbiol. 12. doi: 10.3389/ fmicb.2021.651426

Gaziano, R., Sabbatini, S., Roselletti, E., Perito, S., and Monari, C. (2020). Saccharomyces cerevisiae-based probiotics as novel antimicrobial agents to prevent and treat vaginal infections. Front. Microbiol. 11. doi: 10.3389/fmicb.2020.00718

Guerra, B., Ghi, T., Quarta, S., Morselli-Labate, A. M., Lazzarotto, T., Pilu, G., et al. (2006). Pregnancy outcome after early detection of bacterial vaginosis. Eur. J. Obstet. Gynecol. Reprod. Biol. 128, 40–45. doi: 10.1016/j.ejogrb.2005.12.024

Hedges, S. R., Barrientes, F., Desmond, R. A., and Schwebke, J. R. (2006). Local and systemic cytokine levels in relation to changes in vaginal flora. J. Infect. Dis. 193, 556562. doi: 10.1086/499824

Ilhan, Z. E., Łaniewski, P., Thomas, N., Roe, D. J., Chase, D. M., and HerbstKralovetz, M. M. (2019). Deciphering the complex interplay between microbiota, HPV, inflammation and cancer through cervicovaginal metabolic profiling. eBioMedicine 44, 675–690. doi: 10.1016/j.ebiom.2019.04.028

Jacobsson, B., Pernevi, P., Chidekel, L., and Jörgen-Platz-Christensen, J. (2002). Bacterial vaginosis in early pregnancy may predispose for preterm birth and postpartum endometritis. Acta Obstet. Gynecol. Scand. 81, 1006–1010. doi: 10.1034/ j.1600-0412.2002.811103.x

Jurkiewicz, D., and Zielnik-Jurkiewicz, B. (2018). Bacterial lysates in the prevention of respiratory tract infections. Otolaryngol. Pol. 72, 1–8. doi: 10.5604/01.3001.0012.7216

Kaambo, E., Africa, C., Chambuso, R., and Passmore, J.-A. S. (2018). Vaginal microbiomes associated with aerobic vaginitis and bacterial vaginosis. Front. Public Health 6. doi: 10.3389/fpubh.2018.00078

Kalia, N., Singh, J., and Kaur, M. (2019). Immunopathology of recurrent vulvovaginal infections: new aspects and research directions. Front. Immunol. 10. doi: 10.3389/fimmu.2019.02034

Kauffman, C. A. (2006). Fungal infections. Proc. Am. Thorac. Soc. 3, 35–40. doi: 10.1513/pats.200510-110JH

Kaufmann, E., Sanz, J., Dunn, J. L., Khan, N., Mendonça, L. E., Pacis, A., et al. (2018). BCG educates hematopoietic stem cells to generate protective innate immunity against tuberculosis. Cell 172, 176–190.e19. doi: 10.1016/j.cell.2017.12.031

Kavoussi, S. K., Pearlman, M.D., Burke, W.M., and Lebovic, D.I. (2006). Endometrioma complicated by tubo-ovarian abscess in a woman with bacterial vaginosis. Infect. Dis. Obstet. Gynecol. 2006, 084140. doi: 10.1155/IDOG/2006/84140

Leitich, H., Bodner-Adler, B., Brunbauer, M., Kaider, A., Egarter, C., and Husslein, P. (2003). Bacterial vaginosis as a risk factor for preterm delivery: A meta-analysis. Am. J. Obstet. Gynecol. 189, 139–147. doi: 10.1067/mob.2003.339

Liu, G.-Y., Liu, Y., Lu, Y., Qin, Y.-R., Di, G.-H., Lei, Y.-H., et al. (2016). Short-term memory of danger signals or environmental stimuli in mesenchymal stem cells: implications for therapeutic potential. Cell Mol. Immunol. 13, 369–378. doi: 10.1038/ cmi.2015.11

Ma, X., Wu, M., Wang, C., Li, H., Fan, A., Wang, Y., et al. (2022). The pathogenesis of prevalent aerobic bacteria in aerobic vaginitis and adverse pregnancy outcomes: a narrative review. Reprod. Health 19, 21. doi: 10.1186/s12978-021-01292-8

Mangano, K., Vergalito, F., Mammana, S., Mariano, A., De Pasquale, R., Meloscia, A., et al. (2017). Evaluation of hyaluronic acid-P40 conjugated cream in a mouse model of dermatitis induced by oxazolone. Exp. Ther. Med. 14, 2439–2444. doi: 10.3892/ etm.2017.4810

Mohankumar, B., Shandil, R. K., Narayanan, S., and Krishnan, U. M. (2022). Vaginosis: Advances in new therapeutic development and microbiome restoration. Microbial. Pathogen. 168, 105606. doi: 10.1016/j.micpath.2022.105606

Netea, M. G., Joosten, L. A. B., Latz, E., Mills, K. H. G., Natoli, G., Stunnenberg, H. G., et al. (2016). Trained immunity: A program of innate immune memory in health and disease. Science 352, aaf1098. doi: 10.1126/science.aaf1098

Niu, X.-X., Li, T., Zhang, X., Wang, S.-X., and Liu, Z.-H. (2017). Lactobacillus crispatus Modulates Vaginal Epithelial Cell Innate Response to Candida albicans. Chin. Med. J. 130, 273–279. doi: 10.4103/0366-6999.198927

O'Laughlin, D. J., and McCoy, R. G. (2023). Diabetes and vulvovaginal conditions. Clin. Diabetes 41, 458–464. doi: 10.2337/cd23-0011

Odds, F. C. (1987). Candida infections: an overview. Crit. Rev. Microbiol. 15, 1–5. doi: 10.3109/10408418709104444

Ohashi, M., Amagai, T., Ushijima, T., Imanishi, J., Kishida, T., and Ozaki, Y. (1983). Mode of protection of mice against herpes simplex virus type 2 infection by propionibacterium. Microbiol. Immunol. 27, 601–609. doi: 10.1111/j.13480421.1983.tb00621.x

Pappas, P. G. (2006). Invasive candidiasis. Infect. Dis. Clin. North Am. 20, 485–506. doi: 10.1016/j.idc.2006.07.004 Pfaller, M. A., and Diekema, D. J. (2007). Epidemiology of invasive

candidiasis: a persistent public health problem. Clin. Microbiol. Rev. 20, 133–163. doi: 10.1128/ CMR.00029-06

Pfefferle, P. I., Prescott, S. L., and Kopp, M. (2013). Microbial influence on tolerance and opportunities for intervention with prebiotics/probiotics and bacterial lysates. J. Allergy Clin. Immunol. 131, 1453–1463. doi: 10.1016/j.jaci.2013.03.020

Plisko, O., Zodzika, J., Jermakova, I., Pcolkina, K., Prusakevica, A., Liepniece-Karele, I., et al. (2021). Aerobic vaginitis—Underestimated risk factor for cervical intraepithelial neoplasia. Diagnostics 11, 97. doi: 10.3390/diagnostics11010097

Rahman, N., Mian, M. F., Hayes, C. L., Nazli, A., and Kaushic, C. (2024). G. vaginalis increases HSV-2 infection by decreasing vaginal barrier integrity and increasing inflammation in vivo. Front. Immunol. 15. doi: 10.3389/fimmu.2024.1487726

Ravel, J., Gajer, P., Abdo, Z., Schneider, G. M., Koenig, S. S. K., McCulle, S. L., et al. (2011). Vaginal microbiome of reproductive-age women. Proc. Natl. Acad. Sci. U.S.A. 108, 4680–4687. doi: 10.1073/pnas.1002611107

Rothman, K. J., Funch, D. P., Alfredson, T., Brady, J., and Dreyer, N. A. (2003). Randomized field trial of vaginal douching, pelvic inflammatory disease and pregnancy. Epidemiology 14, 340–348. doi: 10.1097/01.EDE.0000059230.67557.D3

Salinas, A. M., Osorio, V. G., Pacha-Herrera, D., Vivanco, J. S., Trueba, A. F., and MaChado, A. (2020). Vaginal microbiota evaluation and prevalence of key pathogens in Ecuadorian women: an epidemiologic analysis. Sci. Rep. 10, 18358. doi: 10.1038/ s41598-020-74655-z

Spaggiari, L., Ardizzoni, A., Ricchi, F., Pedretti, N., Squartini Ramos, C. A., Squartini Ramos, G. B., et al. (2024). Fungal burden, dimorphic transition and candidalysin: Role in Candida albicans-induced vaginal cell damage and mitochondrial activation in vitro. PloS One 19, e0303449. doi: 10.1371/journal.pone.0303449

Spaggiari, L., Squartini Ramos, G. B., Squartini Ramos, C. A., Ardizzoni, A., Pedretti, N., Blasi, E., et al. (2023). Anti-candida and anti-inflammatory properties of a vaginal gel formulation: novel data concerning vaginal infection and dysbiosis. Microorganisms 11, 1551. doi: 10.3390/microorganisms11061551

Srinivasan, S., and Fredricks, D. N. (2008). The human vaginal bacterial biota and bacterial vaginosis. Interdiscip. Perspect. Infect. Dis. 1–22. doi: 10.1155/2008/750479

Talaei, Z., Sheikhbahaei, S., Ostadi, V., Ganjalikhani Hakemi, M., Meidani, M., Naghshineh, E., et al. (2017). Recurrent vulvovaginal candidiasis: could it be related to cell-mediated immunity defect in response to candida antigen? Int. J. Fertil. Steril. 11, 134–141. doi: 10.22074/ijfs.2017.4883

Triantafillou, V., Workman, A. D., Patel, N. N., Maina, I. W., Tong, C. C. L., Kuan, E. C., et al. (2019). Broncho-Vaxom® (OM-85 BV) soluble components stimulate sinonasal innate immunity. Int. Forum Allergy Rhinol. 9, 370–377. doi: 10.1002/alr.22276

Turovskiy, Y., Sutyak Noll, K., and Chikindas, M. L. (2011). The etiology of bacterial vaginosis: Aetiology of bacterial vaginosis. J. Appl. Microbiol. 110, 1105–1128. doi: 10.1111/j.1365-2672.2011.04977.x

West, A. P., Shadel, G. S., and Ghosh, S. (2011). Mitochondria in innate immune responses. Nat. Rev. Immunol. 11, 389–402. doi: 10.1038/nri2975

Yang, F., Qin, X., Zhang, T., Lin, H., and Zhang, C. (2019). Evaluation of small molecular polypeptides from the mantle of pinctada martensii on promoting skin wound healing in mice. Molecules 24, 4231. doi: 10.3390/molecules24234231

Zhang, Z., Li, T., Zhang, D., Zong, X., Bai, H., Bi, H., et al. (2021). Distinction between vaginal and cervical microbiota in high-risk human papilloma virus-infected women in China. BMC Microbiol. 21, 90. doi: 10.1186/s12866-021-02152-y

Zhang, X., and Mosser, D. (2008). Macrophage activation by endogenous danger signals. J. Pathol. 214, 161–178. doi: 10.1002/path.2284

CHAPTER 2

Candida albicans as a Trailblazer for Herpes Simplex Virus-2 Infection Against an *In Vitro* Reconstituted Human Vaginal Epithelium

Francesco Ricchi[1], Stefania Caramaschi[1,2], Arianna Sala[3], Laura Franceschini[4], Luca Fabbiani[2], Andrea Ardizzoni[5], Elisabetta Blasi[5] and Claudio Cermelli[5]

[1] Clinical and Experimental Medicine Ph.D. Program, Department of Biomedical, Metabolic, and Neural Sciences, University of Modena and Reggio Emilia, 41125 Modena, Italy;

[2] Pathology Unit, Department of Medical and Surgical Sciences for Children and Adults, University of Modena and Reggio Emilia, 41125 Modena, Italy;

[3] Molecular Microbiology and Virology Unit, University Hospital Policlinico, 41124 Modena, Italy;

[4] Department of Biomedical, Metabolic, and Neural Sciences, University of Modena and Reggio Emilia, 41125 Modena, Italy;

[5] Department of Surgery, Dentistry, Morphological Sciences Related to Transplant, Oncology and Regenerative Medicine, University of Modena and Reggio Emilia, 41125 Modena, Italy.

***Microorganisms*. 2025, doi:10.3390/microorganisms13040905**

1. INTRODUCTION

Genital infections represent a significant public health concern worldwide. Among them, Herpes Simplex Virus-Type 2 (HSV-2) and *Candida albicans* are two of the most prevalent pathogens. HSV-2 primarily causes genital herpes, while *C. albicans* is the leading cause of vulvovaginal candidiasis (Workowski et al., 2021; NyirjesY et al., 2022). Genital herpes is characterized by painful vesicular lesions in the genital region, although infections can be asymptomatic, leading to an underestimation of their prevalence. The virus establishes latency in the sacral ganglia and can be reactivated due to various triggers, including stress, immunosuppression, and co-infections (Omarova et al., 2022). HSV-2 infection is endemic globally, with estimates indicating that approximately 12% of the population aged 15–49 years is seropositive for HSV-2 (Looker et al., 2012). This prevalence varies with demographic factors, including age, sex, and geographical location (Gupta et al., 2007). *C. albicans* is a commensal fungus found in various body sites, including the gastrointestinal tract, mouth, and vagina. Overgrowth of this fungus leads to candidiasis; substantial clinical manifestations depend on the site of infection and on the host's condition (Lopes et al., 2022). Common presentations include vulvovaginal candidiasis, oropharyngeal candidiasis (thrush), and deep-seated/invasive candidiasis in immunocompromised individuals. Symptoms of vulvovaginal candidiasis include itching, burning, and a thick, white discharge, which may overlap, at least partly, with the initial symptoms of HSV-2 infection (Gaziano et al., 2023). The incidence of vulvovaginal candidiasis is estimated to be around 75% in women during their lifetime, with recurrent infections affecting approximately 20–25% of these women (Farr et al., 2021).

Coinfections are an increasingly recognized phenomenon, particularly in patients with weakened immune systems, resulting in severe and difficult-to-treat diseases (Frisan T.,2021). Some studies have shown that the presence of a primary infectious agent can predispose the host to a second infection, likely also implying pathogen-to-pathogen synergistic interplay (Murray et al., 2014; Higgins et al., 2022). Among various combinations of genital dual infections, *C. albicans* species and HSV-2 are noteworthy due to their overlapping risk factors and shared propensity to exploit host immunosuppression. Increasing data indicate that HSV-2 may enhance fungal colonization by affecting the integrity of the mucosal barrier and immune responses, as well as the host's microbiome. As an example, HSV-2-induced epithelial disruption facilitates fungal adhesion and invasion, increasing susceptibility to secondary infections (Panasiti et al., 2007; Plotkin et al., 2020). Moreover, cytokines produced during HSV-2 infection may also enhance *C. albicans* virulence, suggesting a complex interplay between the immune response elicited by HSV-2 and *C. albicans* pathogenic potential (Jayaraman et al., 2020).

Although poorly investigated, genital co-infection with HSV-2 and *C. albicans* is emerging as an important area of interest. Co-infection, occurring especially among patients with repeated episodes of genital herpes, may lead to more severe symptoms and complications, necessitating attentive management strategies, simultaneously tailored towards both HSV-2 and *C. albicans* (Kaul et al., 2007; Suazo et al., 2015). Antiviral therapy for HSV-2 and antifungal treatment for *C. albicans* should be considered concurrently, emphasizing the importance of integrated care and differential diagnoses. Additionally, the psychological impact of recurrent HSV-2 episodes can lead to increased stress and immunosuppression, further predisposing individuals to candidiasis (Fichorova et al., 2020). Therefore, increased knowledge is needed on the interplay between these two pathogens to improve prompt and complete diagnosis and tailored treatment and, in turn, ameliorate patient management. Further research is imperative to elucidate the mechanisms behind their interactions, potentially leading to improved therapeutic strategies and patient outcomes.

Most pathogens enter the human body through mucosal barriers, which represent the first environment to be breached prior to establishing a successful infection (Biswas et al., 2024). Animal models have greatly improved our understanding of the initial steps of microbial pathogenesis; however, numerous limitations occur when assessing mucosal infections, given the complexity of the microenvironment and the multiplicity of cross-talks among different pathogens and hosts (Schaller et al., 2006). Here, we report an *in vitro* model of human epithelial cell line differentiated into a reconstituted multilayered epithelium, using which we evaluated susceptibility to single or dual infection by HSV-2 and *C. albicans*, virus vs. fungus growth, cell damage, secretion profile, and oxidative stress.

2. MATERIALS AND METHODS

2.1 Epithelial cells

All the experiments were carried out on the A-431 cell line, from a human epidermoid skin carcinoma (ATCC CLR-1555); such a cell line has been widely used to produce monolayers or multilayers mimicking the physiological epithelium (Schaller et al., 2006; Giard et al., 1973). The cells were cultured in DMEM (Sial S.r.l., Rome, Italy) supplemented with L-glutamine (2 mM) (Gibco, Thermo Fisher Scientific Italia, Segrate, Italy), 100 U/mL Penicillin–Streptomycin (Lonza Walkersville Inc., Walkersville, MD, USA), ciprofloxacin (2.5 mg/mL) (Gibco, Fisher Scientific Italia, Segrate, Italy), and heat-inactivated fetal bovine serum (Sial S.r.l., Rome, Italy) at 10% (growth medium, used at cell seeding) or 5% (maintenance medium, used after 5 days of cell growth, during the experimental procedures). The cell line was kept viable by subculturing twice a week and incubation at 37 °C with 5% CO_2. The cells were used between the 30th and the 40th sub-culture passage.

2.2 Fungal Strain and Growth Conditions

The reference strain *C. albicans* SC5314 (ATCC MYA-2876) was employed. The fungal strain was stored as frozen stocks at −80 °C in Sabouraud Dextrose Broth (Condalab, Madrid, Spain) supplemented with 15% glycerol. After thawing, the fungal cells were grown in a liquid YPD medium (Scharlab S.L., Barcelona, Spain) and incubated at 37 °C under aerobic conditions for 24 h. Fungal cultures in the exponential growth phase were used in each experiment.

2.3 HSV-2 Strain

A clinical isolate of HSV-2, initially identified by a monoclonal antibody and laboratory adapted through serial passages (>50) on Vero cells, was used. The viral suspensions used in the experiments were obtained upon the centrifugation of lysates of virus-infected Vero cells, which had been cultured for 2–3 days and showed a diffused cytopathic effect (more than 80% of monolayer destruction), as detailed elsewhere (Sala et al., 2024). Prior to being used, the virus batches were titrated on A-431 cells, aliquoted, and kept frozen at −80 °C; all the experiments were carried out using the same batch.

2.4 Establishment of A-431 Monolayer Cultures and Reconstituted Epithelium (RVE)

Cells were organized as monolayers or as reconstituted vaginal epithelium multilayers, with cultures initially seeded at 4×10^5 cells/mL (1 mL per well) in 24-well plates (Corning, New York, NY, USA). For the epithelial monolayers, A-431 cells were incubated overnight at 37 °C with 5% CO_2, while, to obtain the RVE cultures, the A-431 cells were incubated for 5 days, with a fresh growth medium replacement at day 3.

2.5 Immunohistochemical (IHC) Staining for Cytokeratin 5/6 Detection

The monolayers and RVE cultures were processed for immunohistochemistry (IHC), with cells plated at 2×10^5 cells/mL (400 µL per well) in chamber slides, following the same seeding and incubation protocol as used for the 24-well plates. After 1 or 5 days (for the epithelial monolayer or RVE, respectively), the slides were fixed in 95% ethylic alcohol for 10 min. IHC staining for cytokeratin 5/6 (CK 5/6) was performed using the anticytokeratin 5/6 mouse monoclonal primary antibody, clone D5/16B4, at an approximate concentration of 10.4 µg/mL (Roche Diagnostics-Ventana Medical Systems, Tucson, AZ, USA). Staining procedures were conducted using BenchMark IHC/ISH automated instruments (Ventana Medical Systems, Tucson, AZ, USA) according to standard antigen retrieval protocol. Antibody reactivity was visualized using a Ventana OptiView Universal DAB IHC Detection Kit and 3,3′-diaminobenzidine (DAB) chromogen (Roche Diagnostics—Ventana Medical Systems, Tucson, AZ, USA). Subsequently, the slides were counterstained with Hematoxylin II—a modified Mayer's hematoxylin (Roche Diagnostics—Ventana Medical Systems, Tucson, AZ, USA) to highlight cell morphology. Cells exhibiting membranous and/or cytoplasmic brown staining were considered positive for cytokeratin 5/6. Each well was scored as negative (<10% of positive cells), partially positive (10–80%), or diffuse expression (>80%). The intensity of staining was semi-quantitatively graded as weak (1), moderate (2), or strong (3).

2.6 Infection Protocol

The infection protocol included the use of the monolayers and the RVE cultures, replaced with fresh maintenance medium before the infection; in selected wells, synthetic vaginal fluid (SVF) was also added (10% vol/vol), according to the protocol of Owen et al. and Del Gaudio et al. (Owen et al., 1999; Del Gaudio et al., 2013). The SVF, intended to simulate human vaginal fluid, had the following formulation for 1 L of solution, given as a compound and its weight (g): calcium, 0.120; potassium, 0.978; sodium, 1.38; chloride, 2.13; albumin, 0.018; lactic acid, 2.00; acetic acid, 1.00; glycerol, 0.16; urea, 0.4; and glucose, 5.0. The final pH value was 4.2. Next, the cultures were infected with *C. albicans* (250 µL of fungal suspension/well), at a Multiplicity of Infection (MOI, fungal cells:epithelial cells) of 0.5:1; after a 3 h incubation at 37 °C, 250 µL of the HSV-2 suspension was added to a final MOI (virus: cells) of 0.1:1. The final working volume was 1 mL/well. Then, the cultures were incubated for a further 21 h at 37 °C prior to being assessed as detailed below.

2.7 Evaluation of Microorganisms-Induced Cell Damage by Quantification of LDH Release

Epithelial cell damage was quantified by analyzing the lactate dehydrogenase (LDH) release in the supernatant (Shekhawat et al., 2025); a commercially available kit (Roche, via Merk Life Science S.r.l., Milan, Italy) was employed, following the manufacturer's instructions. The percentage of damage was calculated as follows:

$$\%\ \text{of cell damage} = \frac{\text{test sample} - \text{low control}}{\text{high control} - \text{low control}} \times 100$$

where test sample is the O.D. value of the sample, low control is the mean value of uninfected cells, and high control is the mean value of uninfected cells lysed with 1% (vol/vol) Triton X-100 (Fluka Chemicals, via Merk Life Science S.r.l., Milan, Italy) (Sala et al., 2023). In selected experiments, the LDH assay was compared with the MTT assay (see Supplementary Material).

2.8 Pathogen Growth Quantification

C. albicans quantification on the epithelial cells was assessed using the CFU assay. At 24 h, cells were lysed with Triton X-100 (a final concentration of 0.1%), and serial dilutions from each well were performed and then seeded on Sabouraud agar plates, which were further incubated for 24 h at 37 °C. The resulting CFUs were counted. Each sample was assessed in triplicate.

For HSV-2 load quantification, a commercial Real Time-PCR was used (Elite InGEnius SP200, Elitech, Torino, Italy) after DNA extraction by means of a commercial kit (HSV2 ELITe MGB® Kit, Elitech, Torino, Italy), according to the manufacturer's instructions. The PRC protocol was as follows: decontamination at 50 °C/2 min, initial denaturation at 94 °C/2 min, and then at 94 °C/10 s, 60 °C/30 s, and 72 °C/20 s for 45 cycles.

In selected experiments, the results of the molecular assay were compared with those obtained by a plaque reduction assay, performed as previously described (Sala et al., 2024). The rate of HSV-2-infected RVE cells was also checked with an indirect immunofluorescence assay using a monoclonal antibody against a HSV-2 capsid antigen (Merck Millipore, Milan, Italy), and a representative image is presented in the Supplementary Materials Section.

2.9 Oxidative Stress Determination

The production of mitochondrial reactive oxygen species (mtROS) by epithelial cells, infected as detailed above, was measured at time 24 h. MitoSOX™ Red (2.5 μM/well) (Invitrogen™, Fisher Scientific Italia, Segrate, Italy) was added to each well immediately after infection. Then, the plates were evaluated using Fluoroskan (Thermo Scientific, Segrate, Italy) at 37 °C, for 24 h; the fluorescence emission was analyzed at an excitation/emission length of 544/590. The results at 24 h were depicted as a heatamp.

2.10 Quantification of IL-1α, IL-1β, IL-8 and Mucin-1 Production

The levels of IL-1α, IL-1β, IL-8, and mucin-1 were measured in 100 μL of A-431 cell-free supernatants at 24 h, using specific commercially available ELISA kits (PeproTech™, Fisher Scientific Italia, Segrate, Italy for IL-1α; Invitrogen™, Fisher Scientific Italia, Segrate, Italy, for IL-1β and IL-8; Elabscience Biotechnology, Huston, TX, USA for mucin-1) according to the manufacturer's instructions.

2.11 Statistical Analysis

Unless differently indicated, each experiment was repeated 4–6 times, and the samples were assessed in triplicate. The Shapiro–Wilk test was used to analyze the data distribution within each experimental group. Subsequently, statistical analysis was performed using one-way ANOVA or the Kruskal–Wallis test, depending on the distribution of data; Tukey's multiple comparisons were chosen as post hoc tests. For the heatmap obtained in the mtROS assay, the Area Under the Curve (AUC) was calculated to summarize the curve into a single value. Subsequently, statistical analysis was performed comparing the AUC values of each experimental group, using one-way ANOVA. All statistical analyses were carried out using GraphPad Prism 10 software. Values of * $p < 0.05$ and ** $p < 0.01$ were considered statistically significant.

3. RESULTS

3.1. Cytokeratin-5/6 Expression in A-431 Epithelial Cells Maintained at Different Culture Conditions

Initially, we investigated the expression of cytokeratin 5/6, a well-established marker of epithelial cell differentiation. Thus, A-431 cells, cultured for 1 day (monolayer) or 5 days (RVE) with or without SVF, were processed and stained for IHC analysis. As detailed in Figure 1, the RVE showed a strong and diffused expression of this marker (intensity grade 3) in comparison to the cell monolayer (intensity grade 2); a further enhancement of positivity was observed if the RVE had been cultivated in the presence of SVF. Importantly, in this latter case, a more marked localization of the cytokeratin at the cell membrane level was evident.

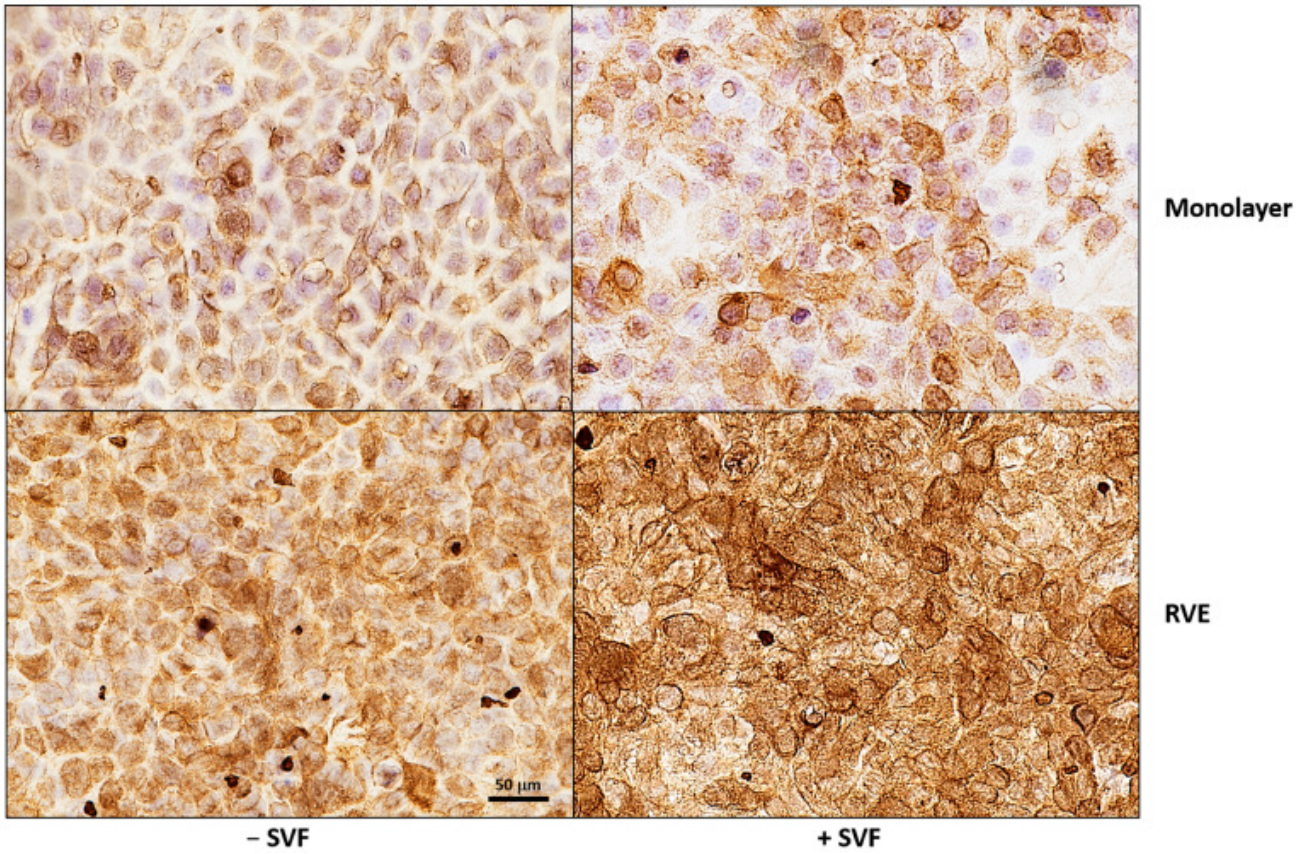

Figure 1
Cytokeratin 5/6 staining in A-431 cells, cultured for 1 or 5 days, in the absence or presence of SVF. Cells were immunohistochemically stained, with an anti-cytokeratin 5/6 mouse monoclonal primary antibody, using BenchMark IHC/ISH automated instruments according to standard antigen retrieval protocol. Representative images from two experiments are shown (magnification 40×). Immunohistochemical staining for CK5/6 shows diffused expression in the RVE, with stronger intensity observed in SVF.

3.2. *Candida albicans* and HSV-2 Load in A-431 RVE Infected with or Without SFV

The amount of fungal cells (expressed as CFUs) and virus production (expressed as DNA copies) was assessed in the RVE, infected with a single pathogen or both, in the presence and the absence of SVF. Figure 2A shows that *C. albicans* growth was significantly higher (>1 Log difference in CFU) in the samples cultured with SVF compared to the controls without SVF. Figure 2B shows the levels of HSV-2 DNA copies, determined using RT-PCR. The amount of viral DNA ranged between 3.9×10^5 copies/mL and 7.3×10^6 copies/mL, with no significant changes with respect to the presence of SVF. Yet, in the absence of SVF, the viral infectious titers slightly decreased in cells that had also been infected with *C. albicans* while, in contrast, in the presence of SVF, the HSV-2 DNA copies approximately doubled in dually infected cells with respect to A-431 cells infected with the virus alone. A similar trend of data was observed when the infectious titers were measured using the plaque assay (Figure 2C).

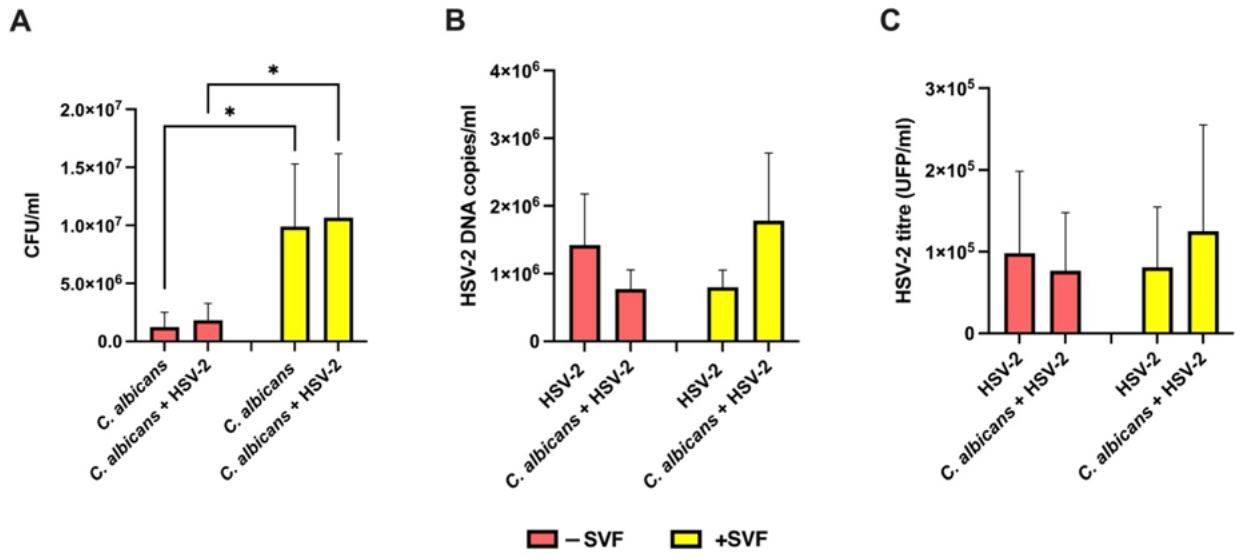

Figure 2
Quantification of fungal and viral loads in the RVE cultured with or without SVF. Five-day RVE cultures were infected with *C. albicans* (fungus:epithelial cell ratio = 0.5:1), and, after 3 h, HSV-2 (virus:cell ratio = 0.1:1) was added. Fungal and virus quantification was carried out after 24 h incubation using the CFU method on Sabouraud agar for *C. albicans* (**A**) and both RT-PCR (**B**) and the plaque reduction assay (**C**) for HSV-2. * $p < 0.05$.

3.3. Damage of A-431 RVE upon Infection with One or Two Pathogens, in the Presence or Absence of SFV

The LDH assay was used to determine the levels of A-431 cell damage, induced by a single or a dual infection, in the presence or absence of SVF (Figure 3). HSV-2 alone did not affect epithelial cell viability (<2% of cytotoxicity), irrespective of the presence or absence of SVF. Conversely, *C. albicans* significantly damaged epithelial cells, with the cytotoxicity percentage rising from 16% without SVF to 24% in the presence of SVF. In the dually infected cultures, the LDH levels showed a further slight, insignificant increase. In selected experiments, the cell damage was also determined using the MTT assay, and the results were completely superimposable (see Supplementary Materials).

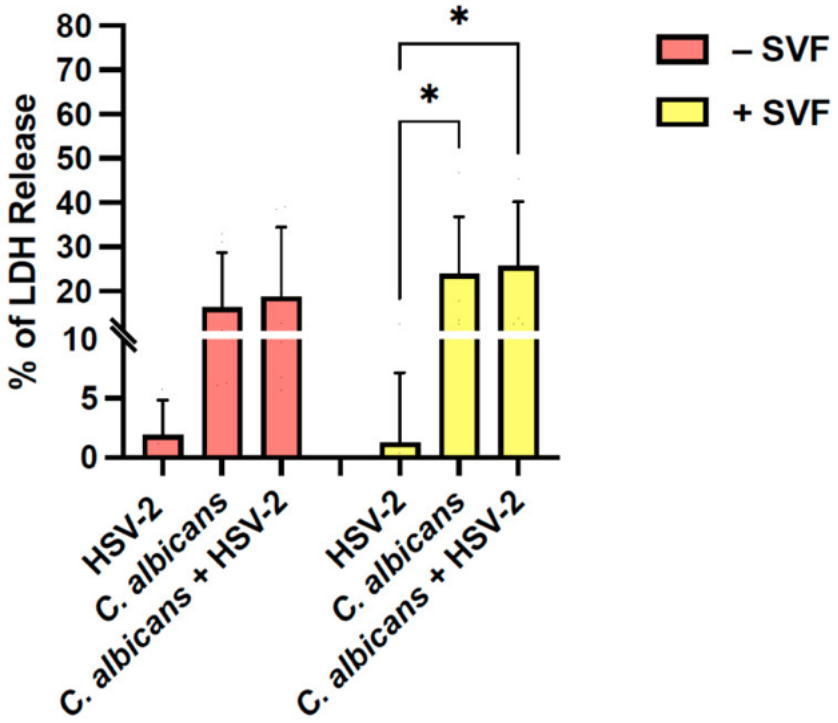

Figure 3
Levels of A-431 cell damage after single or dual infection in the presence or absence of SVF. Five-day RVE cultures were infected with *C. albicans* (fungus:epithelial cell ratio = 0.5:1), and, after 3 h, HSV-2 (virus:cell ratio = 0.1:1) was added. At 24 h, the LDH assay was performed to quantify the percentage of LDH release in the RVE exposed to one or two pathogens, in the presence or in the absence of SVF. * $p < 0.05$.

3.4. Oxidative Stress in A-431 RVE Infected with *Candida albicans* and/or HSV-2, With or Without SFV

The A-431 RVE samples infected with *C. albicans* and/or HSV-2, in the presence or absence of SVF, were tested for oxidative stress and measured as mtROS production. The heatmap is shown in Figure 4. On the right line, the reference lane is depicted. The values indicated by the different colors represent the amounts of mtROS detected in each sample at 24 h. As shown in the figure, in all conditions, the ROS levels were higher in the samples with SVF compared to those without SVF. A clear additive effect was evident in the dually infected cells cultured with SVF, displaying levels that were approximately double those of the mono-infected samples. This was evident only when SVF was present.

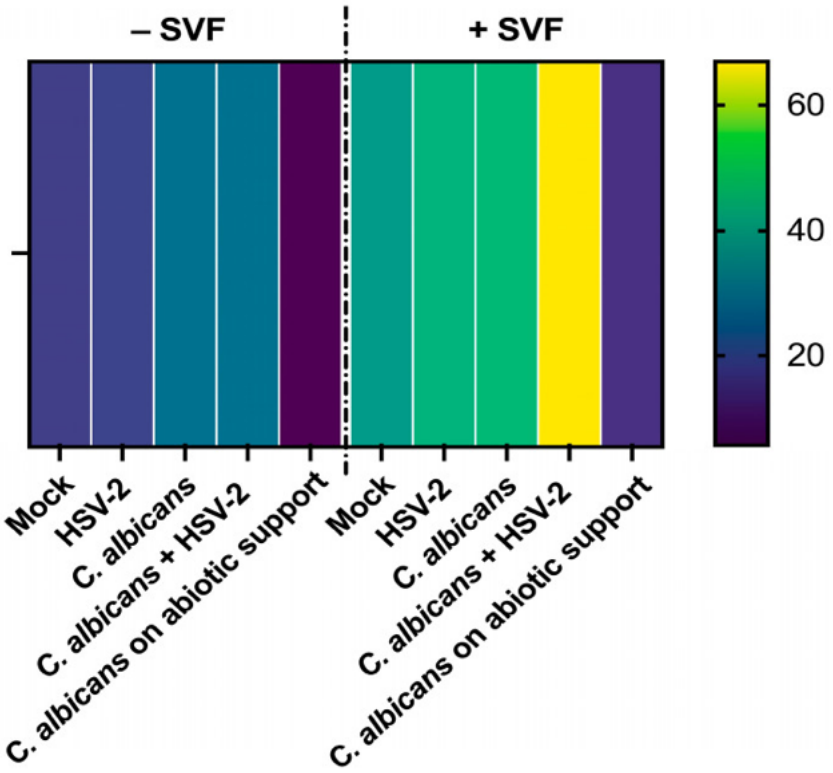

Figure 4
Mitochondrial ROS production by A-431 cells, exposed to single or dual infection in the presence or absence of SVF. Five-day RVE cultures were infected with *C. albicans* (fungus:epithelial cell ratio = 0.5:1), and, after 3 h, HSV-2 was added (virus:cell ratio = 0.1:1). Then, MitoSOX™ Red was added to each well and the plates were evaluated using Fluoroskan at 37 °C, for 24 h. A representative heatmap of the quantification of mtROS production at 24 h is shown. The mock line refers to A-431 cells alone; an inoculum of *C. albicans* without cells was included as a negative control (abiotic support). The values corresponding to the different colors represent the Area Under the Curve calculated to summarize the curve of the 24 h determination into a single value.

3.5. Secretion Pattern of A-431 Epithelial Cells Exposed to Single or Dual Infection, With or Without SVF

Levels of IL-1α, IL-1β, IL-8, and mucin-1 were assessed in cell-free supernatants of A-431 cells infected with HSV-2 and/or *C. albicans* in the presence or absence of SVF. As shown in Figure 5, IL-1α and IL-1β were not detectable in the uninfected A-431 cells; induction occurred only by *C. albicans*, with no relevant differences when comparing mono and dual infection. As shown, in the presence of SVF, the production of IL-1α and IL-1β was greatly affected, with their levels being doubled (30 pg/mL vs. 60 pg/mL for IL-1 α and 6 pg/mL vs. 12 pg/mL for IL-1β). As for IL-8, this chemokine was basally produced by A-431 cells and significantly increased upon infection with *C. albicans*, but not with HSV-2. Unexpectedly, SVF caused a decrease in IL-8 levels (44 pg/mL vs. 28 pg/mL). As for mucin-1 production, enhanced levels were observed upon SVF addition (13 ng/mL vs. 22 ng/mL) in the uninfected cultures. In contrast, each infectious agent caused a decrease in mucin-1 production, which was significant for *C. albicans* (22 ng/mL vs. 11 ng/mL) but not for HSV-2 (22 ng/mL vs. 18 ng/mL). Moreover, the dual infection did not have any additive effect, since the mucin-1 levels remained almost unaffected (11 ng/mL with *C. albicans* alone; 13 ng/mL with both pathogens).

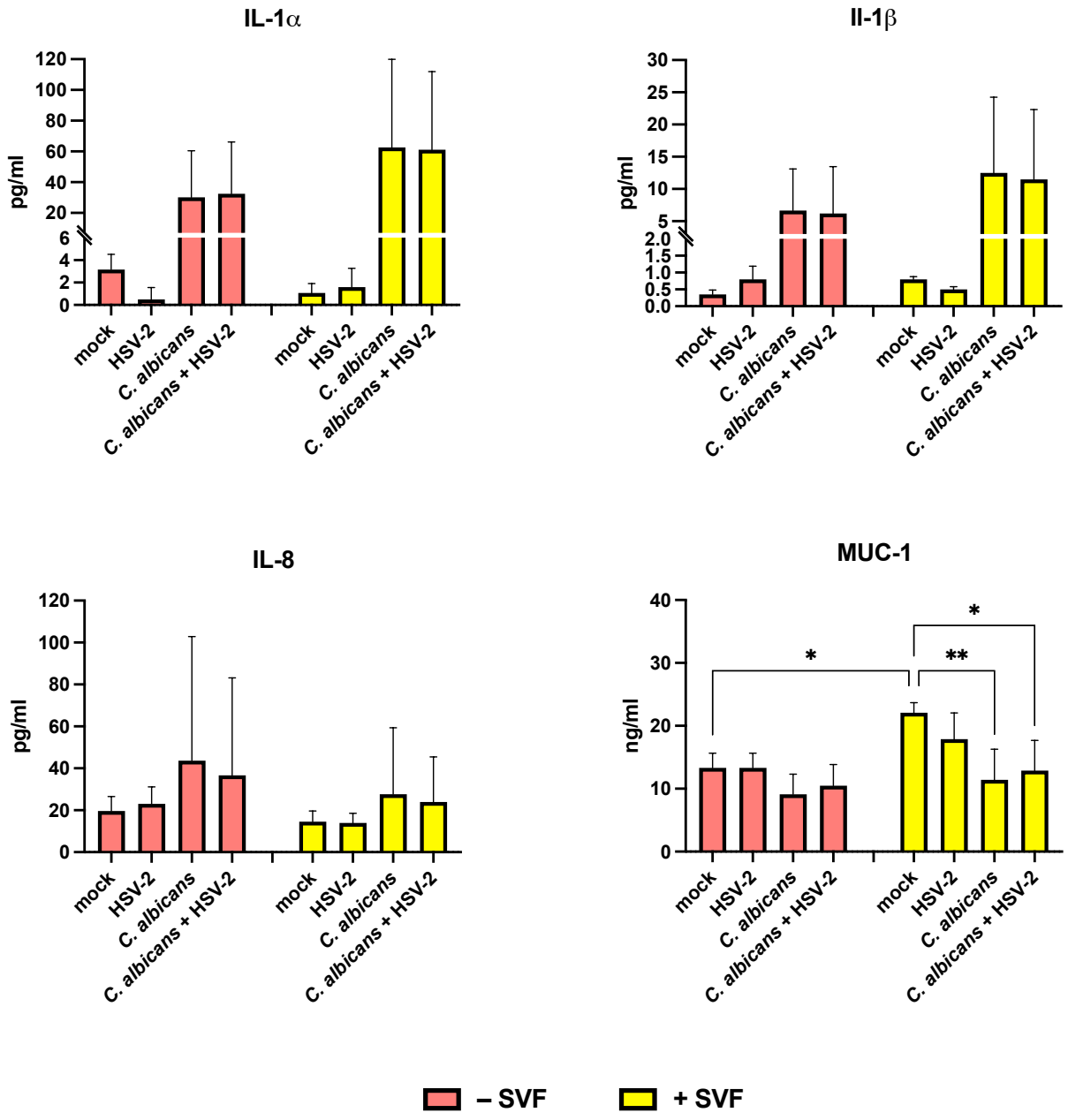

Figure 5
Secretory profile of the RVE infected with *C. albicans* and/or HSV-2, in the presence or absence of SVF. Five-day RVE cultures were infected with *C. albicans* (fungus:epithelial cell ratio = 0.5:1), and, after 3 h, HSV-2 was added (virus:cell ratio = 0.1:1). Following 24 h incubation, quantification of the secretion product was performed on the supernatants using commercial ELISA. * $p < 0.05$; ** $p < 0.01$.

In the Supplementary Materials, we provide a summary of RVE peculiarities with respect to SVF addition and infection with one or two pathogens.

4. DISCUSSION

In the era of molecular diagnostics, increasingly sensitive techniques are showing how polymicrobial infections, at a mucosal level, are frequent and certainly underestimated events (Frisan T., 2021). Scant research documents the frequency of double vaginal infections by HSV-2 and *C. albicans* (Plotkin et al., 2020; Kaul et al., 2007), and even less is known about the pathogenic mechanisms involved and the possible synergistic action whereby one microorganism favors the other. We have previously demonstrated how C. albicans biofilm favors the persistence of HSV-1 and Coxsackie Virus B5 over time; importantly, the fungal pathogenic potential seems to increase further, since the presence of *C. albicans* biofilm protects viral infectious particles from the immune response, drugs, and disinfectants (Mazaheritehrani et al., 2014; Ascione et al., 2017). Similarly, the co-presence of HSV-1 or HHV-6 and *C. albicans* or *Cryptococcus neoformans* dysregulates monocyte-mediated immune functions (Cermelli et al., 2006; Cermelli et al., 2008).

Here, to study the interplay between HSV-2 and *C. albicans* at the mucosal level, we describe an *in vitro* epithelial model using the A-431 cell line, that depending on the culture conditions, forms a monolayer (1 day) or a differentiated stratified (5 days) epithelium (Ridge et al., 1991). The A-431 line exhibits a range of characteristics that are quintessentially typical of epithelial cells (Wahl et al., 1988; Atsumi et al., 1994) including the high expression of keratins, structural proteins that not only support cellular architecture but also play a crucial role in the resilience and protective function of the epithelial barrier (Waseem et al., 1999). In the present study, to render our model as close as possible to the *in vivo* condition, the culture medium was treated with synthetic vaginal fluid (SVF), according to the previously established protocol (Owen et al., 1999; Del Gaudio et al., 2013). Initially, we demonstrate that the 5-day RVE displays a strong and diffused expression of cytokeratin 5/6 with respect to the 1-day monolayers, and, interestingly, the addition of SVF further increases the expression of such a differentiation marker, especially in the RVE. Thus, hereafter, we focus on the RVE model as the condition providing the highest degree of epithelial cell differentiation.

The RVE appears to be a suitable *in vitro* model for studying single or dual infection by *C. albicans* or HSV-2. Indeed, we show that fungal growth occurs and significantly increases upon the addition of SVF. This result is not surprising since the acidic pH of the SVF and its high glucose concentration are parameters greatly favorable to *C. albicans* persistence and growth, both *in vitro* and *in vivo*. Interestingly, *C. albicans* CFUs are not affected upon HSV-2 co-infection, excluding any pro-*C. albicans* effect by the viral agent. Concerning viral quantification, SVF addition tends to reduce viral load. Possibly, changes in the extracellular environment induced by the fluid, including pH lowering, increased viscosity, and high levels of polysaccharides, may limit the initial epithelial cell–virus

interaction, as shown in other infection models (Pinna et al., 2008; Ray et al., 2021). Moreover, in the co-infection, two opposite patterns of results have been observed with respect to SVF addition. In the absence of SVF, the viral load is reduced by the co-presence of *C. albicans*, while it is increased when the co-infection is performed with SVF. These data suggest that by utilizing the SVF content, fungal overgrowth may have led to fluid consumption and the restoration of conditions suitable for viral infection and replication. If this process has an *in vivo* counterpart, we can envision significant cooperation between fungal and viral agents that enhances their pathogenic potential at the mucosal level.

As established using the LDH release assay, epithelial cell damage is only attributable to *C. albicans*, as the contribution of HSV-2, alone or in co-infection, happens to be extremely limited regardless of the presence of SVF. This result may be due to the overgrowth of the fungus observed in cultures treated with SFV. The negligible contribution of the virus to epithelial cell damage may not be attributed to a low rate of viral infection since, as assessed using an immunofluorescence assay, more than 60% of the cells became infected (Figure S1 in the Supplementary Materials). Likely, the lack of LDH release may be related to the short incubation time chosen in our protocol (24 h), as the inverted light microscope observation of the cell cultures reveals a limited cytopathic effect.

An imbalance in the redox state towards oxidant conditions is a key event during viral infections, also mediating tissue damage (Foo et al., 2022; Gain et al., 2023). In particular, the involvement of ROS has been demonstrated in many viral infections, including HSV-1, where the dynamics of viral replication change, leading to increased viral loads and persistence within the host cell (Protto et al., 2020). In the case of *C. albicans*, the presence of ROS correlates with reduced fungal viability and virulence, emphasizing their role as hosts' essential defense mechanisms (Dantas Ada et al., 2015; Cui et al., 2023). In our model, the epithelial cell infection by either *C. albicans* or HSV-2 alone causes a partial-to-negligible ROS response, while SVF alone increases ROS with respect to basal levels. Interestingly, in the presence of SVF, the two pathogens exert an additive effect with respect to ROS production, which is indeed more than doubled. Thus, we may conclude that A-431 epithelial cells, supported by SVF, better respond to the concomitant *C. albicans* and HSV-2 infection in terms of ROS production; however, this condition favors viral replication, as indicated by the viral loads that are augmented in the samples with double infection.

Besides oxidative stress, cytokines play a pivotal role in shaping the inflammatory response against infections. Among many, IL-1α and IL-1β are pro-inflammatory signals that crucially act in hosts' defenses. Indeed, upon HSV-1 infection, epithelial cells release IL-1α that in turn induces necrosis and cell lysis. Meanwhile, IL-1α predominantly acts at the site of tissue damage, working as a further

“alarmin” to locally signal injury (Milora et al., 2014; Smith et al., 2022). In our model, the secretion of IL-1α does not change when the cells are infected with the virus alone, and this is in line with the limited cellular damage occurring in these same samples. Concerning IL-1β, it is known that such a cytokine is primarily secreted following activation of the inflammasome (Fu and Wu, 2023). Interestingly, HSV-2 affects the activation of the NLRP3 inflammasome by two specific viral proteins (Fakioglu et al., 2008) and, in turn, reduces IL-1β production. Our data show no changes in IL-1β production by HSV-2 in parallel with minor virus-mediated cell damage.

Increasingly, the literature has shown that IL-1α is released from epithelial cells during fungal invasions, acting as an early alarm signal to recruit immune cells (Wüthrich et al., 2013; Caffrey-Carr et al., 2017). Upon binding to specific pattern recognition receptors, *C. albicans* activates the NLRP3 inflammasome via NF-κB, in turn triggering IL-1β production (Fang et al., 2023). In our model, both IL-1α and IL-1β are induced by *C. albicans* without any significant additive effect from the presence of HSV-2. Interestingly, upon the addition of SVF, IL-1α and IL-1β production is enhanced, indicating that this culture condition favors epithelial cell reactivity against *C. albicans*. Furthermore, IL-8, a well-known pro-inflammatory chemokine (Matsushima et al., 2022), shows no relevant variations in our model, irrespective of whether SVF is present or the epithelial cells have been infected by HSV-2 and/or *C. albicans*. Finally, mucin-1, released through the apical surface of epithelial cells, is crucial in protecting mucosal surfaces and provides barrier functions and immune regulation (Dhar and Auley, 2019; Ballester et al., 2021). HSV-2 displays several mechanisms to evade mucin action, including downregulation of MUC1 gene expression (Trybala et al., 2021). Similarly, *C. albicans* can elude mucin-1 by secreting aspartyl proteases that promptly degrade mucins (Dühring et el, 2015), allowing hyphal active penetration and tissue invasion through the mucosal barrier (Mayer et al., 2013). The results we obtained in our dual infection model add evidence for the ability of the two pathogens to modulate mucin-1 production. In particular, *C. albicans* and HSV-2, either alone or in co-infection, can reduce levels of mucin-1, the phenomenon being particularly evident in cultures with SVF.

Overall, using an *in vitro* RVE obtained from the A-431 cell line, we first show that *C. albicans* induces important cell damage, associated with a scant release of inflammatory cytokines and a relevant reduction in mucin, likely reflecting the complex double-face interplay between fungal and host cells occurring at the mucosal level. Second, superinfection with HSV-2 does not result in a modification of *C. albicans* behavior nor in a further increase in epithelial cell damage and response. Third, *C. albicans* favors viral replication, whose load in fact increases in cells already infected by *C. albicans* compared to uninfected cells, in the presence of the SVF. Bearing in mind the limitations of

such an epithelial tumor cell-line model, we aim to implement it through (i) the addition of neutrophils, as the first line and most abundant immune cell recruited at the site of infection, and (ii) the use of synthetic scaffolds, as inert cell support, to produce three-dimensional culture structures, hopefully, better mimicking the *in vivo* architecture of the vaginal epithelium.

In conclusion, the A-431-based RVE represents a ductile and easy-to-perform model for *in vitro* studies on polymicrobial infections occurring at the mucosal level; the addition of SVF provides a first step ahead in mimicking the vaginal environment.

SUPPLEMENTARY MATERIAL

Parameters assessed	Role of the SVF	
Epithelial cell differentiation (IHC staining for cytokeratin 5/6)	↑↑ staining intensity and membrane localization	
Mucin-1 release (ELISA)	↑↑ basal levels	
	Single infection	**Double infection**
Candida albicans growth (CFU assay)	↑↑	↑↑
HSV-2 load (DNA copies)	↓	↑
Epithelial cell damage (LDH release)	↑↑ by *Candida albicans* No change by HSV-2	↑↑ by *Candida albicans* No change by HSV-2
Oxidative stress (mtROS)	↑ by *Candida albicans* No change by HSV-2	↑↑ by *Candida albicans* ↑↑ by HSV-2
IL-1α production (ELISA)	↑ by *Candida albicans* ↓ by HSV-2	↑↑ by *Candida albicans* ↔ by HSV-2
IL-1β production (ELISA)	↑ by *Candida albicans* ↔ by HSV-2	↑↑ by *Candida albicans* ↔ by HSV-2
IL-8 production (ELISA)	↑↑ by *Candida albicans* ↔ by HSV-2	↑ by *Candida albicans* ↔ by HSV-2
Mucin-1 production (ELISA)	↔ by *Candida albicans* ↑ by HSV-2	↓ by *Candida albicans* ↓ by HSV-2

Table S1. Summary of events occurring in the RVE model in the presence and in the absence of SVF.

Table S1 provides a schematic summary of the results obtained, visualizing the differences between A-431 cells, exposed or not to SVF, regarding *C. albicans* proliferation, virus load, epithelial cell damage, IL-1 α, IL-1 β, and mucin-1 production. We have shown that the SVF promotes A-431 cell differentiation and exerts a pro- *C. albicans* role. The SVF impairs viral replication, that, in contrast, is enhanced in the presence of *C. albicans*. Epithelial cell damage, ROS production and cytokine response are essentially ascribed to *C. albicans*, and, mostly, in the presence of the SVF. Whether these *in vitro* phenomena may have an *in vivo* counterpart remains to be investigated. In any case, the RVE may be proposed as a useful model to assess *in vitro* the complex interplay between vaginal epithelium and single or multiple pathogens.

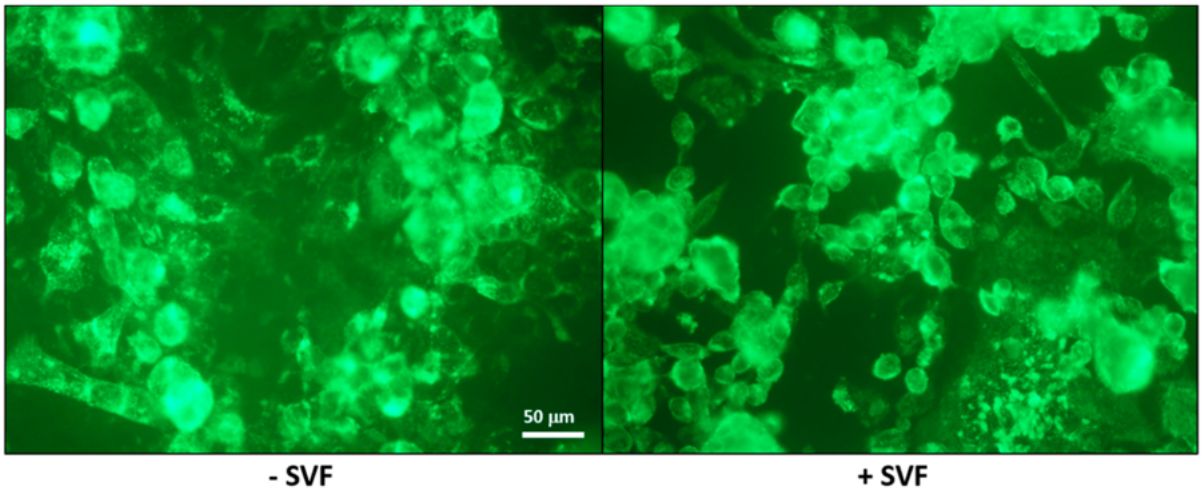

Figure S1. Immunofluorescence assay for HSV-2 detection in RVE cultured with or without SVF.
A-431 cells grown for 5 days on chamber slides were infected with HSV-2 (virus:cell ratio = 0.1:1). After 24 h incubation, the slides were then fixed in acetone for 15 min. at room temperature and then incubated with a monoclonal antibody against HSV-2 capsid antigen for 35 min. After 3 washes with PBS, a goat anti-mouse IgG antibody labelled with FITC was added for 35 min and, following 3 washes with PBS, the slides were counterstained with Evan's blu.

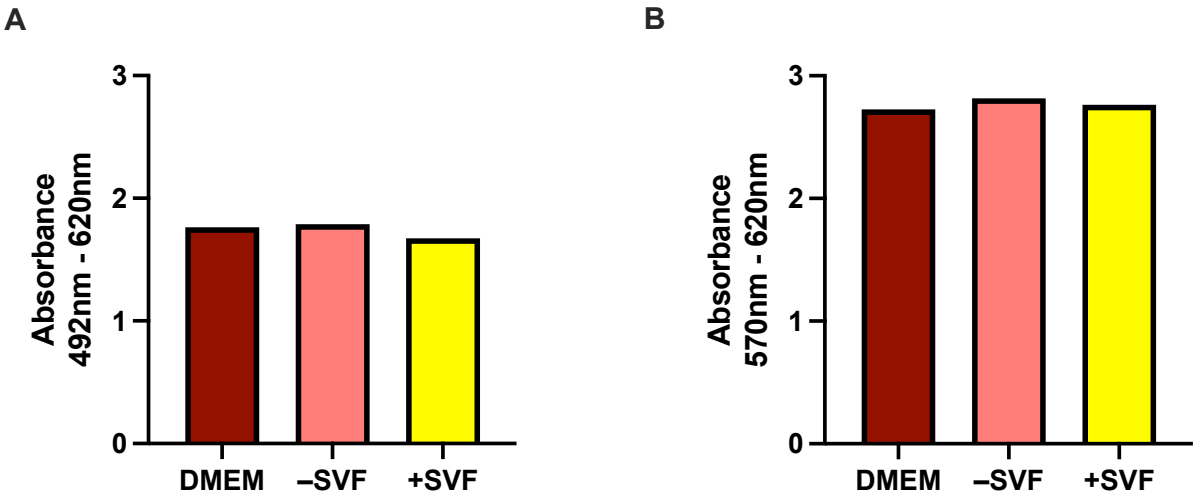

Figure S2. Comparison between LDH (A) and MTT (B) assays for the evaluation of cell damage in RVE cultured with or without SVF.
Five day RVE cultures were incubated with or without SVF for further 24 h and then the two cytotoxicity assays were carried out in parallel. The results are completely superimposable.

REFERENCES

Ascione, C.; Sala, A.; Mazaheri-Tehrani, E.; Paulone, S.; Palmieri, B.; Blasi, E.; Cermelli, C. Herpes simplex virus-1 entrapped in Candida albicans biofilm displays decreased sensitivity to antivirals and UVA1 laser treatment. Ann. Clin. Microbiol. Antimicrob. 2017, 16, 72.

Atsumi, T.; Hosoi, K.; Ueha, T. Involvement of high-affinity binding site for EGF receptor in formation of rounding in A-431 epidermoid carcinoma cells. Horm. Metab. Res. 1994, 26, 141–144.

Ballester, B.; Milara, J.; Cortijo, J. The role of mucin 1 in respiratory diseases. Eur. Respir. Rev. 2021, 30, 200149.

Biswas, M.; Nurunnabi, M.; Khatun, Z. Understanding Mucosal Physiology and Rationale of Formulation Design for Improved Mucosal Immunity. ACS Appl. Bio Mater. 2024, 7, 5037–5056.

Caffrey-Carr, A.K.; Kowalski, C.H.; Beattie, S.R.; Blaseg, N.A.; Upshaw, C.R.; Thammahong, A.; Lust, H.E.; Tang, Y.-W.; Hohl, T.M.; Cramer, R.A.; et al. Interleukin 1α Is Critical for Resistance against Highly Virulent Aspergillus fumigatus Isolates. Infect. Immun. 2017, 85, 1–19.

Cermelli, C.; Cenacchi, V.; Beretti, F.; Pezzini, F.; Luca, D.D.; Blasi, E. Human herpesvirus-6 dysregulates monocyte-mediated anticryptococcal defences. J. Med. Microbiol. 2006, 55, 695–702.

Cermelli, C.; Orsi, C.F.; Ardizzoni, A.; Lugli, E.; Cenacchi, V.; Cossarizza, A.; Blasi, E. Herpes simplex virus type 1 dysregulates anti-fungal defenses preventing monocyte activation and downregulating toll-like receptor-2. Microbiol. Immunol. 2008, 52, 575–584.

Cui, Y.; Wang, D.; Nobile, C.J.; Dong, D.; Ni, Q.; Su, T.; Jiang, C.; Peng, Y. Systematic identification and characterization of five transcription factors mediating the oxidative stress response in Candida albicans. Microb. Pathog. 2023, 187, 106507.

Dantas Ada, S.; Day, A.; Ikeh, M.; Kos, I.; Achan, B.; Quinn, J. Oxidative stress responses in the human fungal pathogen, Candida albicans. Biomolecules 2015, 5, 142–165.

Del Gaudio, G.; Lombardi, L.; Maisetta, G.; Esin, S.; Batoni, G.; Sanguinetti, M.; Senesi, S.; Tavanti, A. Antifungal Activity of the Noncytotoxic Human Peptide Hepcidin 20 against Fluconazole-Resistant Candida glabrata in Human Vaginal Fluid. Antimicrob. Agents Chemother. 2013, 57, 4314–4321.

Dhar, P.; McAuley, J. The Role of the Cell Surface Mucin MUC1 as a Barrier to Infection and Regulator of Inflammation. Front. Cell. Infect. Microbiol. 2019, 9, 117.

Dühring, S.; Germerodt, S.; Skerka, C.; Zipfel, P.F.; Dandekar, T.; Schuster, S. Host-pathogen interactions between the human innate immune system and Candida albicans—Understanding and modeling defense and evasion strategies. Front. Microbiol. 2015, 6, 625.

Fakioglu, E.; Wilson, S.S.; Mesquita, P.M.M.; Hazrati, E.; Cheshenko, N.; Blaho, J.A.; Herold, B.C. Herpes simplex virus downregulates secretory leukocyte protease inhibitor: A novel immune evasion mechanism. J. Virol. 2008, 82, 9337–9344.

Fang, X.; Lian, H.; Liu, S.; Dong, J.; Hua, X.; Li, W.; Liao, C.; Yuan, X. A positive feedback cycle between the alarmin S100A8/A9 and NLRP3 inflammasome-GSDMD signalling reinforces the innate immune response in Candida albicans keratitis. Inflamm. Res. 2023, 72, 1485–1500.

Farr, A.; Effendy, I.; Frey Tirri, B.; Hof, H.; Mayser, P.; Petricevic, L.; Ruhnke, M.; Schaller, M.; Schaefer, A.P.A.; Sustr, V.; et al. Guideline: Vulvovaginal candidosis (AWMF 015/072, level S2k). Mycoses 2021, 64, 583–602.

Fichorova, R.N.; Morrison, C.S.; Chen, P.-L.; Yamamoto, H.S.; Govender, Y.; Junaid, D.; Ryan, S.; Kwok, C.; Chipato, T.; Salata, R.A.; et al. Aberrant cervical innate immunity predicts onset of dysbiosis and sexually transmitted infections in women of reproductive age. PLoS ONE 2020, 15, e0224359.

Foo, J.; Bellot, G.; Pervaiz, S.; Alonso, S. Mitochondria-mediated oxidative stress during viral infection. Trends Microbiol. 2022, 30, 679–692.

Frisan, T. Co-and polymicrobial infections in the gut mucosa: The host-microbiota-pathogen perspective. Cell. Microbiol. 2021, 23, e13279.

Fu, J.; Wu, H. Structural Mechanisms of NLRP3 Inflammasome Assembly and Activation. Annu. Rev. Immunol. 2023, 41, 301–316.

Gain, C.; Song, S.; Angtuaco, T.; Satta, S.; Kelesidis, T. The role of oxidative stress in the pathogenesis of infections with coronaviruses. Front. Microbiol. 2023, 13, 1111930.

Gaziano, R.; Sabbatini, S.; Monari, C. The Interplay between Candida albicans, Vaginal Mucosa, Host Immunity and Resident Microbiota in Health and Disease: An Overview and Future Perspectives. Microorganisms 2023, 11, 1211.

Giard, D.J.; Aaronson, S.A.; Todaro, G.J.; Arnstein, P.; Kersey, J.H.; Dosik, H.; Parks, W.P. In vitro cultivation of human tumors: Establishment of cell lines derived from a series of solid tumors. JNCI J. Natl. Cancer Inst. 1973, 51, 1417–1423.

Gupta, R.; Warren, T.; Wald, A. Genital herpes. Lancet 2007, 370, 2127–2137.

Higgins, E.; Gupta, A.; Cummins, N.W. Polymicrobial Infections in the Immunocompromised Host: The COVID-19 Realm and Beyond. Med. Sci. 2022, 10, 60.

Jayaraman, M.; Leela, K.V.; Rajalakshmi, E. Superadded bacterial and fungal infections in oral and genital herpes simplex lesions. Int. J. Med. Sci. Public Health 2020, 9, 468–474.

Kaul, R.; Nagelkerke, N.J.; Kimani, J.; Ngugi, E.; Bwayo, J.J.; Macdonald, K.S.; Rebbaprgada, A.; Fonck, K.; Temmerman, M.; Ronald, A.R.; et al. Prevalent herpes simplex virus type 2 infection is associated with altered vaginal flora and an increased susceptibility to multiple sexually transmitted infections. J. Infect. Dis. 2007, 196, 1692–1697.

Looker, K.J.; Magaret, A.S.; May, M.T.; Turner, K.M.; Vickerman, P.; Gottlieb, S.L.; Newman, L.M. Global and Regional Estimates of Prevalent and Incident Herpes Simplex Virus Type 1 Infections in 2012. PLoS ONE 2015, 10, e0140765.

Lopes, J.P.; Lionakis, M.S. Pathogenesis and virulence of Candida albicans. Virulence 2022, 13, 89–121.

Matsushima, K.; Yang, D.; Oppenheim, J.J. Interleukin-8: An evolving chemokine. Cytokine 2022, 153, 155828.

Mayer, F.L.; Wilson, D.; Hube, B. Candida albicans pathogenicity mechanisms. Virulence 2013, 4, 119–128.

Mazaheritehrani, E.; Sala, A.; Orsi, C.F.; Neglia, R.G.; Morace, G.; Blasi, E.; Cermelli, C. Human pathogenic viruses are retained in and released by Candida albicans biofilm in vitro. Virus Res. 2014, 179, 153–160.

Milora, K.A.; Miller, S.L.; Sanmiguel, J.C.; Jensen, L.E. Interleukin-1α released from HSV-1-infected keratinocytes acts as a functional alarmin in the skin. Nat. Commun. 2014, 5, 5230.

Murray, J.L.; Connell, J.L.; Stacy, A.; Turner, K.H.; Whiteley, M. Mechanisms of synergy in polymicrobial infections. J. Microbiol. 2014, 52, 188–199.

Nyirjesy, P.; Brookhart, C.; Lazenby, G.; Schwebke, J.; Sobel, J.D. Vulvovaginal Candidiasis: A Review of the Evidence for the 2021 Centers for Disease Control and Prevention of Sexually Transmitted Infections Treatment Guidelines. Clin. Infect. Dis. 2022, 74 (Suppl. S2), S162–S168.

Omarova, S.; Cannon, A.; Weiss, W.; Bruccoleri, A.; Puccio, J. Genital Herpes Simplex Virus-An Updated Review. Adv. Pediatr. 2022, 69, 149–162.

Owen, D.H.; Katz, D.F. A vaginal fluid simulant. Contraception 1999, 59, 91–95.

Panasiti, V.; Devirgiliis, V.; Borroni, R.; Spataro, A.; Melis, L.; Petrella, M.; Pala, S. Atypical cutaneous manifestation of HSV-2 with Candida albicans co-infection in a patient with HIV-1. J. Infect. 2007, 54, e55–e57.

Pinna, D.; Oreste, P.; Coradin, T.; Kajaste-Rudnitski, A.; Ghezzi, S.; Zoppetti, G.; Rotola, A.; Argnani, R.; Poli, G.; Manservigi, R.; et al. Inhibition of herpes simplex virus types 1 and 2 in vitro infection by sulfated derivatives of Escherichia coli K5 polysaccharide. Antimicrob. Agents Chemother. 2008, 52, 3078–3084.

Plotkin, B.J.; Sigar, I.M.; Kaminski, A.; Kreamer, J.; Ito, B.; Kacmar, J. Kinetics of Candida albicans and Staphylococcus aureus Biofilm Initiation on Herpes Simplex Virus (HSV-1 and HSV-2) Infected Cells. Adv. Microbiol. 2020, 10, 583–598.

Protto, V.; Tramutola, A.; Fabiani, M.; Marcocci, M.E.; Napoletani, G.; Iavarone, F.; Vincenzoni, F.; Castagnola, M.; Perluigi, M.; Di Domenico, F.; et al. Multiple Herpes Simplex Virus-1 (HSV-1) Reactivations Induce Protein Oxidative Damage in Mouse Brain: Novel Mechanisms for Alzheimer's Disease Progression. Microorganisms 2020, 8, 972.

Ray, B.; Ali, I.; Jana, S.; Mukherjee, S.; Pal, S.; Ray, S.; Schütz, M.; Marschall, M. Antiviral Strategies Using Natural Source-Derived Sulfated Polysaccharides in the Light of the COVID-19 Pandemic and Major Human Pathogenic Viruses. Viruses 2021, 14, 35.

Ridge, J.; Muller, J.; Noguchi, P.; Chang, E.H. Dynamics of differentiation in human epidermoid squamous carcinoma cells (A431) with continuous, long-term γ-IFN treatment. Vitr. Cell. Dev. Biol. Anim. 1991, 27, 417–424.

Sala, A.; Ardizzoni, A.; Spaggiari, L.; Vaidya, N.; van der Schaaf, J.; Rizzato, C.; Cermelli, C.; Mogavero, S.; Krüger, T.; Himmel, M.; et al. A New Phenotype in Candida-Epithelial Cell Interaction Distinguishes Colonization- versus Vulvovaginal Candidiasis-Associated Strains. mBio 2023, 14, e00107-23.

Sala, A.; Ricchi, F.; Giovati, L.; Conti, S.; Ciociola, T.; Cermelli, C. Anti-Herpetic Activity of Killer Peptide (KP): An In Vitro Study. Int. J. Mol. Sci. 2024, 25, 10602.

Schaller, M.; Zakikhany, K.; Naglik, J.R.; Weindl, G.; Hube, B. Models of oral and vaginal candidiasis based on in vitro reconstituted human epithelia. Nat. Protoc. 2006, 1, 2767–2773.

Shekhawat, K.S.; Bhatia, P.; Bhatnagar, K.; Shandilay, S.; Chaudhary, S. Roadmap to Cytotoxicity: Exploring Assays and Mechanisms. ASSAY Drug Dev. Technol. 2025.

Smith, J.B.; Herbert, J.J.; Truong, N.R.; Cunningham, A.L. Cytokines and chemokines: The vital role they play in herpes simplex virus mucosal immunology. Front. Immunol. 2022, 13, 936235.

Suazo, P.A.; Tognarelli, E.I.; Kalergis, A.M.; González, P.A. Herpes simplex virus 2 infection: Molecular association with HIV and novel microbicides to prevent disease. Med. Microbiol. Immunol. 2015, 204, 161–176.

Trybala, E.; Peerboom, N.; Adamiak, B.; Krzyzowska, M.; Liljeqvist, J.; Bally, M.; Bergström, T. Herpes Simplex Virus Type 2 Mucin-Like Glycoprotein mgG Promotes Virus Release from the Surface of Infected Cells. Viruses 2021, 13, 887.

Wahl, M.; Carpenter, G. Regulation of epidermal growth factor-stimulated formation of inositol phosphates in A-431 cells by calcium and protein kinase C. J. Biol. Chem. 1988, 263, 7581–7590.

Waseem, A.; Alam, Y.; Lalli, A.; Dogan, B.; Tidman, N.; Purkis, P.; Jackson, S.; Machesney, M.; Leigh, I.M. Keratin 15 expression in stratified epithelia: Downregulation in activated keratinocytes. J. Investig. Dermatol. 1999, 112, 362–369.

Workowski, K.A.; Bachmann, L.H.; Chan, P.A.; Johnston, C.M.; Muzny, C.A.; Park, I.; Reno, H.; Zenilman, J.M.; Bolan, G.A. Sexually Transmitted Infections Treatment Guidelines, 2021. MMWR Recomm. Rep. 2021, 70, 1–187.

Wüthrich, M.; LeBert, V.; Galles, K.; Hu-Li, J.; Ben-Sasson, S.Z.; Paul, W.E.; Klein, B.S. Interleukin 1 enhances vaccine-induced antifungal T-helper 17 cells and resistance against Blastomyces dermatitidis infection. J. Infect. Dis. 2013, 208, 1175–1182.

CHAPTER 3

Fungal burden, dimorphic transition and candidalysin: Role in *Candida albicans*-induced vaginal cell damage and mitochondrial activation *in vitro*

Luca Spaggiari[1], Andrea Ardizzoni[2], Francesco Ricchi[1], Natalia Pedretti[2], Caterina Alejandra Squartini Ramos[2], Gianfranco Bruno Squartini Ramos[2], Samyr Kenno[3], Francesco De Seta[4,5], Eva Pericolini

[1] Clinical and Experimental Medicine PhD Program, University of Modena and Reggio Emilia, Modena, Italy;

[2] Department of Surgical, Medical, Dental and Morphological Sciences with Interest in Transplant, Oncological and Regenerative Medicine, University of Modena and Reggio Emilia, Modena, Italy;

[3] Institute for SystemicI nflammation Research, University of Lübeck, Lübeck, Germany;

[4] Department of Medical Sciences, University of Trieste, Trieste, Italy;

[5] Institute for Maternal and Child Health-IRCCS, Burlo Garofolo, Trieste, Italy.

***PloS one*. 2024, doi:10.1371/journal.pone.0303449**

1. INTRODUCTION

Candida albicans (*C. albicans*) is one of the most known human fungal pathogens. It is responsible of significant clinical conditions, spanning from mild mucosal to severe invasive infections. This species has been recently included by WHO within the critical priority group of pathogenic fungi (Parums DV, 2022).

C. albicans is a part of the vaginal microbiota of healthy women: when occurring in low numbers it is normally tolerated as a commensal yeast on the mucosal surface, where it does not trigger any epithelial immune response (Ardizzoni et al., 2021; Jabra-Rizk et al., 2016). However, in immunocompromised hosts or in specific clinical conditions such as VVC that can occur in immunocomopetent women, *C. albicans* behaves as an opportunistic pathogen increasing the local fungal burden and its virulence; these events in turn may exceed the tolerance threshold of epithelial cells thus causing an intense inflammatory response, which is the main responsible of the vulvovaginal candidiasis (VVC) symptoms (Ardizzoni et al., 2021). Such tolerance threshold is defined as tolerability levels of human cells host to *Candida* presence without triggering an inflammatory response (Ardizzoni et al., 2021); it varies among women according to several individual factors (i.e. presence of lactobacilli, pH, estrogen levels and many others).

Among mucosal infections, VVC is a very common condition in healthy women in their reproductive age. Therefore, here *C. albicans* behaves like a primary pathogen.

In vitro studies shown the involvement of several components during the vaginal epithelial cells response to *C. albicans* and it is more and more evident that epithelial cells, in addition to their role as mechanical barriers, are capable to polarize host response against infections (Pekmezovic et al., 2021).

Host mitochondria play a crucial role in the innate immune responses by several mechanisms, such as Reactive Oxygen Species (ROS) production (West et al., 2011). The latter include many derivatives of molecular oxygen, such as hydrogen peroxide H_2O_2 (prototype of the group of "twoelectron non-radical ROS") and the superoxide anion radical O_2^{*-} (as prototype of the group of "free radical ROS"). The major endogenous enzymatic sources of O_2^{*-} and H_2O_2 are transmembrane NADPH oxidases (NOXs) (Bedard and Krause, 2007; Knock GA, 2019; Parascandolo and Laukkanen, 2019) and the mitochondrial electron transport chain (ETC) (Murphy MP, 2009), as well as various other sources. At physiological conditions, mitochondrial ROS (mtROS) production promotes the so-called "oxidative eustress", responsible of cell differentiation, proliferation, migration and vasodilation (Clempus et al., 2007; Dikalov S., 2011; Ayer et al., 2014): under these

conditions, cells regulate mtROS levels by maintaining a balance between their production and their elimination, avoiding thus their harmful effects (Tsao et al., 2007; Zhao et al., 2017). Indeed, mitochondrial activation is also one of the primary responses of the host cells when they are subjected to different external stimuli (including microbes), and such activation is important for the regulation of innate and adaptive immune response (Weinberg et al., 2015). Activation of TLRs 1, 2, and 4 leads to the recruitment of mitochondria to macrophage phagosomes, where they enhance mtROS production (Tiku et al., 2020). It has been reported that methicillin-resistant *Staphylococcus aureus* (MRSA) induces the generation of mitochondria-derived vesicles containing mtROS that, in turn, help the clearance of intracellular bacteria via TLR signaling (Abuaita et al., 2018). Furthermore, oral epithelial cells treated with candidalysin (CL) showed a rapid production of mtROS, triggering numerous cellular stress responses that ultimately lead to oral epithelial cell necrotic death (Blagojevich et al., 2021). The activation of mtROS in response to different microbial infections has been demonstrated to modulate host cells proliferation, vitality and death and to improve the antimicrobial function of the innate immune cells (Sancho et al., 2017). Interestingly, type I interferon pathway seems to play a key protective role, depending on the time and species, in epithelial response against *Candida* infection through mitochondrial activation (Pekmezovic et al., 2021; Pekmezovic et al., 2022; Sala et al., 2023).

However, excessive amounts of mtROS can cause “oxidative distress”, that results in degradation of intracellular lipids, proteins and DNA, which in turn lead to cell damage and triggers several cell death patterns (Foyer and Noctor, 2005; Chen et al., 2009; Sies and Jones, 2020). It has been recently reported that *C. albicans* causes cellular oxidative stress and cell death upon activation and mtROS production (Ren et al., 2020).

During VVC immunopathogenesis, human cells, fungi, and microbiota alteration, all contribute to the disease onset. Therefore, *C. albicans* virulence in the vaginal environment is also mediated by its capacity to proliferate, form hyphae, and produce toxic molecules such as Secreted Aspartyl Proteinases (SAPs) and CL (the latter produced only by hyphal forms), that seem to play a key role in the immunopathogenesis of VVC (Pekmezovic et al., 2021; Russel et al., 2023; Pericolini et al, 2015). In particular, CL has been recently shown to induce a potent epithelial cell damage and inflammation both *in vitro* and in a murine model of VVC (Moyes et al., 2016; Naglik et al., 2019). Indeed, challenge *C. albicans* lacking hyphal-associated gene ECE1 or CL deletion mutant strains in a murine model of VVC resulted in a reduction of the immunopathology, including a decreased proinflammatory cytokines production, neutrophils recruitment and tissue damage, as compared to the challenge with the WT strain. Given that, the CL mutants still robustly form hyphae in vaginal

lumen, these results clearly show that hyphal growth is required but not sufficient for VVC immunopathology development. CL is likely the virulence factor that drives these responses (Richardson et al., 2018).

Here we focus on the role of three main factors such as fungal load, morphogenesis and CL in the induction of the epithelial response to *C. albicans* by RVE infection model *in vitro*. The production of mtROS and cell damage will be analysed since we observed, in our preliminary data, that *C. albicans* induces a time-dependent production of mtROS in vaginal epithelial cells. Interestingly, the morphology, CL, and fungal load are all regulators of mtROS production and cellular damage.

2. RESULTS

2.1 Mitochondrial activation by BLI-Ca

We started by analyzing the mtROS production in response to Ca infection, using the RVE infection model (Ridge et al, 1999; Pericolini et al., 2017), both by BLI-Ca yeasts and preformed hyphae with low Multiplicity Of Infection (MOI) 1:1 and high MOI 1:5 (epithelial cells: *Candida*) (Hopke et al., 2016). As far as we know, this is the first time that mtROS production by RVE is monitored kinetically after Ca yeasts or hyphae infection. Therefore, we chose 5 min reading cycles up to 12 h to collect as much data as possible to describe the phenomenon.

Our results show that at MOI 1:1 (epithelial cells/*Candida*) the mtROS occurred at around 7 h post-infection (84 reading cycles) with yeasts and at around 3.5 h post-infection (40 reading cycles) with hyphae (Figure 1A and 1B—left panels and Figure 4A—left panel). Differently, the response to infection at MOI 1:5 was quicker, i.e., at 3.5 h for yeasts (42 reading cycles) and at 2.5 h for hyphae (30 reading cycles) (Figure 1A and 1B—right panels and Figure 4A—right panel).

A side-by-side analysis of epithelial response to Ca yeasts and hyphae shows that at MOI 1:1 mtROS induction by hyphae was quicker than mtROS induction by yeasts; moreover, hyphae induced mtROS levels were significantly higher than those induced by yeasts (Figure 1C—left panel and Figure 4B – left panel). The difference in the mtROS activation times could not be observed upon epithelial cells infection with the higher fungal inoculum (MOI 1:5). Indeed, under this experimental condition, the mtROS induction in response to both yeasts and hyphae was overlapping, at least up to 10 h post-infection (Figure 1C—right panel). However, at 12.5 h post-infection hyphae-induced mtROS levels were higher (albeit not significantly) than yeasts-induced mtROS levels (Figure 1C—right panel and Figure 4B—right panel).

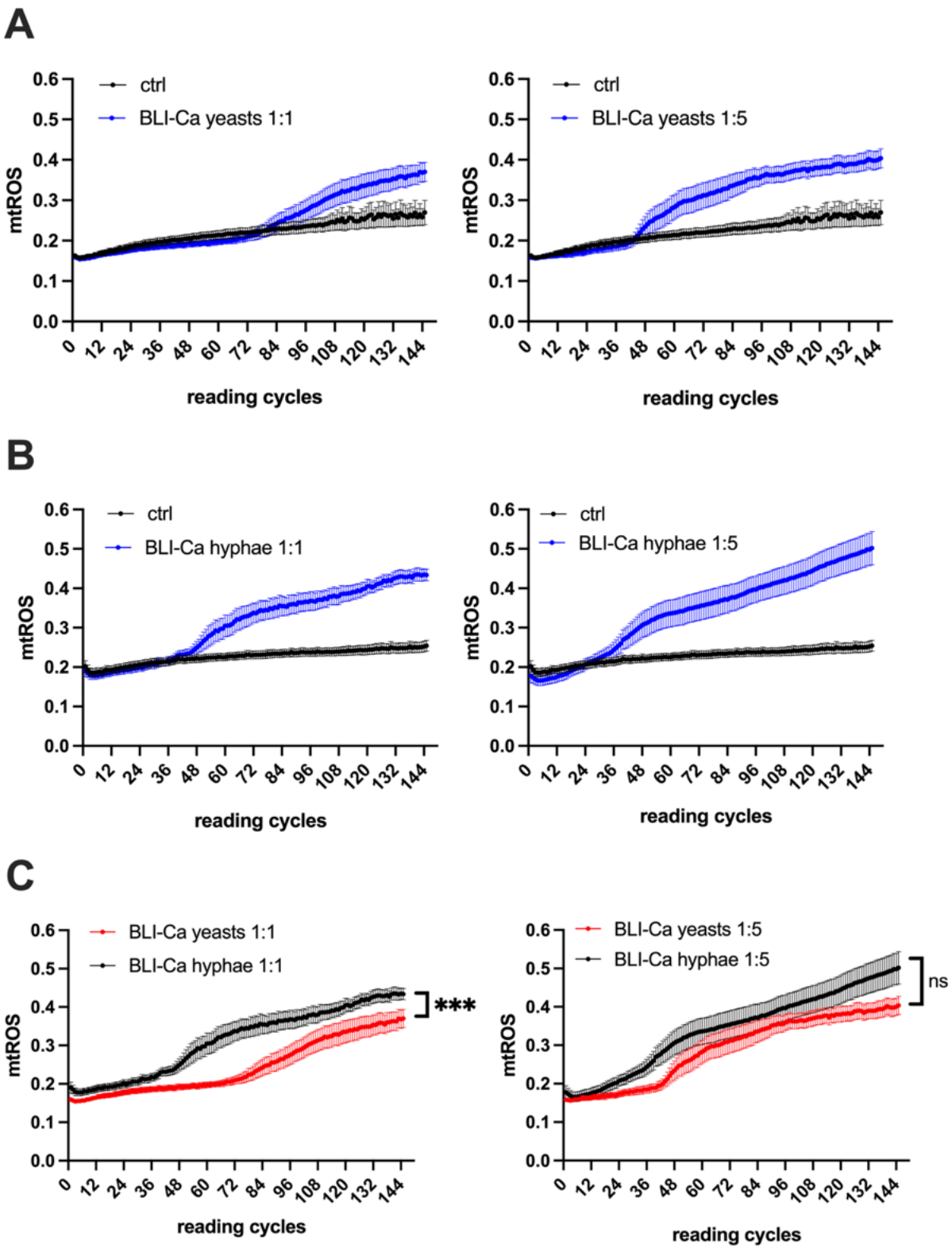

Figure 1. Kinetics of mtROS production by BLI-Ca infected RVE. RVE has been infected with BLI-Ca in yeasts (**A**) or hyphae (**B**) either at MOI 1:1 (left panels) or MOI 1:5 (right panels). In (**C**) the comparisons between mtROS productionby BLI-Ca yeasts and hyphae at MOI 1:1 (left panel) and MOI 1:5 (right panel) is shown. The mtROS production was evaluated by fluorescence emission after addition of MitoSOX™ Red probe, as detailed in Materials and Methods section. Reading cycles were perfomed at 5minutes intervals. Ctrl = uninfected RVE. Data are expressed as mean ± SEM. Data are from at least 3different experiments performed in triplicate. Statistical analysis was performed by using Mann-Whitney U test ***$p < 0.001$.

2.2 Mitochondrial activation by Ca PCA-2

To better understand this observation, we challenged RVE with Ca PCA-2 by the same experimental set-up. The Ca PCA-2 strain is unable to switch from yeast to mycelial form (Bistoni et al., 1986), so that we could establish only the role played by the fungal load in inducing mtROS. The results shown in Figure 2 and 4A demonstrate that Ca PCA-2 strain could induce mtROS after 7.5 h of infection at MOI 1:1 (92 reading cycles) and after 4.5 h post-infection at MOI 1:5 (54 reading cycles). Therefore, at the same fungal loads, Ca PCA-2 induced mtROS 1 h (MOI 1:5) and 0.5 h (MOI 1:1) later then BLI-Ca yeasts. In addition, the levels of mtROS 12.5 h post-infection were higher at MOI 1:5 than at MOI 1:1, thus demonstrating that higher fungal loads were decisive in increasing levels of mtROS by RVE (Figure 4B).

2.3 Mitochondrial activation by 529L Ca

In order to better clarify the role of hyphae in the mtROS induction, we employed the Ca strain 529L, characterized by an impaired production of CL (Rahman et al., 2007). Our results show that mtROS activation from Ca 529L yeasts at MOI 1:1 could not be observed at least up to 11 h post-infection (132 reading cycles). Differently, mtROS activation from yeasts started after 8.5 h at MOI 1:5 (102 reading cycles) (Figures 3A and 4A). Moreover, we observed mtROS production from hyphae after 9 h at MOI 1:1 (108 reading cycles) and after 6 h at MOI 1:5 (72 reading cycles) (Figures 3B and 4A).

A comparison between BLI-Ca and Ca 529L strains, shows that the former in hyphal form was able to induce significantly higher mtROS levels and more quickly than the latter, both at MOI 1:1 and at MOI 1:5 (Figures 3C and 4B).

The scheme in Figure 4A summarizes the time required by Ca-infected RVE to trigger mtROS production, that was always quicker in BLI-Ca when compared to Ca 529L. Similarly, the scheme in Figure 4B summarizes the levels of mtROS induced at the end of the experiments, i.e., 12.5 h after RVE infection, showing that they were always higher in BLI-Ca than in Ca 529L.

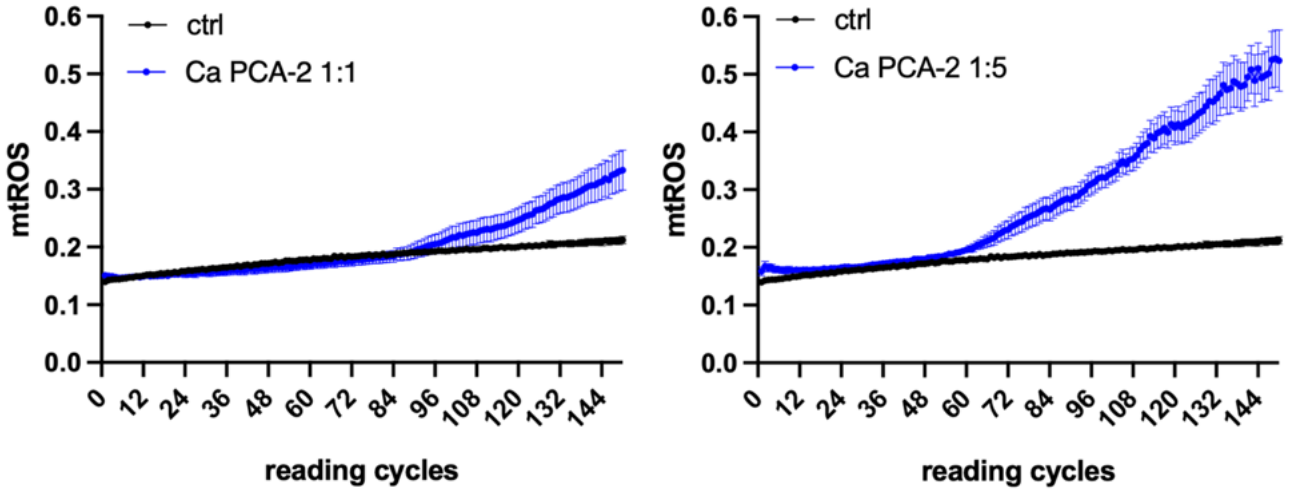

Figure 2. Kinetics of mtROS production by Ca PCA-2 infected RVE. RVE has been infected with Ca PCA-2 either at MOI 1:1 (left panel) or MOI 1:5 (right panel). The mtROS production was evaluated by fluorescence emission after addition of MitoSOX™ Red probe, as detailed in Materials and Methods section. Reading cycles were perfomed at 5minutes intervals. Ctrl = unifected RVE. Data are expressed as mean ± SEM. Data are from at least 3 different experiments performed in triplicate.

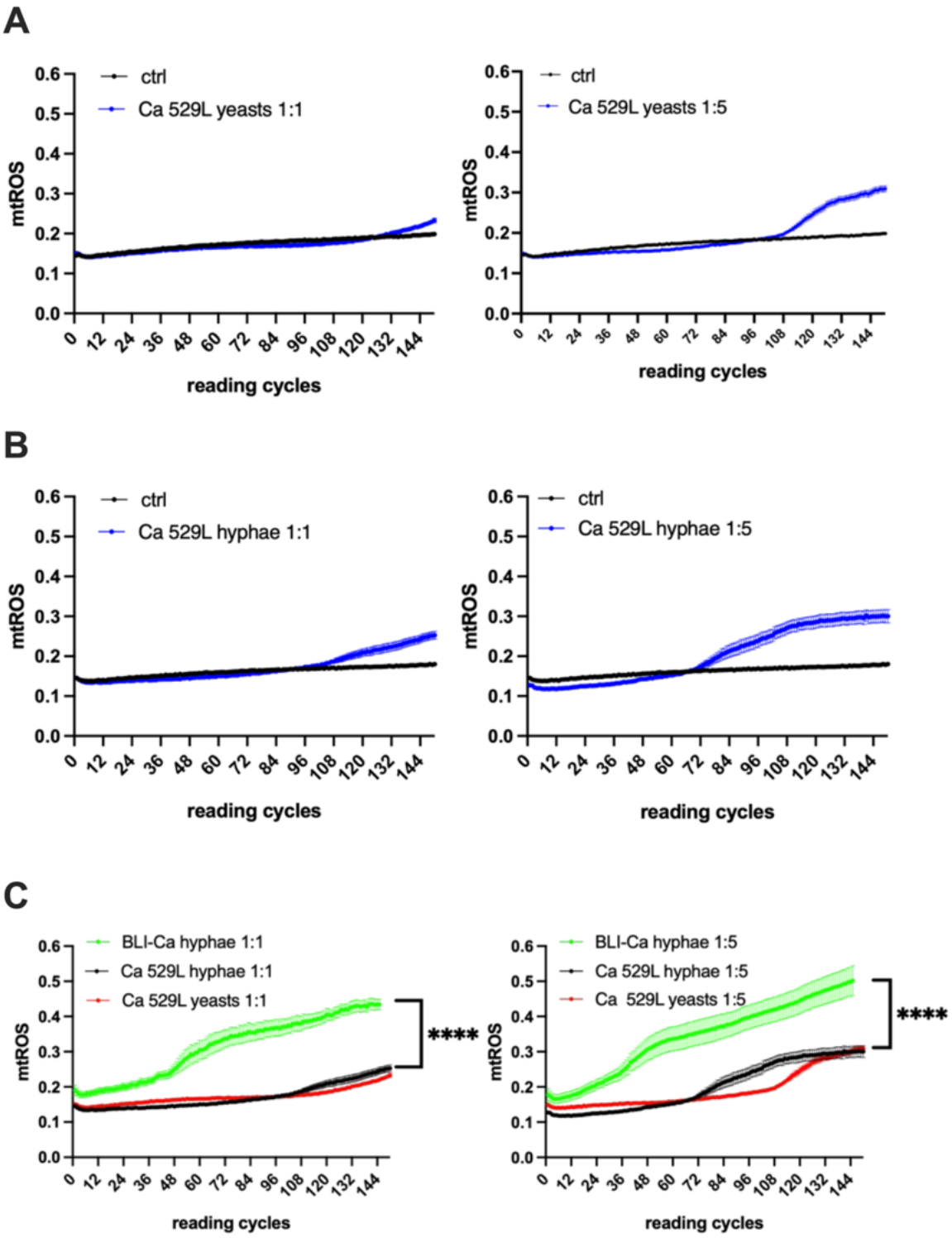

Figure 3. Kinetics of mtROS production by Ca 529L infected RVE. RVE has been infected with Ca 529L in yeasts (**A**) or hyphae (**B**) either at MOI 1:1 (left panels) or MOI 1:5 (right panels). In (**C**) the comparisons between mtROS productionby Ca 529L yeasts and hyphae and BLI-Ca hyphae at MOI 1:1 (left panel) and MOI 1:5 (right panel) are shown. The mtROS productionwas evaluated by fluorescence emission after addition of MitoSOX™ Red probe, as detailed in materials and methods section. Reading cycles were perfomed at 5 minutes intervals. Ctrl = unifected RVE. Data are expressed as mean ± SEM. Data are from at least 3 different experiments performed in triplicate. Statistical analysis was performed by using Mann-Whitney U test ****$p < 0.0001$.

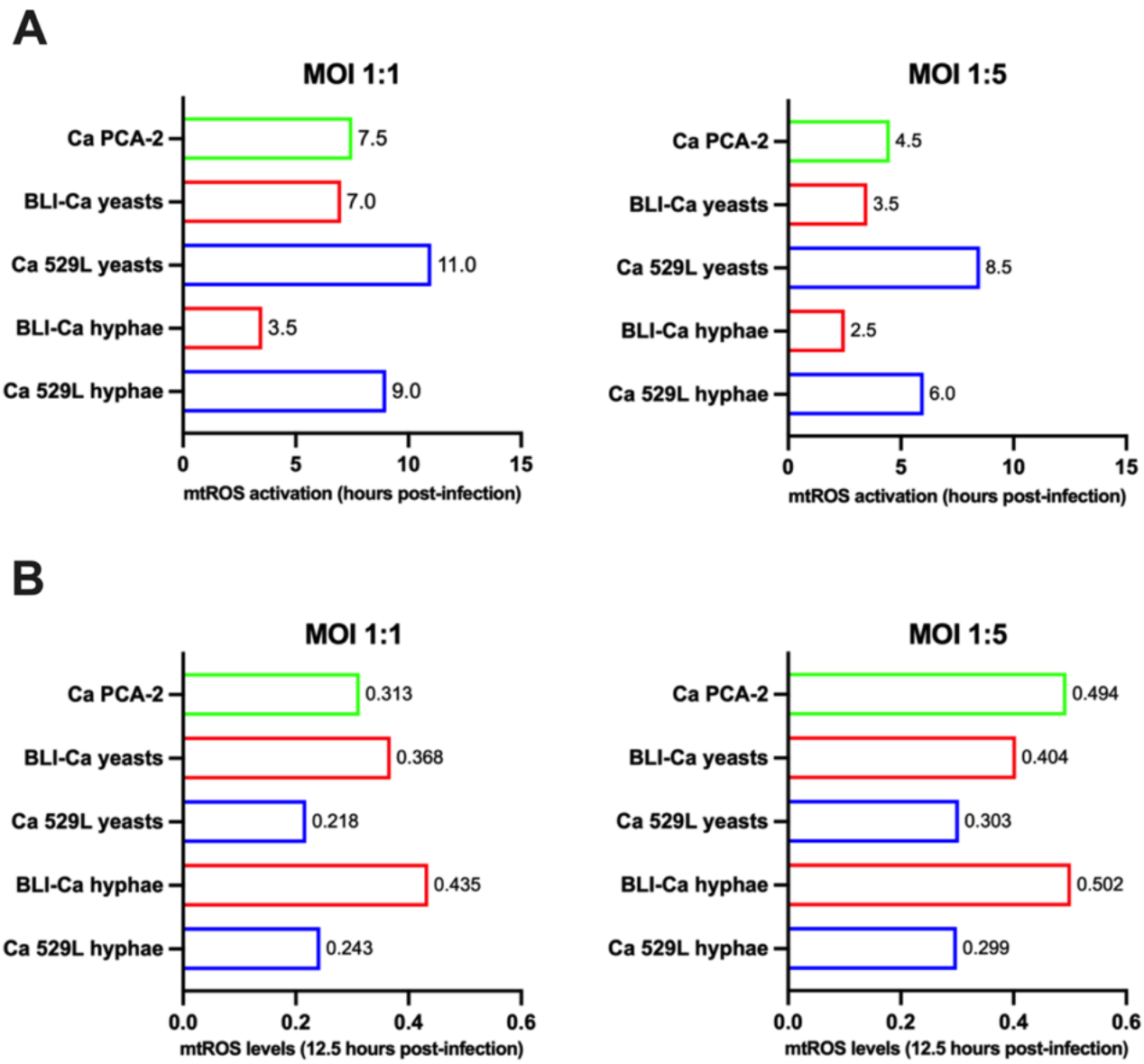

Figure 4. Schematic representation of mtROS activation times and levels. (**A**) Times of induction of mtROS after RVE infection with the different Ca strains at the different experimental conditon sare shown at MOI 1:1 (left panel) and MOI 1:5 (right panel). (**B**) The levels of mtROS production reached after 12.5 h of RVE infection with the different Ca strains at the different experimental conditons are shown at MOI 1:1 (left panel) and MOI 1:5 (right panel).

2.4 Cell damage after Ca infection

The assessment of epithelial cell damage is an important datum to define Ca virulence; therefore, we analyzed cell damage after 24 h of RVE infection with yeasts of Ca PCA-2 and yeasts and hyphae of BLI-Ca and Ca 529L both at MOI 1:1 and MOI 1:5. Interestingly, at low fungal burden (MOI 1:1) and in both yeast and hyphal form, Ca 529L induced significantly lower cell damage when compared to BLI-Ca. Notably, at MOI 1:1, Ca 529L yeasts did not induce any damage to RVE (below 5% of cell damage), whereas Ca 529L hyphae induced damage was around 20%, i.e. much lower than BLI-Ca yeasts- and hyphae-induced damage (more than 80%).

Differently, at high fungal load (MOI 1:5) both BLI-Ca and Ca 529L severely damaged the RVE, irrespective of the morphological stage or CL. Ca PCA-2 induced a cell damage comparable to the cell damage induced by BLI-Ca yeasts at both MOIs (Figure 5).

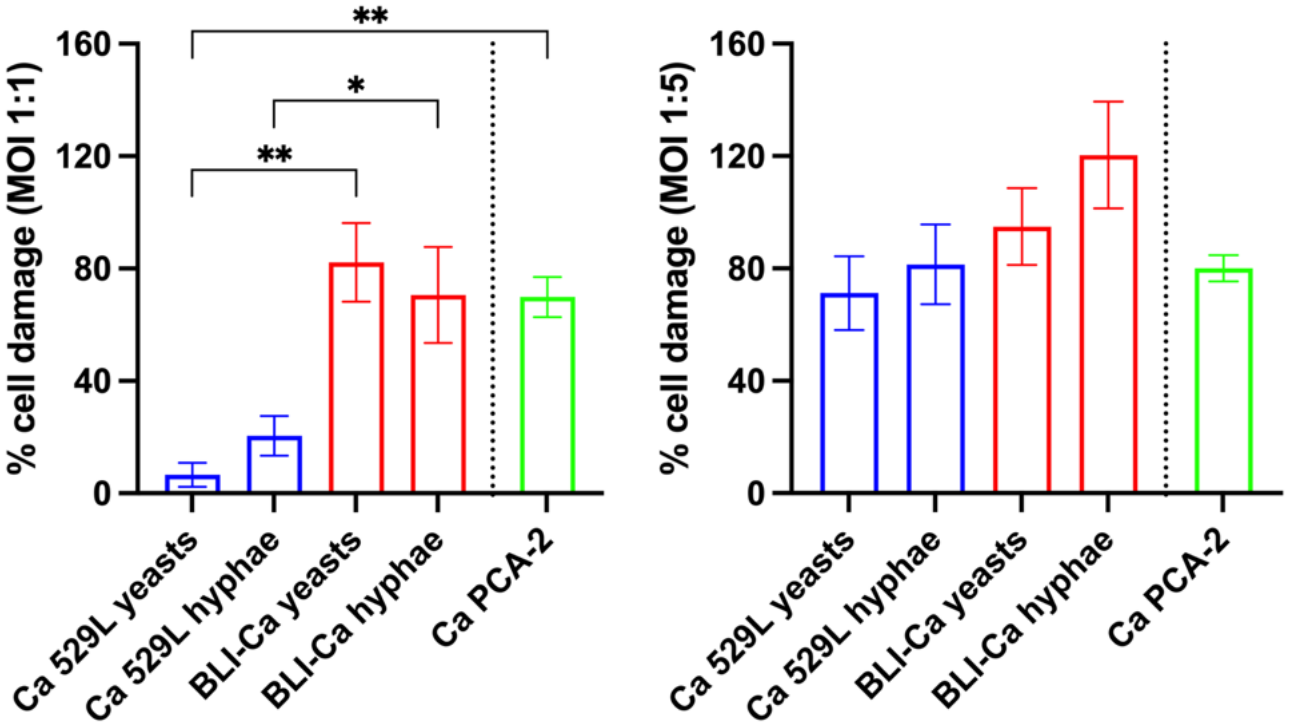

Figure 5. Cell damage after RVE infection with BLI-Ca, Ca 529L and Ca PCA-2. The percent (%) of cell damage after 24h of RVE infection with BLI-Ca and Ca 529L, both in yeasts and hyphal forms, and Ca PCA-2 yeasts at MOI 1:1 (left panel) and MOI 1:5 (right panel) is shown. Statistical analysis was performed by OneWay ANOVA followed by Tukey's multiple comparisons test. Data are expressed as mean ± SEM. Data are from at least 3 different experiments performed in triplicate. *$p < 0.05$; **$p < 0.01$.

2.5 Role of Ca-induced mtROS in cell damage and fungal growth

Finally, we performed experiments where RVE was infected for 24h with BLI-Ca yeasts at MOI 1:1 in the presence or absence of ascorbic acid (Vitamin C). It is acknowledged that ascorbic acid functions as a potent antioxidant in mitochondria of human cells, therefore in this context, it is used as mtROS scavenger (Wenzel U., 2003). Our results show that the addition of Vitamin C resulted in a significant reduction of BLI-Ca yeasts induced mtROS (Figure 6A). In the same experimental setting, we quantified fungal growth after RVE infection or culture on an abiotic surface. Our results show that fungal growth was significantly higher on the abiotic surface than on the RVE (Figure 6B).

Notably, by adding Vitamin C to culture medium, a significant increase in fungal growth could be observed in RVE as compared to the fungal growth on abiotic surface (Figure 6C). Moreover, no changes in cell damage after 24 h of RVE infection, could be observed after the addition of Vitamin C to the culture medium (Figure 6D).

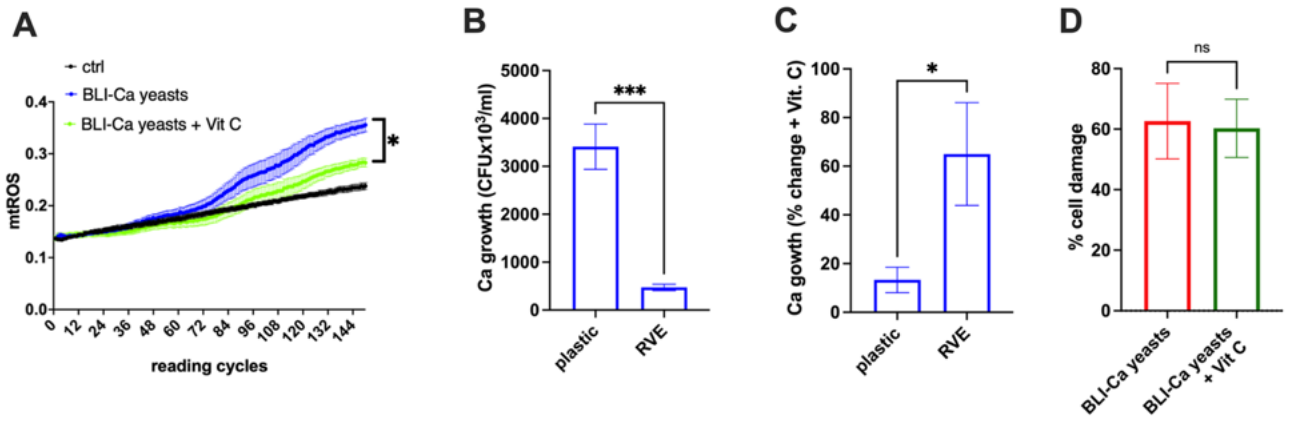

Figure 6. mtROS production, fungal growth and cell damage after RVE infection with BLI-Ca yeasts in the presence of a ROS scavenger.
RVE has been infected with BLI-Ca yeasts at MOI 1:1 in the presence or absence of ascorbic acid (Vit C, 1000 µM) used as ROS scavenger. (**A**) The mtROS production was evaluated by fluorescence emission after addition of MitoSOX™ Red probe, as detailed in materials and methods section. Recording cycles were perfomed at 5 minutes intervals. Ctrl =unifected RVE. Statistical analysis was performed by using unpaired t-test. *$p < 0.05$. (**B**) Comparison of BLI-Ca yeasts growth on abiotic surface (plastic) and on RVE. Data are expressed as CFU x10^3/ml. (**C**) Percentage increase of BLI-Ca yeasts growth on abiotic surface (plastic) and on RVE after addition of Vit C in the culture medium. (**D**) Percentage of cell damage induced by BLI-Ca yeasts on RVE in the presence or absence of Vit C. Data are expressed as mean ± SEM. Data are from at least 3 different experiments performed in triplicate.

3. DISCUSSION

In healthy women, *C. albicans* can behave as a commensal of the vaginal microbiota. Indeed, although *Candida* cell wall antigens interact with the Pattern Recognition Receptors (PRRs), the epithelial cells tolerate *Candida*, as well as any other resident microorganism, without triggering any inflammatory response. In this state of tolerance, it is thought that *Candida* colonizes the mucosal membranes mainly in the form of yeast and with a low fungal load. Nevertheless, if the tolerance threshold is exceeded, this balanced situation breaks down, *Candida* proliferates (therefore increasing its fungal load) and undergoes mycelial transition (Ardizzoni et al., 2021; Sala et al., 2023).

The increased fungal burden, the production of hyphae, as well as toxic molecules such as CL and SAP, have all been described as factors involved in triggering the inflammatory response and the disease onset (Ardizzoni et al., 2021).

The production of mtROS has been recognized as a key mechanism used by the host cells to react against non-self antigens, thus polarizing the immune response (Weinberg et al., 2015). Indeed, mtROS antimicrobial activity after innating immune cells activation has been widely described. Less known is the role exerted by mtROS produced by infected epithelial cells, after fungal infection. Here, we assessed the role of fungal burden, mycelial transition, and CL production in mtROS induction by epithelial cells, and also the potential implication of mtROS production in cell damage and fungal growth.

We started by investigating the role played by the mycelial transition and the fungal burden in the induction of mtROS. Our data show that by employing BLI-Ca, at MOI 1:1, hyphae stimulate mtROS production after 3.5 hours post-infection, whereas at the same MOI, yeasts necessitate of at least 7 hours to induce mtROS and such delay has been shown to be significant (Figure 1C—left panel). Differently, when RVE is infected by a high fungal load (MOI 1:5), also yeasts induce mtROS almost as early as hyphae, suggesting thus that, under such conditions, it is not necessary for Ca to undergo dimorphic transition to induce a quick epithelial activation, as demonstrated by the rapid induction of mtROS. In addition, the short delay in inducing mtROS by yeasts at high fungal load (only 1 h) lacks statistical significance (as shown in Figure 1C—right panel). To support these data, we employed PCA-2, a Ca strain that is constitutively unable to undergo dimorphic transition. As shown in Figure 2 and in Figure 4A, the mtROS production by such strain closely mirrors the mtROS production by the BLI-Ca yeasts, supporting the idea that fungal load is a key element, other than dimorphic transition, that triggers mitochondrial activation, as demonstrated by the similar levels of mtROS induced at MOI 1:5 by Ca PCA-2 and BLI-Ca hyphae and yeasts (Figure 4B). Even though Ca PCA-

2 is not able to form hyphae (and therefore it should be unable to secrete CL) (Moyes et al., 2016), it always stimulates higher levels of mtROS production compared to Ca 529L. This suggestes the Ca PCA-2 might replicate quicker that Ca 529L therefore reaching a higher burden in a shorten time.

Regarding the role of hyphae and pseudohyphae, *in vitro* and *ex vivo* data from the literature describe Ca morphological transition (i.e., the formation of true hyphae) as the main event responsible for the epithelial activation which drives the immunopathology (Pericolini et al., 2018; Moyes et al., 2011). Differently, another study supports the idea that pseudohyphae, rather than hyphae, may play a key role in the activation of the inflammatory process that leads to VVC onset (Rosselletti et al., 2019). Fungal morphogenesis is an important virulence factor that facilitates invasion of host tissues, escape from phagocytes, and dissemination in the blood stream. The innate immune system is the first line of defense against *C. albicans* infections and is influenced by recognition of wall components that vary in composition in different morphological forms (Mukaremera et al., 2017).

Our data suggest that a high fungal load may be sufficient to trigger mtROS production irrespective of the morphology of the fungus. Such mitochondrial activation may also play a key role in induction of inflammation.

The data presented here show that true hyphae always stimulate more quickly mtROS production by epithelial cells at all the experimental conditions assessed, i.e., low, and high fungal load.

Ca 529L, characterized by the impaired production of CL (Liu et al., 2021), has been employed to determine if such toxin plays a role in mithochondrial activation, in addition to morphological transition and fungal burden. Our results have shown that by infecting epithelial cells with Ca 529L, the induction of mtROS occurs much later (and at lower levels) with respect to infections by BLI-Ca. By employing Ca 529L yeasts at MOI 1:1, mtROS induction has not been observed until 11 h post-infection, whereas at MOI 1:5, Ca 529L yeasts have been able to induce mtROS only 8.5 h post-infection. In addition, the mtROS levels induced 12.5 h post-infection by Ca 529L are always lower than those induced by BLI-Ca, irrespective of the MOI. Therefore, by comparing these results with those obtained by infecting the RVE with BLI-Ca, we hypothesize that the yeasts of this latter strain start to undergo morphological transition and the CL produced by the hyphae can accelerate the induction of mtROS. The yeasts of the Ca 529L undergo morphological transition as well, but their impaired production of CL makes them unable to induce mtROS (at low fungal burden) or delays such induction (at high fungal burden). A similar delay in mtROS induction can be observed also with respect to Ca PCA-2. The data obtained by infecting epithelial cells with Ca 529L hyphae once again show a delay in mtROS induction, as compared to the infection with BLI-Ca hyphae (9 h vs

3.5 h at MOI 1:1 and 6 h vs 2.5 h at MOI 1:5). Similarly to what observed with Ca 529L yeasts, Ca 529L hyphae induce also lower levels of mtROS when compared to BLI-Ca hyphae. Again, these data point to the relevance of the CL in inducing mtROS. Therefore, according to these results, we hypothesize that CL is a key element to accelerate and potentiate the Ca-induced mitochondrial activity in vaginal epithelial cells.

Interestingly, oral epithelial cells treated with CL showed rapid production of mtROS (Blagojevic et al., 2021).

Moreover, we have assessed the damage of epithelial cells infected by the BLI-Ca and Ca 529L. In line with studies from other reaserch groups (Russel et al., 2023), our results show that CL is a key player in Ca-induced epithelial damage, as demonstrated by the low damage levels detected in Ca 529L-infected cells. Interestingly, such effect has been observed only at low fungal burden (MOI 1:1), whereas, at higher fungal burden (MOI 1:5), the epithelial cell damage reaches higher levels, irrespective of the CL production and fungal morphology. Therefore, CL is necessary to induce damage at low fungal burden indicating that, in such condition, the simple presence of hyphae is not enough to damage epithelial cells.

Mitochondrial activity after *C. albicans* infection was also tested in the presence of the mtROS scavenger ascorbic acid (Vitamin C). Interestingly, we show that the mtROS scavenging leads to an increased fungal growth only when *C. albicans* is infecting RVE but not when the fungus is growing on an abiotic surface. This result suggests that mtROS may be a key element of vaginal epithelial cell response to *C. albicans*.

Collectively, our data show that mtROS are differentially regulated by vaginal epithelial cells according to fungal burden, presence or hyphae and secretion of CL. It has been demonstrated that oral epithelial cells respond to CL treatment with a rapid production of mtROS, disruption of mitochondria activity and mitochondrial membrane potential, ATP depletion and cytochrome c release, demonstrating that oral epithelial cells respond to CL by triggering numerous cellular stress responses (Blagojevic et al., 2021). To the best of our knowledge, this is the first work that shows how a *Candida* strain whose production of candidalysin is impaired (Ca 529L), is weakened in its capacity to induce mtROS by RVE.

In line with to what observed in oral epithelial cells after CL treatment, our future work will be devoted to unravelling the precise role of mtROS activation in the interplay between vaginal epithelial cells and *Candida*.

4. MATERIALS AND METHODS

4.1 Microbial strains and growth conditions

The bioluminescent strain of *Candida albicans* CA1398 carrying the bioluminescence ACT1pgLUC59 fusion product (BLI-Ca) (Enjalbert et al., 2009) was chosen in order to use the relative luminescence units (RLU) to count the preformed hyphae, as detailed below in "Establishment of a standard curve to count BLI-Ca hyphae". The *Candida albicans* strain PCA-2 (Ca PCA-2), was employed because it is unable to undergo dymorphic transition (Bistoni et al., 1986). The *C. albicans* strain 529L (Ca 529L) was employed because of its impaired production of candidalysin (Rahman et al., 2007). The strains have been stored in frozen stocks at -80˚C in Sabouraud Dextrose Broth (Condalab, Spain) supplemented with 15% glycerol. Every six months strains were reactivated, subcultured and new frozen stocks were prepared. After thawing, the fungi were grown in liquid YPD medium (Yeast extract—Peptone—Dextrose, Scharlab S.L., Spain) and incubated at 37 °C under aerobic conditions for 24 h. Fungal cultures were maintained by passages onto SAB agar biweekly. For infection we employed two different protocols to produce yeasts or hyphae as detailed below.

4.2 Production of *C. albicans* yeasts

For the infection with yeasts, a loop of BLI-Ca, Ca PCA-2, or Ca 529L were seeded in 5 ml of YPD broth and incubated at 30 °C under agitation overnight. Then fungi were washed with PBS, counted with an heamocitometer by excluding dead cells with Trypan blue staining and resuspended to a working strength MOI 1:1 or 1:5 in DMEM-5% heat inactivated FBS with respect to vaginal cells.

4.3 Production of *C. albicans* hyphae

For the infection with hyphae, hyphal fragments were produced according to a protocol established by Hopke and Wheeler (Hopke and Wheeler, 2017). According to this protocol, chosen because it had been specifically set up for *C. albicans*, BLI-Ca and Ca 529L were seeded in 5 ml of YPD broth and grown at 30 °C under agitation overnight. Then fungi were washed, counted by heamocitometer to exclude dead cells with Trypan blue staining and resuspended in 35 ml of RPMI1640 at concentration of $2.5x10^6$/ml and distributed in 6 tubes, each containing 5 ml of fungal suspensions. Such tubes were incubated overnight under agitation at 30 °C. After incubation, fungi were washed, all the pellets were put together and resuspended in 1 ml of PBS.

To count BLI-Ca hyphae, 1 µl of coelenterazine (Synchem, 1 mg/ml) was added to 100 µl of BLI-Ca suspension and measured by Fluoroskan (ThermoFischer Scientific). The use of coelenterazine was necessary because such molecule is the natural substrate of luciferase enzyme occurring on the cell wall of BLI-Ca (Enjalbert et al., 2009). Only values of Relative Luminescence Units (RLU) substracted of the blank (a well containing 100 µl of PBS and 1 µl of coelenterazine), were used to calculate the CFU in reference to a standard curve previously established (as detailed below).

The OD_{570} values corresponding to 100 µl of either BLI-Ca or Ca 529L hyphae were analyzed by a spectrophotometer (SunRise Tecan). The CFU of Ca 529L were calculated by comparison to the BLI-Ca CFU values that had been estimated from the standard curve.

4.4 Establishment of a standard curve to count BLI-Ca hyphae

To quantify hyphal fragments by using luminescence emission, a calibration curve was generated. Serial dilutions of BLI-Ca hyphae were prepared. One hundred µl of each dilution was seeded in Sabouraud agar plates, incubated for 24–48 h at 30 °C and then the CFU were counted. The same dilutions were dispensed in the wells of a 96-well black microtiter plate (100 µl/well) and luminescent signal was read at Fluoroskan after addition of coelenterazine (1 µl/well, 1 mg/ml). The generated calibration curve allowed an estimation of the CFU from the RLU.

4.5 A-431 epithelial cells

The human epithelial A-431 cell line derived from a vaginal epithelial squamous cell carcinoma was used. The cell line was puchased from LGC Standards, catalogue number ATCC-CRL-1555. This cell line is widely employed to produce monolayers or multilayers mimicking the vaginal epithelium (Pekmezovic et al., 2021; Pericolini et al., 2017). These cells were cultured in DMEM medium (Dulbecco's Modified Eagle Medium, PAN Biotech) supplemented with L-glutamine (2 nM) (Euroclone SpA, Italy), penicillin (100 U/ml) (Euroclone SpA, Italy), streptomycin (100 µl/ml) (Euroclone SpA, Italy), ciprofloxacin (20 mg/ml) (Euroclone SpA, Italy) and heat-inactivated Fetal Bovine Serum (h.i. FBS, 10% or 5%, SIGMA-Aldrich, USA); specifically, medium containing 10% h.i. FBS was used to allow the establishment of the Reconstituted Vaginal Epithelium (RVE), whereas medium containing 5% h.i. FBS was used for the infection. The cell line was kept in culture by-passages in fresh medium twice a week and incubated at 37 °C and 5% CO_2.

4.6 Reconstituted vaginal epithelium (RVE) infection and mtROS production analysis

A-431 cells $5x10^5$/ml ($1x10^5$ in 200 µl/well) were grown in DMEM + 10% h.i. FBS for 5 days in a 96-well black-trasparent plates. At days 2 and 4 the medium was replaced with fresh medium. RVE was then infected with the different Ca strains (yeasts or hyphae) MOI 1:1 or 1:5. For the determination of mtROS production, MitoSOX™ Red (2.5 µM/well) (Invitrogen™, ThermoFisher Scientific) was added in each well immediately after infection. Then, the plates were kinetically measured every 5 min (5 min = 1 reading cycle) by Fluoroskan under stable temperature of 37 °C. The fluorescence emission was analyzed at excitation/emission 544/590.

In selected experiments, the antioxidant molecule ascorbic acid (Vitamin C, 1000 µM; Sigma Aldrich) (Guaiquil et al., 2001) was added during RVE infection with BLI-Ca yeasts (MOI 1:1) and then mtROS production has been kinetically analyzed as above described.

4.7 Analysis of cell damage

RVE was infected with Ca PCA-2 yeasts, BLI-Ca and Ca 529L yeasts or hyphae at both MOI 1:1 and MOI 1:5. Twenty-four hours post-infection, cell damage was quantified by the analysis of Lactate dehydrogenase (LDH) release in the growth medium by using a specific colorimetric kit (Abcam). In selected experiments, RVE was infected with BLI-Ca yeasts (MOI 1:1) in the presence or absence of ascorbic acid (Vitamin C, 1000 µM; Sigma Aldrich). After 24h of infection, cell damage was assessed by LDH kit.

4.8 Fungal growth

RVE was infected with BLI-Ca yeasts (MOI 1:1) in the presence or absence of ascorbic acid (Vitamin C, 1000 µM; Sigma Aldrich). After 24 h of infection, cells were lysed with 0.1% Triton X-100 and serial dilutions were performed for CFU counting. As a control, the same concentration of BLI-Ca yeasts was grown under the same experimental conditions but without RVE.

4.9 Statistical analysis

Shapiro-Wilk test was used to analyze the distribution of data within experimental groups. All statistical analyses were performed by using GraphPad Prism 10.3 software.

The statistical analysis of kinetic data was performed following the “GraphPad guide to comparing dose-response or kinetic curves” (Motulsky H., 1998). For each kinetic curve obtained in the

experimental procedures, the Area Under the Curve (AUC) was calculated to summarize the curve into a single value. Subsequently, statistical analysis was performed on the AUC values of each experimental group using unpaired *t*-test or a Mann-Whitney test (see Figure legends), depending on the distribution of data. Statistical differences between groups for non-kinetic data were assessed by One-Way ANOVA followed by Tukey's multiple-comparisons test.

Values of $*p<0.05$, $**p<0.01$, $***p<0.001$ and $****p<0.0001$ were considered statistically significant.

REFERENCES

Abuaita BH, Schultz TL, O'Riordan MX. 2018. Mitochondria-Derived Vesicles Deliver Antimicrobial Reactive Oxygen Species to Control Phagosome-Localized Staphylococcus aureus. Cell Host & Microbe 24:625–636.e5. pmid:30449314

Ardizzoni A, Wheeler RT, Pericolini E. 2021. It Takes Two to Tango: How a Dysregulation of the Innate Immunity, Coupled With Candida Virulence, Triggers VVC Onset. Front Microbiol 12:692491. pmid:34163460

Ayer A, Gourlay CW, Dawes IW. 2014. Cellular redox homeostasis, reactive oxygen species and replicative ageing in Saccharomyces cerevisiae. FEMS Yeast Res 14:60–72.

Bedard K, Krause K-H. 2007. The NOX Family of ROS-Generating NADPH Oxidases: Physiology and Pathophysiology. Physiological Reviews 87:245–313. pmid:17237347

Bistoni F, Vecchiarelli A, Cenci E, Puccetti P, Marconi P, Cassone A. 1986. Evidence for macrophage-mediated protection against lethal Candida albicans infection. Infect Immun 51:668–674. pmid:3943907

Blagojevic M, Camilli G, Maxson M, Hube B, Moyes DL, Richardson JP, et al. 2021. Candidalysin triggers epithelial cellular stresses that induce necrotic death. Cellular Microbiology 23. pmid:34085369

Chen Y, Azad MB, Gibson SB. 2009. Superoxide is the major reactive oxygen species regulating autophagy. Cell Death Differ 16:1040–1052. pmid:19407826

Clempus RE, Sorescu D, Dikalova AE, Pounkova L, Jo P, Sorescu GP, et al. 2007. Nox4 is required for maintenance of the differentiated vascular smooth muscle cell phenotype. Arterioscler Thromb Vasc Biol 27:42–48. pmid:17082491

Dikalov S. 2011. Cross talk between mitochondria and NADPH oxidases. Free Radical Biology and Medicine 51:1289–1301. pmid:21777669

Enjalbert B, Rachini A, Vediyappan G, Pietrella D, Spaccapelo R, Vecchiarelli A, et al. 2009. A multifunctional, synthetic Gaussia princeps luciferase reporter for live imaging of Candida albicans infections. Infect Immun 77:4847–4858. pmid:19687206

Foyer CH, Noctor G. 2005. Oxidant and antioxidant signalling in plants: a re-evaluation of the concept of oxidative stress in a physiological context. Plant Cell Environ 28:1056–1071.

Guaiquil VH, Vera JC, Golde DW. 2001. Mechanism of vitamin C inhibition of cell death induced by oxidative stress in glutathione-depleted HL-60 cells. J Biol Chem 276:40955–40961. pmid:11533037

Hopke A, Nicke N, Hidu EE, Degani G, Popolo L, Wheeler RT. 2016. Neutrophil Attack Triggers Extracellular Trap-Dependent Candida Cell Wall Remodeling and Altered Immune Recognition. PLoS Pathog 12:e1005644. pmid:27223610

Hopke A, Wheeler RT. 2017. In vitro Detection of Neutrophil Traps and Post-attack Cell Wall Changes in Candida Hyphae. Bio Protoc 7:e2213. pmid:28670603

Jabra-Rizk MA, Kong EF, Tsui C, Nguyen MH, Clancy CJ, Fidel PL, et al. 2016. Candida albicans Pathogenesis: Fitting within the Host-Microbe Damage Response Framework. Infect Immun 84:2724–2739. pmid:27430274

Knock GA. 2019. NADPH oxidase in the vasculature: Expression, regulation and signalling pathways; role in normal cardiovascular physiology and its dysregulation in hypertension. Free Radical Biology and Medicine 145:385–427. pmid:31585207

Liu J, Willems HME, Sansevere EA, Allert S, Barker KS, Lowes DJ, et al. 2021. A variant ECE1 allele contributes to reduced pathogenicity of Candida albicans during vulvovaginal candidiasis. PLoS Pathog 17:e1009884. pmid:34506615

Motulsky H. 1998. The GraphPad guide to comparing dose-response or kinetic curves. GraphPad Software, San Diego, CA.

Moyes DL, Murciano C, Runglall M, Islam A, Thavaraj S, Naglik JR. 2011. Candida albicans Yeast and Hyphae are Discriminated by MAPK Signaling in Vaginal Epithelial Cells. PLoS ONE 6:e26580. pmid:22087232

Moyes DL, Wilson D, Richardson JP, Mogavero S, Tang SX, Wernecke J, et al. 2016. Candidalysin is a fungal peptide toxin critical for mucosal infection. Nature 532:64–68. pmid:27027296

Mukaremera L, Lee KK, Mora-Montes HM, Gow NAR. 2017. Candida albicans Yeast, Pseudohyphal, and Hyphal Morphogenesis Differentially Affects Immune Recognition. Front Immunol 8:629. pmid:28638380

Murphy MP. 2009. How mitochondria produce reactive oxygen species. Biochem J 417:1–13. pmid:19061483

Naglik JR, Gaffen SL, Hube B. 2019. Candidalysin: discovery and function in Candida albicans infections. Current Opinion in Microbiology 52:100–109. pmid:31288097

Parascandolo A, Laukkanen MO. 2019. Carcinogenesis and Reactive Oxygen Species Signaling: Interaction of the NADPH Oxidase NOX1-5 and Superoxide Dismutase 1–3 Signal Transduction Pathways. Antioxid Redox Signal 30:443–486. pmid:29478325

Parums DV. 2022. Editorial: The World Health Organization (WHO) Fungal Priority Pathogens List in Response to Emerging Fungal Pathogens During the COVID-19 Pandemic. Med Sci Monit 28. pmid:36453055

Pekmezovic M, Dietschmann A, Gresnigt MS. 2022. Type I interferons during host–fungus interactions: Is antifungal immunity going viral? PLoS Pathog 18:e1010740. pmid:36006878

Pekmezovic M, Hovhannisyan H, Gresnigt MS, Iracane E, Oliveira-Pacheco J, Siscar-Lewin S, et al. 2021. Candida pathogens induce protective mitochondria-associated type I interferon signalling and a damage-driven response in vaginal epithelial cells. Nat Microbiol pmid:33753919

Pericolini E, Gabrielli E, Amacker M, Kasper L, Roselletti E, Luciano E, et al. 2015. Secretory Aspartyl Proteinases Cause Vaginitis and Can Mediate Vaginitis Caused by Candida albicans in Mice. mBio 6:e00724. pmid:26037125

Pericolini E, Gabrielli E, Ballet N, Sabbatini S, Roselletti E, Cayzeele Decherf A, et al. 2017. Therapeutic activity of a Saccharomyces cerevisiae-based probiotic and inactivated whole yeast on vaginal candidiasis. Virulence 8:74–90. pmid:27435998

Pericolini E, Perito S, Castagnoli A, Gabrielli E, Mencacci A, Blasi E, et al. 2018. Epitope unmasking in vulvovaginal candidiasis is associated with hyphal growth and neutrophilic infiltration. PLoS ONE 13:e0201436. pmid:30063729

Rahman D, Mistry M, Thavaraj S, Challacombe SJ, Naglik JR. 2007. Murine model of concurrent oral and vaginal Candida albicans colonization to study epithelial host–pathogen interactions. Microbes and Infection 9:615–622. pmid:17383212

Ren T, Zhu H, Tian L, Yu Q, Li M. 2020. Candida albicans infection disturbs the redox homeostasis system and induces reactive oxygen species accumulation for epithelial cell death. FEMS Yeast Research 20:foz081. pmid:31769804

Richardson JP, Mogavero S, Moyes DL, Blagojevic M, Krüger T, Verma AH, et al. 2018. Processing of Candida albicans Ece1p Is Critical for Candidalysin Maturation and Fungal Virulence. mBio 9. pmid:29362237

Ridge J, Muller J, Noguchi P, Chang EH. 1991. Dynamics of differentiation in human epidermoid squamous carcinoma cells (A431) with continuous, long-term gamma-IFN treatment. In Vitro Cell Dev Biol 27A:417–424. pmid:1712768

Roselletti E, Perito S, Sabbatini S, Monari C, Vecchiarelli A. 2019. Vaginal Epithelial Cells Discriminate Between Yeast and Hyphae of Candida albicans in Women Who Are Colonized or Have Vaginal Candidiasis. J Infect Dis 220:1645–1654. pmid:31300818

Russell CM, Rybak JA, Miao J, Peters BM, Barrera FN. 2023. Candidalysin: Connecting the pore forming mechanism of this virulence factor to its immunostimulatory properties. Journal of Biological Chemistry 299:102829. pmid:36581211

Sala A, Ardizzoni A, Spaggiari L, Vaidya N, Van Der Schaaf J, Rizzato C, et al. 2023. A New Phenotype in Candida -Epithelial Cell Interaction Distinguishes Colonization- versus Vulvovaginal Candidiasis-Associated Strains. mBio 14:e00107–23.

Sancho D, Enamorado M, Garaude J. 2017. Innate Immune Function of Mitochondrial Metabolism. Front Immunol 8:527. pmid:28533780

Sies H, Jones DP. 2020. Reactive oxygen species (ROS) as pleiotropic physiological signalling agents. Nat Rev Mol Cell Biol 21:363–383. pmid:32231263

Tiku V, Tan M-W, Dikic I. 2020. Mitochondrial Functions in Infection and Immunity. Trends in Cell Biology 30:263–275. pmid:32200805

Tsao S-M, Yin M-C, Liu W-H. 2007. Oxidant Stress and B Vitamins Status in Patients With Non-Small Cell Lung Cancer. Nutrition and Cancer 59:8–13. pmid:1792749

Weinberg SE, Sena LA, Chandel NS. 2015. Mitochondria in the Regulation of Innate and Adaptive Immunity. Immunity 42:406–417. pmid:25786173

Wenzel U. 2003. Ascorbic acid suppresses drug-induced apoptosis in human colon cancer cells by scavenging mitochondrial superoxide anions. Carcinogenesis 25:703–712.

West AP, Shadel GS, Ghosh S. 2011. Mitochondria in innate immune responses. Nat Rev Immunol 11:389–402. pmid:21597473

Zhao Y, Hu X, Liu Y, Dong S, Wen Z, He W, et al. 2017. ROS signaling under metabolic stress: cross-talk between AMPK and AKT pathway. Mol Cancer 16:79. pmid:28407774

CHAPTER 4

An Untargeted Metabolomic Analysis of *Lacticaseibacillus* (*L.*) *rhamnosus*, *Lactobacillus* (*L.*) *acidophilus*, *Lactiplantibacillus* (*L.*) *plantarum* and *Limosilactobacillus* (*L.*) *reuteri* Reveals an Upregulated Production of Inosine from *L. rhamnosus*

Luca Spaggiari[1], Natalia Pedretti[2], Francesco Ricchi[1], Diego Pinetti[3], Giuseppina Campisciano[4], Francesco De Seta[5], Manola Comar[4,6], Samyr Kenno[2], Andrea Ardizzoni[2] and Eva Pericolini[2]

[1] Clinical and Experimental Medicine Ph.D. Program, University of Modena and Reggio Emilia, 41125 Modena, Italy

[2] Department of Surgical, Medical, Dental and Morphological Sciences with Interest in Transplant, Oncological and Regenerative Medicine, University of Modena and Reggio Emilia, 41124 Modena, Italy;

[3] Centro Interdipartimentale Grandi Strumenti, University of Modena and Reggio Emilia, 41125 Modena, Italy;

[4] Institute for Maternal and Child Health-IRCCS, Burlo Garofolo, 34137 Trieste, Italy;

[5] Department of Obstetrics and Gynecology, IRCCS San Raffaele Scientific Institute, University Vita and Salute, 20132 Milan, Italy;

[6] Department of Medical Sciences, University of Trieste, 34129 Trieste, Italy.

***Microorganisms*. 2024, doi:10.3390/microorganisms12040662**

1. INTRODUCTION

Among probiotics, lactic acid bacteria are beneficial microbes for human health, when administered in adequate quantity (Latif et al., 2023; Ayvi et al., 2020). As with all probiotics, lactic acid bacteria have effects on microbial pathogens and on the host. Specifically, lactic acid bacteria compete with pathogens for nutrients and binding to receptors and they also produce antimicrobial molecules. Their beneficial effects on the host include improvement in epithelial barrier function (through the enhanced production of mucus and of tight junction proteins that help to prevent the passage of the pathogens to the blood), the modulation of dendritic cell and T-cell activity (immunomodulatory effects), and the regulation of the production and secretion of several neurotransmitters (Latif et al., 2023; Ayvi et al., 2020). In addition, lactic acid bacteria help to prevent and manage several pathological conditions, such as allergic diseases, cancer, hypercholesterolemia, irritable bowel syndrome, diarrhea, lactose intolerance, and inflammatory bowel disease (Latif et al., 2023; Tang and Lu, 2019). One of the main roles played by probiotic lactic acid bacteria is to help the recovery of the eubiosis state in the host. However, the way this goal is achieved is partly unknown. In particular, the precise role of the metabolites produced by specific bacteria during their life cycle and their impact on the environment where they proliferate is yet to be elucidated. In addition, it must be considered that the use of living bacteria in vulnerable people is linked to possible safety concerns; also, maintaining bacterial viability is a challenging task (Huang et al., 2022). Interestingly, new scientific evidence points out that the health benefits granted by lactic acid bacteria are not necessarily related to viable bacteria. Indeed, their metabolites or bacterial components, collectively indicated as postbiotics, may also be the driving force behind health promotion. Postbiotics have been shown to have several biological activities (antimicrobial, antioxidant, anti-inflammatory, anti-proliferative, and immunomodulatory). Moreover, numerous studies have suggested the significant potential of postbiotics for disease treatment (Liang and Xing, 2023). The metabolites produced by lactic acid bacteria can inhibit the growth of pathogens (Alvarez-Sieiro et al., 2016; Murphy et al., 2013). In addition, during the interaction with the host and other microorganisms that dwell in the same host niche, the metabolites produced by “beneficial microbes” such as lactic acid bacteria may exert a significant impact to counteract the infection process (Mosca et al., 2022; Alonso-Roman et al., 2022). Similarly to the living bacteria, the metabolites produced by probiotics have been demonstrated to have many beneficial effects on the host, such as improvement in barrier function, (stimulating the enhanced production of tight junctions’ proteins and mucous), the promotion of changes in the microbiota composition, and immunomodulatory and anti-inflammatory activities (Mosca et al., 2022; Thoda and Touraki, 2023). Since postbiotics are made up of inactivated microbial cells and/or cell components, their employment is characterized by higher levels of stability and safety for the user.

Consequently, interest is increasing in their possible therapeutic employment, because they can be considered an inexhaustible source of possible new bioactive substances (Abdul Hakim et al., 2023). We recently showed that cell-free supernatants (CFS) obtained from *Lacticaseibacillus rhamnosus* (*L.* RHA), *Lactobacillus acidophilus* (*L.* AC), *Lactiplantibacillus plantarum* (*L.* PLA), and *Limosilactobacillus reuteri* (*L.* REU) can impair *Candida parapsilosis* (C. *parapsilosis*) pathogenic potential in an *in vitro* model of epithelial vaginal infection (Spaggiari et al., 2022). This effect could be ascribed to the direct effect of lactic acid bacteria on *Candida* virulence, and to the production of their metabolites that are able to weaken *C. parapsilosis* virulence (Spaggiari et al., 2022). Moreover, it has been recently shown that *L.* RHA can impair *C. albicans* pathogenicity in a model of intestinal epithelial infection. In this work, Alonso-Roman and coworkers showed that *L.* RHA growth alters the intestinal metabolic environment by removing *Candida* nutrient sources, forcing metabolic changes in *C. albicans* (Alonso-Roman et al., 2022). This suggests that the host niche colonization by specific bacteria can antagonize potential microbial pathogens by reshaping the metabolic environment and forcing microbial adaptation. Therefore, by improving our knowledge of the metabolome of beneficial microorganisms that can act within specific host niches, novel important information becomes available on the mechanisms they use to interact with the resident microbiota and with the host cells. For this reason, here, an untargeted metabolomics approach was applied to compare the metabolome of four different lactic acid bacteria often used as probiotics: *L.* RHA, *L.* AC, *L.* REU, and *L.* PLA. Our data show that such metabolomes are significantly different, resulting in an increased production of some specific metabolites, such as inosine, from *L.* RHA. Since inosine can exert antioxidant, anti-inflammatory, and neuroprotective effects (Doyle et al., 2018), other than displaying relevant properties in the prokaryotic metabolisms, our data suggest that the overproduction of inosine by *L.* RHA could have a positive impact on the host and even on its resident microbiota. By employing an untargeted metabolomic approach, the present study shows that it is possible to predict the presence of compounds with potentially relevant biological activity, therefore accelerating knowledge regarding postbiotics. Indeed, although inanimate, postbiotics may provide health benefits comparable or even higher with respect to probiotics. Postbiotics include a wide range of microbial metabolites that could potentially produce complex beneficial effects by interacting with both resident microbiota and host cells. In addition, postbiotics could be considered as potentially novel therapeutics tools, even though evidence of the effect of postbiotics on microbiota and host cells is scant.

2. MATERIALS AND METHODS

2.1 Lactic Acid Bacterial Strains and Growth Conditions

Four different lactic acid bacterial strains were employed in this study: *Lactobacillus acidophilus* ATCC 314, *Limosilactobacillus reuteri* DSM 17938, *Lacticaseibacillus rhamnosus* ATCC 7469, and *Lactiplantibacillus plantarum* ATCC 8014. The bacterial colonies were inoculated in 5 mL of MRS liquid medium (De Man, Rogosa and Sharpe, Oxoid LTD, Basingstoke, UK) and incubated for 24 h at 37 °C, under agitation. After incubation, bacteria were centrifuged at 2300× g at RT for 5 min, washed twice with PBS (Sial group), counted, and resuspended at 1×10^8/mL in 5 mL of MRS broth and incubated for 24 h at 37 °C under agitation. After incubation, the cell-free supernatants (CFS) were prepared as detailed below.

2.2 Preparation of Cell-Free Supernatants (CFS) from Lactic Acid Bacterial Strains

The cell-free supernatants (CFS) were obtained by centrifugation of the bacterial suspensions carried out at 3000× *g*, at 4 °C for 15 min. The supernatants were then collected and filtered with 0.22 μm syringe filters (Corning Incorporated, Wiesbaden, Germany). Potential bacterial contamination of CFS was excluded by incubating 1 mL of each CFS at 37 °C and checking the turbidity (from 24 h to 72 h) by optical density (OD) assessment through spectrophotometer (SunRise, Tecan). The pH of each CFS was measured by a pH meter (Hanna Instrument, Villafranca Padovana, Italy), returning an average pH = 4, as previously described (Spaggiari et al., 2022). The control samples consisted of sterile MRS medium (blank). The CFS obtained were finally stored at −80 °C until their use.

2.3 Liquid Chromatography–Electrospray/High-Resolution Mass Spectrometry (HPLC-ESI/HRMS)

The CFS, which had been stored at −80 °C, were thawed and centrifuged at 18,000× *g* for 10 min. Subsequently, the CFS were transferred to Amicon-Ultra 0.5 tubes, centrifuged at 18,000× g for 15 min, and then transferred into the autosampler vials pending analysis. The Quality Control pool samples (QC) were prepared by mixing equal volumes of each cohort supernatant and used to minimize technical data variance (Fan et al., 2019).

The analyses were performed using an Ultimate 3000 HPLC connected to a QExactive High-Resolution Mass spectrometer via a HESI-II electrospray ionization source (Thermo Scientific, Waltham, MA, USA), controlled by Xcalibur software (Thermo Scientific, v. 29 build 2926). A 10

µL volume of sample solution was injected onto a Hypersil Gold C18 100 × 2.1 mm ID 1.9 µm ps column (Thermo Scientific) kept at 30 °C and separation was performed at 0.4 mL/min flow with a gradient elution scheme using methanol (Fisher Chemicals, Hampton, NH, USA) (B) and 0.1% formic acid (Carlo Erba, Cornaredo, Italy) in water (A). The mobile phase composition was kept at 2% B for 1 min after injection then linearly raised to 42% B in 60 min and further on to 98% B in 5 min. Methanol was kept at 98% up to minute 74.9, then lowered to 2% at minute 75. The total runtime was 90 min. ESI source was operated in both positive and negative ionization mode. Capillary temperature was set at 320 °C; the following nitrogen flows (arbitrary units) were used to assist the ionization: Sheath Gas 45, Aux Gas 25 (at 290 °C), Sweep Gas 2. The capillary voltage was set to 3.8 kV (3.4 kV for negative ionization) and S-Lens RF level was set at 45 (arbitrary units).

A Data-Dependent Acquisition (DDA) strategy was used to acquire MS2 fragmentation spectra of the Top 5 singly charged precursor ions revealed in Full Scan MS experiments. Positive and Negative ionization DDA experiments were performed in separate analyses. Full MS spectra were obtained from m/z 100 to 1500 at 70,000 FWHM resolving power using an automatic gain control (AGC) of 3 × 106 and a maximum Injection Time (max IT) of 250 ms. Fragmentation Spectra (MS2) acquisition was performed at 17,500 FWHM, with 2 × 105 AGC target and 120 ms max IT. The isolation window for precursor ion selection was set at 1.0 Th and HCD normalized collision energy (NCE) was stepped at 20, 50, and 80. Fragmented precursors were dynamically excluded for 6 s. Inosine standard was purchased from Sigma-Aldrich, St. Louis, MO, USA. The data are from triplicate samples from 3 different experiments.

2.4 Compounds Discoverer Data Analysis

Raw files (triplicate samples from 3 different experiments) were processed by Compound Discoverer (CD) 3.3.2.31 (Copyright 2014-2023 Thermo Fisher Scientific Inc.) using a slightly modified processing workflow template for Untargeted Metabolomics with Statistics Detect Unknowns with ID Using Local Databases. The core of the workflow consisted of Spectra selection from raw files (Retention Time limited from 0.2 to 75 min), Retention Time Alignment (ChromAlign) with respect to a QC sample file, and Compound Detection and Grouping with RT tolerance of 0.3 min and 5 ppm mass deviation. Then, Gap Filling, SERRF QC Correction, and Background removal were performed along with Compound Annotation using Predicted Composition and different types of databases (mzCloud, Metabolika, Human Metabolome Database, ChemSpider, BioCyc) (Züllig et al., 2020). The so-detected compounds were used for differential analysis of sample groups (Nested Design; Generated Ratios: lactobacilli PLA/AC, REU/AC, RHA/AC, REU/PLA, RHA/PLA, and RHA/REU).

3. RESULTS

Here, an untargeted metabolomics approach was used to compare the metabolomes from four different lactic acid bacteria, often used as probiotics: *L. rhamnosus* (*L.* RHA), *L. acidophilus* (*L.* AC), *L. plantarum* (*L.* PLA), and *L. reuteri* (*L.* REU). Principal Component Analysis (PCA)-2 showed that the metabolomes differed between *L.* RHA and the other species, as well as between *L.* AC and the other lactic acid bacteria. Conversely, the metabolomes of *L.* PLA and *L.* REU were found to be similar (Figure 1).

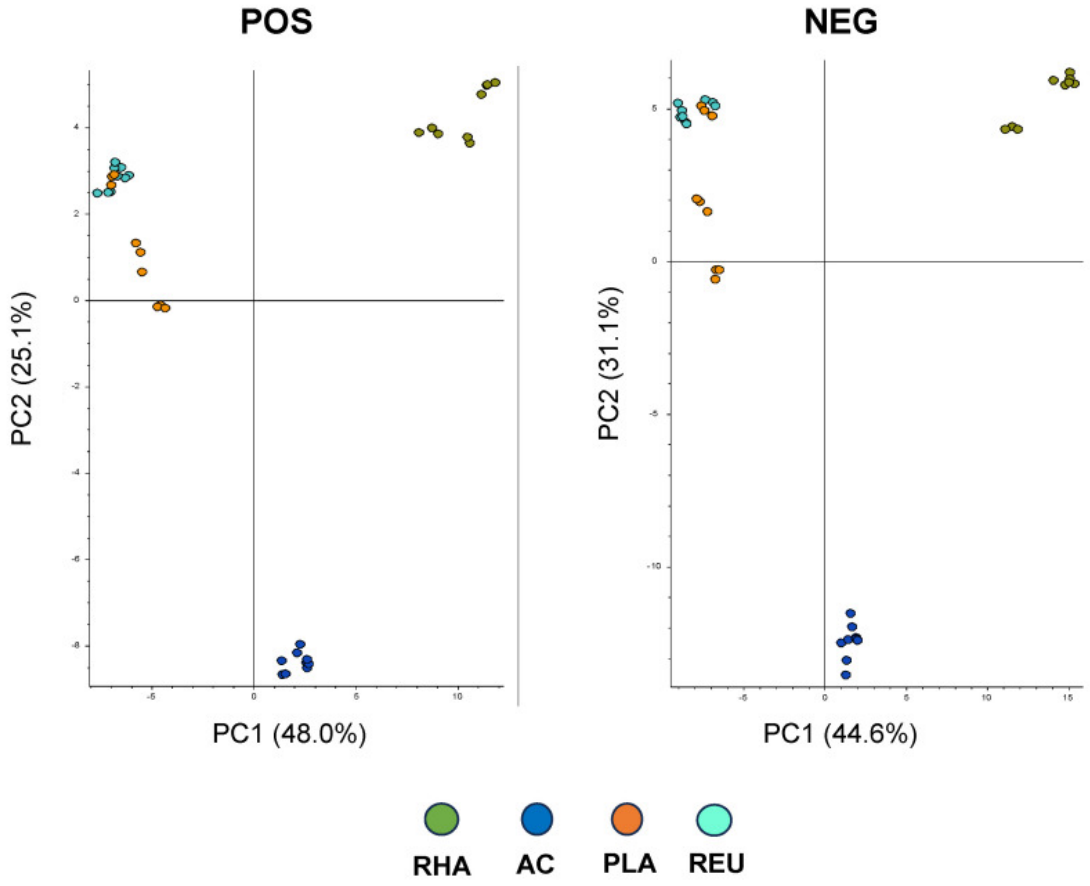

Figure 1
Principal Component Analysis (PCA)-2 of the metabolomes from *L.* RHA, *L.* AC, *L.* PLA, and *L.* REU analyzing in both positive and negative ionization modes. Data are from triplicate samples from 3 different experiments.

A hierarchical clustering analysis, carried out to compare the four metabolomes, revealed a distinct cluster of metabolites overexpressed in the CFS of the different lactic acid bacteria. Once again, *L.* PLA and *L.* REU showed similar metabolome profiles; differently, *L.* RHA and *L.* AC showed a more peculiar metabolome profile (Figure 2). Specifically, *L.* RHA and *L.* AC revealed areas of significantly overexpressed metabolites (p value < 0.01; Log_2 fold change = 2) that strongly differed from the same areas from the other lactic acid bacteria (Figure 2, see red line for *L.* RHA and yellow line for *L.* AC).

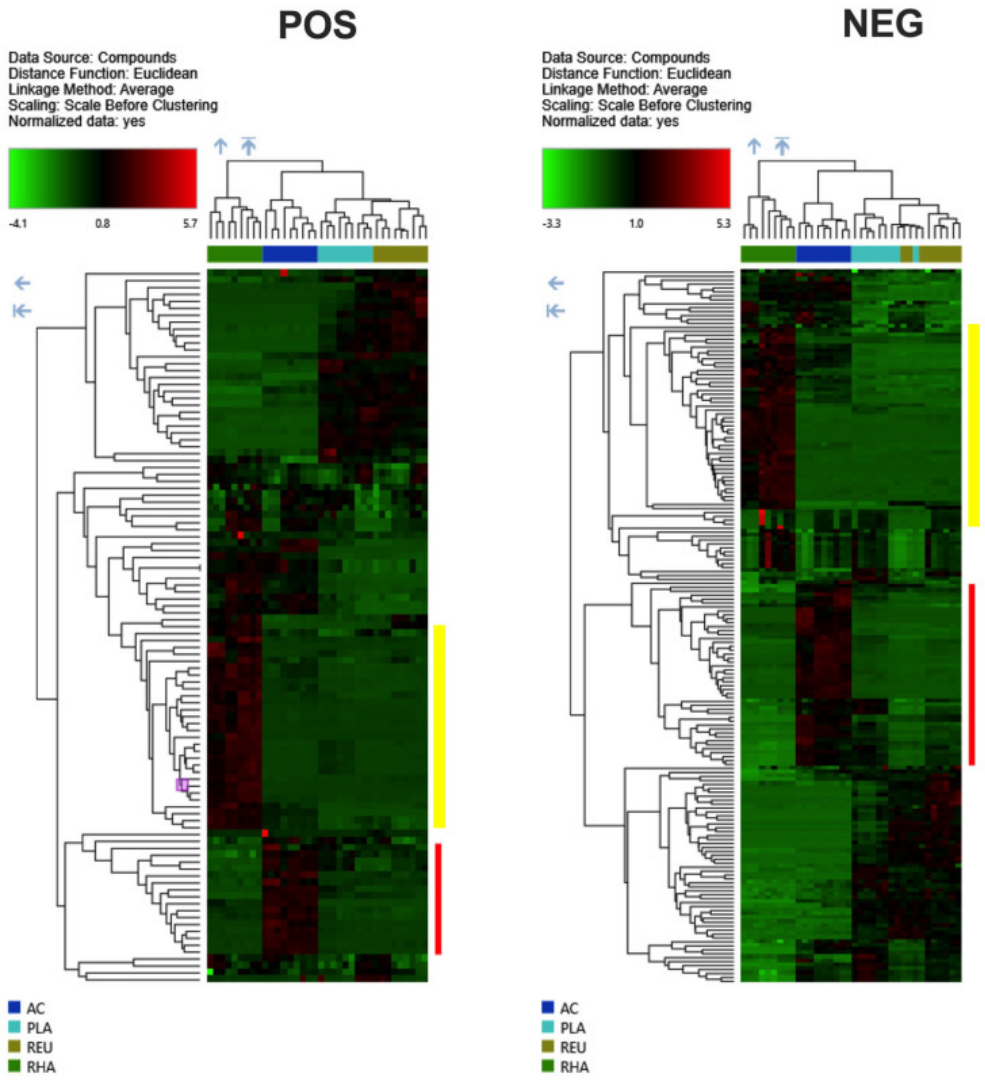

Figure 2
Hierarchical clustering analysis in positive (**left panel**) and negative (**right panel**) ionization mode, carried out to compare the metabolome from *L.* RHA, *L.* AC, *L.* PLA, and *L.* REU according to Compound Discoverer (CD) 3.3.2.31 analysis. Yellow line for *L.* RHA and red line for *L.* AC highlight the distinct cluster of metabolites overexpressed in the respective CFS as compared to the other lactic acid bacteria CFS. Data are from triplicate samples from 3 different experiments.

Therefore, we performed a more detailed analysis of the metabolites included in these specific areas of *L.* RHA and *L.* AC. The identified overexpressed compounds in these areas returned different levels of identification according to the Annotation Sources used by the CD software 3.3.2.31 and listed in Tables 1–4. Only those compounds that the software assigned a name to are reported in Tables 1–4.

Compound Name	Predicted Composition	mzCloud Search	mzValue Search	Metabolika Search	ChemSpider Search	MassList Search
Mevalonolactone	Full Match	Full Match	-	Partial Match	Full Match	Partial Match
N-α-L-Acetyl-arginine	Full Match	Full Match	-	-	Full Match	Full Match
(Ac)2-L-Lys-D-Ala	Full Match	-	-	-	Full Match	-
Inosine	**Full Match**	**Full Match**	**Full Match**	**Full Match**	**Partial Match**	**Partial Match**
(2S,4S)-4-Amino-2-hydroxy-2-methylpentanedioic acid	Full Match	-	-	-	Full Match	-
Confluenine A	Full Match	-	-	-	Partial Match	Full Match
Ala-Leu	Full Match	-	-	-	Full Match	-
O-Succinyl-L-homoserine	Full Match	-	-	Partial Match	Partial Match	Full Match
N-Acetyl-L-leucine	Full Match	Full Match	-	-	Full Match	Full Match
(+)-Flavipucine	Full Match	-	-	-	Partial Match	Full Match
2-(2-amino-3-methylbutanamido)-3-phenylpropanoic acid	Full Match	Full Match	-	-	Partial Match	Partial Match
Acetyl-L-carnitine	Full Match	-	-	-	Partial Match	Full Match
methyl 4-(3,4-dihydroxybenzamido)butanoate	Full Match	-	-	-	-	Full Match
3-amino-4,5,6-trihydroxy-2-methoxy-5-methyl-2-cyclohexen-1-one	Full Match	-	-	-	Partial Match	Full Match
(2S)-2-{[1-(R)-Carboxyethyl]amino}pentanoate	Full Match	-	-	-	Partial Match	Full Match
2-Amino-5-methyl-5-hexencarbonsaeure	Full Match	-	-	-	Partial Match	Full Match
(1S,2R,8aS)-1,2-Dihydroxyindolizidine	Full Match	-	-	-	Full Match	Full Match

Table 1
L. RHA overexpressed compounds identified in positive ionization mode according to Compound Discoverer (CD) 3.3.2.31 analysis. The table includes only those molecules to which the software could assign a name. The dash indicates no results or invalid mass. Data are from triplicate samples from 3 different experiments. The color code mirrors the color code of the software.

Compound Name	Predicted Composition	mzCloud Search	mzValue Search	Metabolika Search	ChemSpider Search	MassList Search
Acetylcholine	Full Match	Full Match	-	-	Partial Match	Full Match
N-Acetyl-S-2-hydroxyethyl-L-cysteine	Full Match	-	-	-	Full Match	-
Palmyrrolinone	Full Match	-	-	-	Partial Match	Full Match
Indole-3-lactic acid	-	Full Match	-	Partial Match	Full Match	Full Match
Gaburedin A	Full Match	-	-	-	Partial Match	Full Match
3-amino-4,5,6-trihydroxy-2-methoxy-5-methyl-2-cyclohexen-1-one	Full Match	-	-	-	Partial Match	Full Match
Louisianin B	Full Match	-	-	Partial Match	Partial Match	Full Match
γ-L-glutamyl-L-leucine	-	-	-	-	-	Full Match
Sistodiolynne	Full Match	-	-	Partial Match	Partial Match	Full Match
Quinoline-2-methanol	Full Match	-	-	-	Partial Match	Full Match

Table 2
L. AC overexpressed compounds identified in positive ionization mode according to Compound Discoverer (CD) 3.3.2.31 analysis. The table includes only those molecules to which the software could assign a name. The dash indicates no results or invalid mass. Data are from triplicate samples from 3 different experiments. The color code mirrors the color code of the software.

Compound Name	Predicted Composition	mzCloud Search	mzValue Search	Metabolika Search	ChemSpider Search	MassList Search
Mevalonic acid	-	-	-	-	-	-
O-Succinyl-L-homoserine	Full Match	-	-	Partial Match	Partial Match	Full Match
N-Acetyl-D-alloisoleucine	-	-	-	-	-	-
O-Succinyl-L-homoserine	Full Match	-	-	Partial Match	Partial Match	Full Match
N-Acetylvaline	-	-	-	-	-	-
Birnbaumin A	Full Match	-	-	-	-	Full Match
methyl 4-(3,4-dihydroxybenzamido)butanoate	Full Match	-	-	-	-	Full Match
3,11-dihydroxy-6,8-dimethyldodecanoic acid	Full Match	-	-	-	-	Full Match
Ala-Leu	-	-	-	-	Full Match	-
Taurochenodeoxycholic acid	-	-	-	-	-	-
Phenamide	Full Match	-	-	-	Partial Match	Full Match
Lorbamate	Full Match	-	-	-	Full Match	-
Pochonicine	Full Match	-	-	-	-	Full Match

Table 3
L. RHA overexpressed compounds identified in negative ionization mode according to Compound Discoverer (CD) 3.3.2.31 analysis. The table includes only those molecules to which the software could assign a name. The dash indicates no results or invalid mass. Data are from triplicate samples from 3 different experiments. The color code mirrors the color code of the software.

Compound Name	Predicted Composition	mzCloud Search	mzValue Search	Metabolika Search	ChemSpider Search	MassList Search
3-Phenyllactic acid	-	-	-	-	-	-
DL-4-Hydroxyphenyllactic acid	-	Full Match	Full Match	Full Match	-	-
2-Hydroxycaproic acid	-	-	-	-	-	-
2-Hydroxyvaleric acid	-	-	-	-	-	-
trans-Cinnamic acid	-	-	-	-	-	-
(+)-Flavipucine	Full Match	-	-	-	Partial Match	Full Match
Indole-3-lactic acid	-	Full Match	-	Partial Match	-	-
zidometacin	Full Match	-	-	-	Full Match	-
(+)-(17R)-apralactone A	Full Match	-	-	-	-	Full Match
2-Oxoglutaric acid	-	-	-	-	-	-
N-Acetyl-L-glutamine	-	Full Match	Full Match	-	-	-
2-Hydroxycinnamic acid	-	-	-	-	-	-
Pochonicine	Full Match	-	-	-	-	Full Match
Peniamidone B	Full Match	-	-	-	-	Full Match
2-Methoxyestradiol	-	-	-	-	-	-
Hopantenic acid	Full Match	-	-	-	Full Match	-
Pantetheine	Full Match	-	-	-	Partial Match	-
methyl 4-(3,4-dihydroxybenzamido)butanoate	Full Match	-	-	-	-	Full Match

Table 4
L. AC overexpressed compounds identified in negative ionization mode according to Compound Discoverer (CD) 3.3.2.31 analysis. The table includes only those molecules to which the software could assign a name. The dash indicates no results or invalid mass. Data are from triplicate samples from 3 different experiments. The color code mirrors the color code of the software.

According to the results of the analysis, inosine from *L.* RHA CFS returned the best identification profile, since it returned four Full Matched and two Partial Matches according to the Annotation Sources as shown in Table 1. Concerning *L.* AC, we found two compounds with a very good identification profile (three Full Matches and one Partial Match): Acetylcholine and Indole-3-lactic acid.

Table 5 shows the identified pathways that included inosine. For each pathway, the mapped and matched compounds and the total compounds in the pathway are shown.

Compound Name	Formula	n° Identified Pathways	Pathways	Mapped Compounds	Matched Compounds	Compoundsin Pathways
Inosine	$C_{10}H_{12}N_4O_5$	1	Superpathway of purine nucleotide salvage	14	10	54
		2	Purine nucleotides degradation II (aerobic)	12	8	27
		3	Purine nucleotides degradation I (plants)	10	7	23
		4	Superpathway of purine degradation in plants	10	7	34

Table 5
Inosine identified pathways according to Compound Discoverer (CD) 3.3.2.31 analysis. Data are from triplicate samples from 3 different experiments.

Interestingly, this molecule has also a well-known biological role. Indeed, inosine is a key intracellular energy substrate for nucleotide synthesis by salvage pathways and it possesses cell protective activity and cell repair properties (Shafy et al., 2012).

To increase the identification confidence over inosine, from probable to possibly confirmed structure (Schymansky et al., 2014), an inosine reference standard solution was used to confirm the $[M+H]^+$ molecular ion mass-to-charge ratio, along with its fragmentation spectrum and retention time (Figures 3 and 4).

Once the identification was confirmed, inosine from *L.* RHA CFS was quantified using a set of calibration samples obtained by adding a proper amount of inosine to MRS covering from 1 to 50 μg/mL concentration range. Inosine of the *L.* RHA sample was quantified in the range of 5–8 μg/mL.

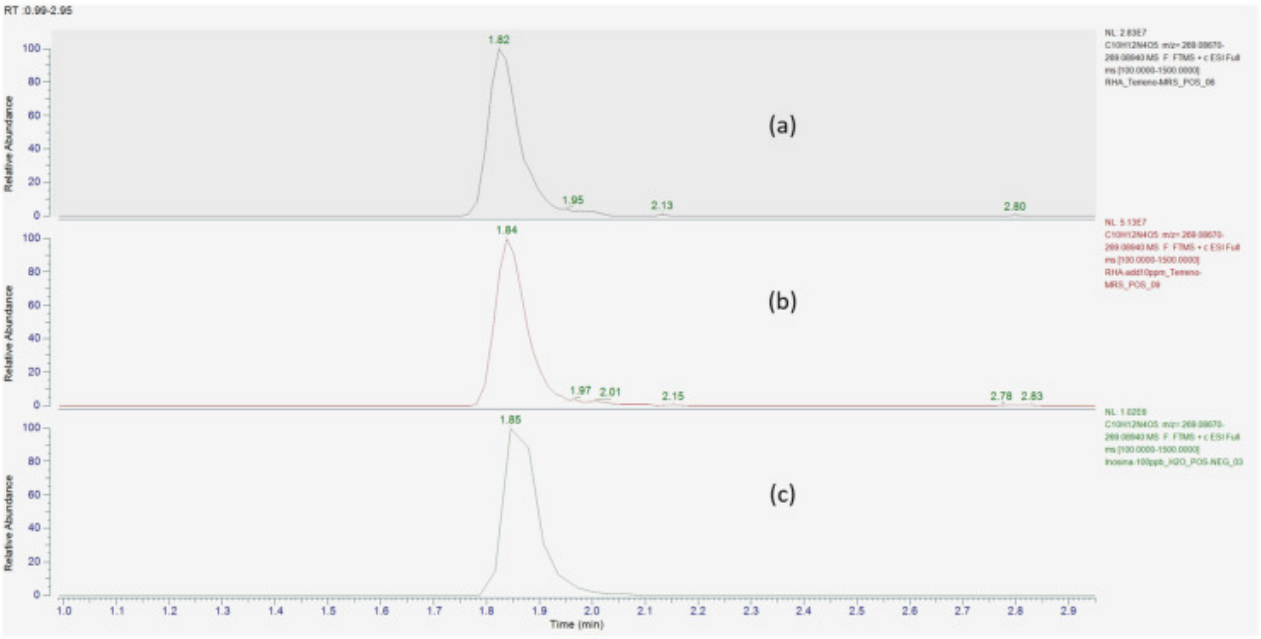

Figure 3
Extracted ion chromatogram of inosine ($C_{10}H_{12}N_4O_5$) theoretical $[M+H]^+$ molecular ion at m/z = 269.08805 (±5 ppm) in (**a**) *L.* RHA CFS, (**b**) *L.* RHA CFS spiked with inosine, and (**c**) inosine standard solution.

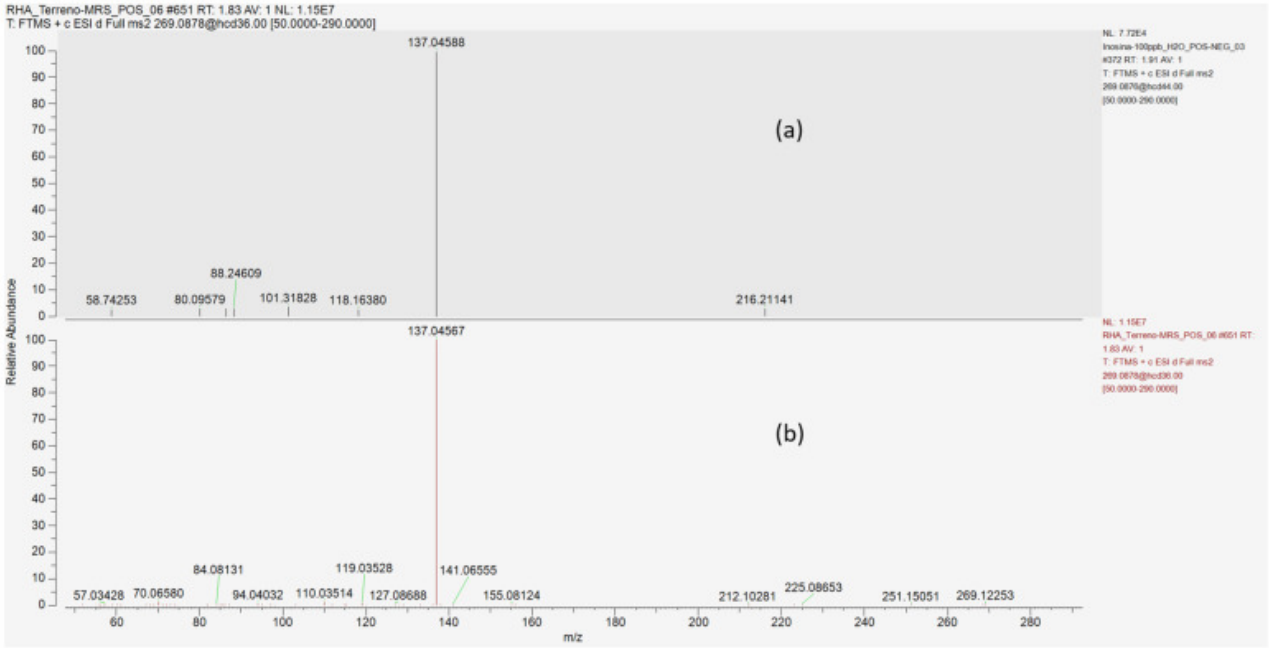

Figure 4
Comparison of HCD fragmentation spectra of m/z = 269.08805 precursor ion at 1.83 min in (**a**) inosine standard solution and (**b**) *L.* RHA CFS.

4. DISCUSSION

Lactic acid bacteria are beneficial microbes, and they are often used as probiotics. The concept of probiotics has been evolving, with the currently accepted definition being "living microorganisms that can benefit the host when consumed in sufficient quantities" (Sanders et al., 2019). Although this definition implies that microorganisms must be viable to be beneficial, increasing evidence suggests that microbial products can also provide benefits to the host (De Almada et al., 2018; Vallejo-Cordoba et al., 2020). Indeed, the so-called postbiotics, also known as metabolites, biogenic or cell-free supernatants (CFS), are defined as "soluble factors secreted by living bacteria or released by bacterial lysis", and their role in providing health benefits to the host has been reported (Martín and Langella, 2019). Hence, today, it is acknowledged that the beneficial effects of lactic acid bacteria are based either on living bacteria (the "probiotics") or on their metabolites/cell lysates (the "postbiotics"). Here, we assess the metabolomic profiles of four different lactic acid bacteria, currently used as safe probiotics: *L.* RHA, *L.* AC, *L.* PLA, and *L.* REU (Zhao et al., 2021). An untargeted metabolomic approach was employed to compare the differences in metabolite production in the CFS from the different lactic acid bacteria under the same culture conditions. Specifically, hierarchical clustering analysis of the compounds released by the four lactic acid bacteria shows for *L.* RHA and *L.* AC specific areas of significantly overexpressed metabolites, which strongly differ from the same areas of the other lactic acid bacteria. It has been shown that CFS from *L.* RHA strain SCB0119 altered the transcription profiles of several genes involved in fatty acid degradation, ion transport, and the biosynthesis of amino acids in *Escherichia coli*, as well as fatty acid degradation, protein synthesis, DNA replication, and ATP hydrolysis in *Staphylococcus aureus*, which are important for bacterial survival and growth (Peng et al., 2022). In addition, *L.* RHA colonization of the epithelial cells has been demonstrated as being responsible for drastic changes in the metabolic environment, forcing metabolic adaptation in *C. albicans* and reducing fungal virulence (Alonso-Roman et al., 2022). Furthermore, antimicrobial properties of *L.* RHA have also been described against *Listeria monocytogenes* (Iglesisas et al., 2017) and *Salmonella* spp. (Muyyarikkandy and Amalaradjou, 2017; Burkholder and Bhunia, 2009). *L.* AC has been found to play important roles in many aspects of human health. It favors the eubiosis of the host intestinal tract through the production of metabolites. Among the molecules produced by *L.* AC, lactic acid is important to reduce the pH, which, in turn, inhibits the growth and virulence of pathogenic bacteria (Gao et al., 2022).

Therefore, according to all the above-mentioned literature data, reporting the antimicrobial activity of *L.* RHA and *L.* AC (Gao et al., 2022; Coman et al., 2014; Song and Lee, 2017; Chew et al., 2015), a detailed investigation was carried out to obtain more information on metabolite overexpressed by

these species. Among the overexpressed compounds, we identified inosine from the CFS of *L.* RHA as the molecule with the best identification profile. We also identified four molecular pathways, including inosine, that could be investigated in future studies. Inosine is a non-canonical nucleotide, mainly occurring in the form of a monophosphate. It base pairs with deoxythymidine, deoxyadenosine, and deoxyguanosine (Alseth et al., 2014). Among the possible roles of such an unconventional nucleotide, it has been reported that the incorporation of inosine in place of guanine modulates translational events (Licht et al., 2019). Several studies carried out in various neuronal cell types have identified the growth-promoting activity of inosine, comparable to that induced by canonical neurotrophic factors such as brain-derived neurotrophic factor (BDNF) or nerve growth factor (NGF) (Benowitz et al., 1998; Irwin et al., 2006). Benowitz and colleagues have shown that inosine promotes axon outgrowth in a rat model of corticospinal tract injury (Benowitz et al., 1999). Furthermore, inosine has been demonstrated to modulate several biological processes through the adenosine receptors, such as the enhancement of neurite outgrowth in depressive disorders (Muto et al., 2014). Because of its antioxidant, anti-inflammatory, pro-axogenic, and neuroprotective functions, inosine is also employed as a therapeutic supplement, and it is prescribed in cases of nerve injury, inflammation, and oxidative stress (Doyle et al., 2018; Haskó et al., 2004). In addition, several drugs used in the treatment of autoimmune and inflammatory diseases (such as adenosine kinase inhibitors) exert their beneficial effects by releasing adenosine (Haskó et al., 2000). Since the latter is readily degraded to inosine in the extracellular space, the direct involvement of inosine in the anti-inflammatory effects of these adenosine-releasing agents is conceivable (Haskó et al., 2000). Inosine has also immunomodulatory effects by contributing to the efficacy of Isoprinosine (inosine pranobex), a synthetic agent formed by inosine combined with the immunostimulant dimepranol acedoben (acetamidobenzoic acid and dimethylaminoisopropanol). Even though many of the biological actions of inosine (particularly in the context of microbial infections) have yet to be described, this molecule is already employed for the treatment of acute respiratory viral infections, genital warts, herpes simplex infections, hepatitis B, and subacute sclerosing panencephalitis (Doyle et al., 2018). Inosine is used also for the treatment of sepsis in infections, and it has been shown to reduce systemic inflammation, organ damage, tissue dysoxia, and vascular dysfunction, resulting in improved survival in a mouse model of septic shock (Liaudet et al., 2001). Therefore, according to our preliminary *in vitro* data demonstrating that *L.* RHA produces biologically significant amounts of inosine, future studies will be devoted to assessing if inosine production also occurs *in vivo*. In addition, it will be necessary to confirm its anti-inflammatory, antioxidant, and antimicrobial activities in *ex vivo* and *in vivo* infection models. The overproduction of inosine by *L.* RHA in an *in vivo* setting might explain the beneficial effect of *L.* RHA as a probiotic because it might set off a

complex intertwining network (where inosine could be one of the key players within the several pathways identified) with beneficial effects on both resident microbiota and host cells.

5. CONCLUSIONS

In conclusion, here, we show that *L.* RHA overproduces inosine during its life cycle, and this might have a significant impact when administered *in vivo*. The data shown in the present manuscript were generated by an *in vitro* experimental system, supplemented by an extremely thorough *in silico* metabolomic analysis. The limitation of the present study is that the analysis was carried out with only one *L.* RHA strain. For this reason, future studies are warranted to confirm if such an overproduction of inosine can also be observed in other *L.* RHA strains. In addition, it will be important to translate these very interesting preliminary results in *ex-vivo* systems. Furthermore, it will be important to assess and contextualize the effects of inosine produced by *L.* RHA in infection models. Finally, our experimental approach should be applied to the study of the metabolome of other lactic acid bacteria to identify metabolites involved in their postbiotic activities.

REFERENCES

Abdul Hakim, B.N.; Xuan, N.J.; Oslan, S.N.H. A Comprehensive Review of Bioactive Compounds from Lactic Acid Bacteria: Potential Functions as Functional Food in Dietetics and the Food Industry. Foods 2023, 12, 2850.

Alonso-Roman, R.; Last, A.; Mirhakkak, M.H.; Sprague, J.L.; Möller, L.; Großmann, P.; Graf, K.; Gratz, R.; Mogavero, S.; Vylkova, S.; et al. Lactobacillus rhamnosus Colonisation Antagonizes Candida albicans by Forcing Metabolic Adaptations That Compromise Pathogenicity. Nat. Commun. 2022, 13, 3192.

Alseth, I.; Dalhus, B.; Bjørås, M. Inosine in DNA and RNA. Curr. Opin. Genet. Dev. 2014, 26, 116–123.

Alvarez-Sieiro, P.; Montalbán-López, M.; Mu, D.; Kuipers, O.P. Bacteriocins of Lactic Acid Bacteria: Extending the Family. Appl. Microbiol. Biotechnol. 2016, 100, 2939–2951.

Ayivi, R.D.; Gyawali, R.; Krastanov, A.; Aljaloud, S.O.; Worku, M.; Tahergorabi, R.; Silva, R.C.D.; Ibrahim, S.A. Lactic Acid Bacteria: Food Safety and Human Health Applications. Dairy 2020, 1, 202–232.

Benowitz, L.I.; Goldberg, D.E.; Madsen, J.R.; Soni, D.; Irwin, N. Inosine Stimulates Extensive Axon Collateral Growth in the Rat Corticospinal Tract after Injury. Proc. Natl. Acad. Sci. USA 1999, 96, 13486–13490.

Benowitz, L.I.; Jing, Y.; Tabibiazar, R.; Jo, S.A.; Petrausch, B.; Stuermer, C.A.; Rosenberg, P.A.; Irwin, N. Axon Outgrowth Is Regulated by an Intracellular Purine-Sensitive Mechanism in Retinal Ganglion Cells. J. Biol. Chem. 1998, 273, 29626–29634.

Burkholder, K.M.; Bhunia, A.K. Salmonella enterica Serovar Typhimurium Adhesion and Cytotoxicity during Epithelial Cell Stress Is Reduced by Lactobacillus rhamnosus GG. Gut Pathog. 2009, 1, 14.

Chew, S.Y.; Cheah, Y.K.; Seow, H.F.; Sandai, D.; Than, L.T.L. Probiotic Lactobacillus rhamnosus GR-1 and Lactobacillus reuteri RC-14 Exhibit Strong Antifungal Effects against Vulvovaginal Candidiasis-causing Candida glabrata Isolates. J. Appl. Microbiol. 2015, 118, 1180–1190.

Coman, M.M.; Verdenelli, M.C.; Cecchini, C.; Silvi, S.; Orpianesi, C.; Boyko, N.; Cresci, A. In Vitro Evaluation of Antimicrobial Activity of Lactobacillus rhamnosus IMC 501®, Lactobacillus paracasei IMC 502® and SYNBIO® against Pathogens. J. Appl. Microbiol. 2014, 117, 518–527.

De Almada, C.N.; De Almada, C.N.; De Souza Sant'Ana, A. Paraprobiotics as Potential Agents for Improving Animal Health. In Probiotics and Prebiotics in Animal Health and Food Safety; Di Gioia, D., Biavati, B., Eds.; Springer International Publishing: Cham, Switzerland, 2018; pp. 247–268. ISBN 978-3-319-71948-1.

Doyle, C.; Cristofaro, V.; Sullivan, M.P.; Adam, R.M. Inosine—A Multifunctional Treatment for Complications of Neurologic Injury. Cell Physiol. Biochem. 2018, 49, 2293–2303.

Fan, S.; Kind, T.; Cajka, T.; Hazen, S.L.; Tang, W.H.W.; Kaddurah-Daouk, R.; Irvin, M.R.; Arnett, D.K.; Barupal, D.K.; Fiehn, O. Systematic Error Removal Using Random Forest for Normalizing Large-Scale Untargeted Lipidomics Data. Anal. Chem. 2019, 91, 3590–3596.

Gao, H.; Li, X.; Chen, X.; Hai, D.; Wei, C.; Zhang, L.; Li, P. The Functional Roles of Lactobacillus acidophilus in Different Physiological and Pathological Processes. J. Microbiol. Biotechnol. 2022, 32, 1226–1233.

Haskó, G.; Kuhel, D.G.; Németh, Z.H.; Mabley, J.G.; Stachlewitz, R.F.; Virág, L.; Lohinai, Z.; Southan, G.J.; Salzman, A.L.; Szabó, C. Inosine Inhibits Inflammatory Cytokine Production by a Posttranscriptional Mechanism and Protects Against Endotoxin-Induced Shock. J. Immunol. 2000, 164, 1013–1019.

Haskó, G.; Sitkovsky, M.V.; Szabó, C. Immunomodulatory and Neuroprotective Effects of Inosine. Trends Pharmacol. Sci. 2004, 25, 152–157.

Huang, R.; Wu, F.; Zhou, Q.; Wei, W.; Yue, J.; Xiao, B.; Luo, Z. Lactobacillus and Intestinal Diseases: Mechanisms of Action and Clinical Applications. Microbiol. Res. 2022, 260, 127019.

Iglesias, M.B.; Viñas, I.; Colás-Medà, P.; Collazo, C.; Serrano, J.C.E.; Abadias, M. Adhesion and Invasion of Listeria monocytogenes and Interaction with Lactobacillus rhamnosus GG after Habituation on Fresh-Cut Pear. J. Funct. Foods 2017, 34, 453–460.

Irwin, N.; Li, Y.-M.; O'Toole, J.E.; Benowitz, L.I. Mst3b, a Purine-Sensitive Ste20-like Protein Kinase, Regulates Axon Outgrowth. Proc. Natl. Acad. Sci. USA 2006, 103, 18320–18325.

Latif, A.; Shehzad, A.; Niazi, S.; Zahid, A.; Ashraf, W.; Iqbal, M.W.; Rehman, A.; Riaz, T.; Aadil, R.M.; Khan, I.M.; et al. Probiotics: Mechanism of Action, Health Benefits and Their Application in Food Industries. Front. Microbiol. 2023, 14, 1216674.

Liang, B.; Xing, D. The Current and Future Perspectives of Postbiotics. Probiotics Antimicrob. Proteins 2023, 15, 1626–1643.

Liaudet, L.; Mabley, J.G.; Soriano, F.G.; Pacher, P.; Marton, A.; Haskó, G.; Szabó, C. Inosine Reduces Systemic Inflammation and Improves Survival in Septic Shock Induced by Cecal Ligation and Puncture. Am. J. Respir. Crit. Care Med. 2001, 164, 1213–1220.

Licht, K.; Hartl, M.; Amman, F.; Anrather, D.; Janisiw, M.P.; Jantsch, M.F. Inosine Induces Context-Dependent Recoding and Translational Stalling. Nucleic Acids Res. 2019, 47, 3–14.

Martín, R.; Langella, P. Emerging Health Concepts in the Probiotics Field: Streamlining the Definitions. Front. Microbiol. 2019, 10, 1047.

Mosca, A.; Abreu Y Abreu, A.T.; Gwee, K.A.; Ianiro, G.; Tack, J.; Nguyen, T.V.H.; Hill, C. The Clinical Evidence for Postbiotics as Microbial Therapeutics. Gut Microbes 2022, 14, 2117508.

Murphy, E.F.; Clarke, S.F.; Marques, T.M.; Hill, C.; Stanton, C.; Ross, R.P.; O'Doherty, R.M.; Shanahan, F.; Cotter, P.D. Antimicrobials: Strategies for Targeting Obesity and Metabolic Health? Gut Microbes 2013, 4, 48–53.

Muto, J.; Lee, H.; Lee, H.; Uwaya, A.; Park, J.; Nakajima, S.; Nagata, K.; Ohno, M.; Ohsawa, I.; Mikami, T. Oral Administration of Inosine Produces Antidepressant-like Effects in Mice. Sci. Rep. 2014, 4, 4199.

Muyyarikkandy, M.S.; Amalaradjou, M. Lactobacillus Bulgaricus, Lactobacillus rhamnosus and Lactobacillus paracasei Attenuate Salmonella enteritidis, Salmonella Heidelberg and Salmonella typhimurium Colonization and Virulence Gene Expression In Vitro. Int. J. Mol. Sci. 2017, 18, 2381.

Peng, H.; Zhou, G.; Yang, X.-M.; Chen, G.-J.; Chen, H.-B.; Liao, Z.-L.; Zhong, Q.-P.; Wang, L.; Fang, X.; Wang, J. Transcriptomic Analysis Revealed Antimicrobial Mechanisms of Lactobacillus rhamnosus SCB0119 against Escherichia coli and Staphylococcus aureus. Int. J. Mol. Sci. 2022, 23, 15159.

Sanders, M.E.; Merenstein, D.J.; Reid, G.; Gibson, G.R.; Rastall, R.A. Probiotics and Prebiotics in Intestinal Health and Disease: From Biology to the Clinic. Nat. Rev. Gastroenterol. Hepatol. 2019, 16, 605–616.

Schymanski, E.L.; Jeon, J.; Gulde, R.; Fenner, K.; Ruff, M.; Singer, H.P.; Hollender, J. Identifying Small Molecules via High Resolution Mass Spectrometry: Communicating Confidence. Environ. Sci. Technol. 2014, 48, 2097–2098.

Shafy, A.; Molinié, V.; Cortes-Morichetti, M.; Hupertan, V.; Lila, N.; Chachques, J.C. Comparison of the Effects of Adenosine, Inosine, and Their Combination as an Adjunct to Reperfusion in the Treatment of Acute Myocardial Infarction. ISRN Cardiol. 2012, 2012, 326809.

Song, Y.-G.; Lee, S.-H. Inhibitory Effects of Lactobacillus rhamnosus and Lactobacillus casei on Candida Biofilm of Denture Surface. Arch. Oral Biol. 2017, 76, 1–6.

Spaggiari, L.; Sala, A.; Ardizzoni, A.; De Seta, F.; Singh, D.K.; Gacser, A.; Blasi, E.; Pericolini, E. Lactobacillus acidophilus, L. plantarum, L. rhamnosus, and L. reuteri Cell-Free Supernatants Inhibit Candida parapsilosis Pathogenic Potential upon Infection of Vaginal Epithelial Cells Monolayer and in a Transwell Coculture System In Vitro. Microbiol. Spectr. 2022, 10, e02696-21.

Tang, C.; Lu, Z. Health Promoting Activities of Probiotics. J. Food Biochem. 2019, 43, e12944.

Thoda, C.; Touraki, M. Immunomodulatory Properties of Probiotics and Their Derived Bioactive Compounds. Appl. Sci. 2023, 13, 4726.

Vallejo-Cordoba, B.; Castro-López, C.; García, H.S.; González-Córdova, A.F.; Hernández-Mendoza, A. Postbiotics and Paraprobiotics: A Review of Current Evidence and Emerging Trends. In Advances in Food and Nutrition Research; Elsevier: Amsterdam, The Netherlands, 2020; Volume 94, pp. 1–34. ISBN 978-0-12-820218-0.

Zhao, X.; Zhong, X.; Liu, X.; Wang, X.; Gao, X. Therapeutic and Improving Function of Lactobacilli in the Prevention and Treatment of Cardiovascular-Related Diseases: A Novel Perspective from Gut Microbiota. Front. Nutr. 2021, 8, 693412.

Züllig, T.; Zandl-Lang, M.; Trötzmüller, M.; Hartler, J.; Plecko, B.; Köfeler, H.C. A Metabolomics Workflow for Analyzing Complex Biological Samples Using a Combined Method of Untargeted and Target-List Based Approaches. Metabolites 2020, 10, 342.

FUNDING

Tesi di dottorato finanziata dall'Unione europea- Next Generation EU, Missione 4, componente 2 "Dalla Ricerca all'Impresa" - Investimento 3.3 "Introduzione di dottorati innovativi che rispondono ai fabbisogni di innovazione delle imprese e promuovono l'assunzione dei ricercatori dalle imprese".